PLEUROTUS OSTREATUS HYDROPHOBINS: SURFACE ACTIVE PROTEINS

Annunziata Armenante

Dottorato in Scienze Biotecnologiche – XXI ciclo
Indirizzo Biotecnologie Industriali
Università di Napoli Federico II

Dottorato in Scienze Biotecnologiche – XXI ciclo
Indirizzo Biotecnologie Industriali
Università di Napoli Federico II

Pleurotus ostreatus hydrophobins: surface active proteins

Annunziata Armenante

Dottoranda:	Annunziata Armenante
Relatore:	Prof.ssa Paola Giardina
Coordinatore:	Prof. Giovanni Sannia

La scienza è la ricerca perpetua di una comprensione intelligente e integrata del mondo in cui viviamo.

Cornelis Bernardus van Niel

Summary

Hydrophobins are a large family of small cysteine rich proteins (about 100 amino acids) that appear to be ubiquitous in the Fungi kingdom. The ability of hydrophobins to modify surface properties by interfacial self-assembly and their high surface activity provide a potential for several applications.

A hydrophobin secreted by the basidiomycete fungus *Pleurotus ostreatus* has been purified, and identified as vmh2-1 (TrEMBL entry Q8WZI2_PLEOS). The hydrophobin production has been optimized using different conditions, the highest production (~60 mg/l) has been obtained when *P. ostreatus* mycelium was grown in minimum medium under static conditions.

The pure protein is insoluble in water, whereas complexes formed between the hydrophobin and glycans, present in culture broth containing amylose (PDY), are water soluble. The structure of these glycans, analyzed by GC-MS, MALDI-MS and NMR, matches to cyclic structures of α 1-4 linked glucose containing from 6 to 16 monomers (cyclodextrins). In the presence of these glycans, the hydrophilicity of the hydrophobin increases, nevertheless the protein is prone to self aggregation. On the other hand when the pure hydrophobin is dissolved in 60% ethanol, its self assembly is prevented.

Recombinant *P. ostreatus* hydrophobin has been expressed in a host microorganism, *Escherichia coli.* The recombinant protein has been obtained fused to GST, separated by an aminoacidic sequence recognized by TEV protease. Purification of the recombinant protein has been achieved using the self-assembling properties of the native hydrophobin. The set up procedure has allowed us to obtain about 12 mg/litre of the pure, correctly structured (by CD analysis) recombinant hydrophobin.

The pure protein from *P. ostreatus*, deposited on a silicon hydrophobic surface, forms a very stable biofilm, whereas the biofilm has not been detected on a oxidized silicon hydrophilic surface. When the water-soluble cyclodextrin-hydrophobin complex was used, thick biofilms have been obtained on both surfaces. The hydrophobin biofilm is resistant to hot 2% SDS and it is able to protect silicon surface from basic dissolution, a procedure used in micromachining process. The pure hydrophobin self-assembles also on other surfaces, like porous silicon and oxidized porous silicon, changing the wettability of these surfaces (from hydrophobic to hydrophilic and *vice versa*) but leaving unaltered the sensing ability of the surface.

The features of the Languimir Blodgett (LB) film formed by the *P. ostreatus* hydrophobin have been investigated. When the LB film is transferred onto a silicon substrate, AFM observations revealed the coexistence of a LB monolayer and rodlets. The observed rodlets have a hydrophilic character and are formed by hydrophobin bilayers embedded in the LB monolayer.

We have also demonstrated that the hydrophobin biofilm is suitable for peptides and proteins immobilization. The monolayer acts as a bioactive substrate to bind other proteins. These results can be the starting point in the manufacture of a new generation of hybrid devices for proteomics applications.

Riassunto

Le idrofobine sono piccole proteine (7000-10000 Da) di origine fungina, importanti per lo svolgimento di un ampio spettro di funzioni, dalla crescita allo sviluppo dei funghi.
La caratteristica peculiare di questa classe di proteine è quella di "auto-assemblare" alle interfacce idrofiliche-idrofobiche in biofilm anfipatici notevolmente insolubili. Il biofilm di idrofobine interagisce stabilmente sia con superfici idrofobiche, rendendole idrofiliche, che con superfici idrofiliche, rendendole idrofobiche. In base alla stabilità del biofilm formato, le idrofobine vengono distinte in due classi: le idrofobine di classe I, prodotte sia da Basidiomiceti che da Ascomiceti, formano biofilm molto stabili (solubilizzabili solo con acido formico o acido trifluoroacetico puro) mentre quelle di classe II, prodotte solo da Ascomiceti, formano biofilm meno stabili (solubilizzabili anche con trattamenti più blandi quali etanolo al 60% oppure SDS caldo al 2%).
Sul piano molecolare le idrofobine sono caratterizzate, a fronte di una scarsa identità di sequenza, da una distribuzione conservata di otto cisteine formanti quattro ponti disolfurici intramolecolari.
SC3 (da *Schizophyllum comune*) è una tra le idrofobine di classe I più studiate. E' caratterizzata da uno stato conformazionale essenzialmente α-elicoidale quando la proteina si pone all'interfaccia tra l'acqua e un solido idrofobico (come il teflon), uno stato *β-sheet,* contraddistinto da una elevata percentuale di struttura β, in seguito all'auto-assemblaggio all'interfaccia acqua-aria ed uno stato relativo alla proteina solubile (41 % di struttura β e 20 % di α-elica). La struttura tridimensionale di un'altra idrofobina di classe I EAS (da *Neurospora crassa*), risolta tramite tecniche di NMR, mostra un'elevata presenza di *β-strand,* costituenti un *β-barrel.* Inoltre questa struttura trova ampio riscontro in quella, risolta per cristallografia ai raggi X, di un idrofobina di classe II, l'HFBII (da *Trichoderma reesei)* costruita da un *β-barrel* contenente due motivi *β-hairpin* legati ad un' α-elica.
Grazie alle loro caratteristiche peculiari le idrofobine possono trovare applicazione in svariati campi, che vanno dalle biotecnologie alimentari, all'industria cosmetica, all'ingegneria biomedica. Possono essere infatti utilizzate:

- per ricoprire dispositivi medici, come cateteri e vene artificiali, riducendo la possibilità di legame da parte di batteri patogeni a tali superfici.
- per la purificazione di proteine ricombinanti, opportunamente fuse alle idrofobine,
- per l'immobilizzazione di enzimi, sfruttando la loro capacità di formare biofilm e di interagire stabilmente con supporti rigidi, lasciando gli enzima liberi di ripiegarsi e di svolgere la propria attività catalitica .
- per la creazione di biosensori, come componenti per *lab-on-chip* con applicazioni chimiche e biochimiche e per il *drug delivery,* essendo in grado di derivatizzare superfici.

Nel gruppo di ricerca presso cui ho svolto la tesi di dottorato è da tempo oggetto di studio il fungo basidiomicete *Pleurotus ostreatus,* il cui corpo fruttifero è di importanza commerciale, in quanto alimento umano. Il micelio è usato in processi di bioconversione di ligno-cellulosa, di scarti agricoli o industriali, oltre che come fonte di enzimi e di altri prodotti utili per applicazioni industriali e mediche. Sono noti almeno 4 geni codificanti idrofobine da *P. ostreatus var. florida*: alcuni espressi solo negli stati vegetativi, altri nel

corpo fruttifero. L'espressione di queste proteine è quindi regolata nel tempo e dallo stadio di sviluppo.

Questo lavoro di ricerca ha avuto come scopi *1)* la determinazione delle condizioni di massima produzione e la messa a punto di protocolli di purificazione sia delle idrofobine secrete che delle idrofobine estrattive dal micelio di *P. ostreatus*; *2)* la produzione di un'idrofobina ricombinante; *3)* la caratterizzazione dell'idrofobina sia in forma solubile che aggregata; *4)* l'ottimizzazione delle condizioni per la formazione di biofilm ordinati dell'idrofobina; *5)* la caratterizzazione ottica e strutturale di biofilm di idrofobine deposti su superfici di diversa natura (idrofilica ed idrofobica); *6)* l'utilizzo di biofilm di idrofobine per applicazioni biotecnologiche.

Idrofobina solubile

Sono state ottimizzate le condizioni di crescita di *P. ostreatus* per la produzione di idrofobine, esplorando condizioni diverse (culture statiche o in agitazione) e differenti terreni (complessi e minimi). Inoltre sono state analizzare sia le idrofobine secrete nel terreno che quelle estratte dal micelio vegetativo. Sfruttando la peculiare tendenza di queste proteine a formare aggregati, si è messo a punto un protocollo di purificazione sia per le idrofobine secrete nel terreno di coltura che per quelle del micelio vegetativo.

Dagli studi effettuati risulta che la maggiore quantità di idrofobina è stata estratta dal micelio cresciuto in terreno minimo (per 15 giorni in coltura statica). La quantità di idrofobine ottenute in queste condizioni (circa 60 mg/litro) è decisamente superiore sia a quella ottenuta dall'estrazione da micelio cresciuto in terreno ricco (circa 30 mg/litro per crescite in coltura agitata) che per le idrofobine secrete dal fungo cresciuto in terreno ricco (circa 1.5 mg/l se cresciuto in coltura in agitazione). Questo risultato può essere interpretato considerando che in condizioni di carenza di nutrienti il micelio necessita di un più alto livello di espressione dell'idrofobina.

L'analisi della struttura primaria dell'idrofobina, effettuata tramite idrolisi *in situ*, spettrometria di massa MALDI-TOF e LC-MS/MS, ha permesso l'identificazione della proteina quale idrofobina nota come vmh2-1 (TrEMBL accession number Q8WZI2) sottoposta ad un successivo processo proteolitico di maturazione.

L'idrofobina, purificata a partire da brodo di coltura PDY (patata-destrosio ed estratto di lievito), è solubile in acqua (Hyd-w) e in tamponi salini come l'ammonio bicarbonato (Hyd-a). D'altro canto, l'idrofobina ottenuta in condizioni differenti, quali ad esempio da brodo di coltura ME (estratto di malto) o terreno minimo, non è solubile in acqua ma in una soluzione di etanolo al 60% (Hyd-et). L'idrofobina derivante dalla crescita in PDY viene comunque solubilizzata in 60% etanolo, ma in questo caso si forma un evidente precipitato, la cui natura è stata opportunamente studiata. Le analisi (GC-MS, MALDI-MS e NMR) effettuate su questo precipitato risolubilizzato in acqua, hanno mostrato preliminarmente una struttura di tipo glucidico: più precisamente si tratta di oligomeri di glucosio α-(1$\rightarrow$4) legato (ciclo destrine) a lunghezza variabile (da 6 a 16 monomeri di glucosio) probabilmente prodotte dall'attività enzimatica del fungo per idrolisi dell'amilosio, presente nell'estratto di patata del terreno di coltura PDY. Evidentemente la formazione di complessi tra l'idrofobina e le ciclodestrine rende la proteina più idrofilica e per questo solublizzabile in acqua. In assenza di ciclodestrine la proteina può essere solubilizzata solo in presenza di solventi meno polari quali l'etanolo.

Considerando che le altre idrofobine note mostrano una buona solubilità in acqua, l'idrofobina da *P. ostreatus* è la proteina nota più idrofobica di questa famiglia. Interazioni tra idrofobine e polisaccaridi erano già state riportate: SC3 interagisce con il polisaccaride prodotto dallo stesso microrganismo *Schizophyllum comune*, lo schizofillano e quest'interazione porta ad una stabilizzazione idrofilica ed ad una diminuzione della tendenza all'aggregazione della proteina.

Nel caso di vmh2, la proteina sciolta in etanolo (Hyd-et) non mostra alcuna tendenza all'aggregazione anche dopo 20 giorni dalla dissoluzione o inducendo l'aggregazione mediante vortexing. Se l'idrofobina pura viene solubilizzata in soluzioni a differenti percentuali di etanolo la sua solubilità decrementa fino al 70% se sciolta in 20% etanolo (Hyd-20et). In queste condizioni però la solubilità dell'idrofobina continua a non variare in seguito ad agitazione.

Il complesso ciclodestrine-idrofobina mostra la naturale tendenza all'aggregazione sia in acqua (Hyd-w) che in tampone ammonio bicarbonato (Hyd-a), particolarmente evidente in quest'ultimo caso (sia per analisi SDS-PAGE che seguendo la variazione di concentrazione) già dopo 24h dalle dissoluzione. Hyd-w invece necessita di circa 24 h per la completa dissoluzione ma successivamente tende comunque ad aggregare seppur più lentamente.

L'analisi conformazionale dell'idrofobina, effettuata attraverso dicroismo circolare, mostra per Hyd-et una struttura con un significativo contributo di α-elica che resta invariata almeno per 20 giorni ed anche in seguito ad agitazione. Gli spettri CD di Hyd-20et mostrano un profilo molto simile a quelli di Hyd-et ed anche in questo caso non si osserva alcuna variazione in seguito ad agitazione della soluzione. Invece per quanto riguarda Hyd-w (idrofobina in presenza di ciclodestrine) si evidenzia un'elevata variabilità degli spettri anche se sempre con contributo di struttura random. In seguito ad aggregazione indotta da agitazione si evidenzia una significativa variazione dello spettro CD con aumento del contributo di struttura β. Analisi CD sono stati effettuate anche al variare della temperatura (tra 30 e 90°C). Lo spettro risulta invariato fino a circa 70°C mentre tra 70 e 80°C si è evidenziata una significativa variazione dello spettro con aumento del contributo di struttura beta.

Analisi preliminari sono state effettuate utilizzando la GrFFF (Gravitational field-flow fractionation), una tecnica separativa a flusso liquido capace di separare gli analiti in un ampio intervallo di dimensioni utilizzando un campo gravitazionale perpendicolare al flusso della fase mobile. Queste analisi hanno mostrato la presenza di una banda corrispondente ad un raggio idrodinamico di circa 3 nm attribuibile all'idrofobina monomerica sia nel caso di Hyd-et che di Hyd-w. Per Hyd-a in particolare è evidente la presenza di un'ulteriore banda corrispondente ad un raggio idrodinamico di circa 8 nm, attribuibile ad aggregati multimerici presenti per questo campione anche nell'analisi SDS-PAGE.

Inoltre si è proceduto all'espressione eterologa dell'idrofobina vmh2 in un opportuno organismo ospite (*Escherichia coli*). È stata possibile la sua produzione come proteina di fusione con la GST (dalla quale è stata separata mediante una sequenza amminoacidica riconosciuta dalla proteasi TEV), e con una coda di istidine all'estremità N-terminale. L'idrolisi con la proteasi, e i successivi metodi di purificazione, hanno reso

possibile, la purificazione dell'idrofobina ricombinante (circa 12 mg/litro di coltura), ad un notevole grado di purezza. La sua corretta strutturazione è stata verificata con analisi CD.

Biofilm di idrofobine

Sono state ottimizzate le condizioni di deposizione di Hyd-et per la formazione di biofilm su superfici di natura idrofobica quale il silicio cristallino (Si). Sui biofilm formati sono state effettuate analisi di stabilità a trattamenti chimici come SDS 2% caldo (100°C), trattamento a cui resistono i biofilm formati da idrofobine di classe I. I biofilm sono stati caratterizzati tramite metodologie quali spettroscopia FTIR, ellissometria, angolo di contatto, AFM.

Ottimizzate le condizioni di deposizione che prevedono l'esposizione del chip ad alte temperature per indurre il cambio conformazionale, queste stesse sono state adottate per formare biofilm su superfici di diversa natura (quali silicio cristallino ossidato, silicio poroso e silicio poroso ossidato) e con Hyd-w al fine di verificare la possibilità di formare biofilm anche con il complesso ciclodestrine-idrofobine. È stato verificato che Hyd-et non forma biofilm stabili su silicio ossidato (ox-Si), mentre il complesso ciclodestrine-idrofobine (Hyd-w) forma biofilm sia su superfici idrofobiche, Si, che idrofiliche, ox-Si, ma di spessore maggiore rispetto ai biofilm formati dall'idrofobina pura sul silicio e molto variabile. I polisaccaridi potrebbero essere quindi indispensabili all'adesione delle idrofobine a superfici idrofili che, come già ipotizzato per altre idrofobine di classe I. Nel caso di Hyd-w però la complessità del sistema glucidico ottenuto può rendere difficile la completa comprensione di queste interazioni.

I biofilm di Hyd-et su silicio sono resistenti anche a trattamenti drastici quali l'esposizione a soluzioni basiche, come NaOH e KOH: quest'ultima soluzione è in genere utilizzata come standard di etching. Infatti una superficie di silicio, esposta ad una soluzione di KOH ad 80 °C per 30 s, viene visibilmente corrosa, mentre se la superficie è coperta da un biofilm di idrofobine, anche sottile, la superficie resta perfettamente omogenea. In quest'ultimo caso l'esposizione prolungata decrementa lo spessore del biofilm fino a circa 4 nm , probabilmente corrispondente al monostrato di idrofobine, che resta poi stabile fino a 20 min di esposizione. Il biofilm può quindi essere utilizzato come "maschera" protettiva per superfici in processi di *micromachining*.

E' stato inoltre verificata la formazione di biofilm stabili anche su silicio poroso (P-Si) e silicio poroso ossidato (ox-P-Si). In questo caso la proteina penetra infiltrandosi nella fitta rete di pori lasciando inalterate le caratteristiche ottiche del silicio poroso, ma variandone la bagnabilità. Infatti è stato osservato, attraverso misure di angolo di contatto, che la formazione del biofilm modifica la natura delle superfici, ad es. rendendo il P-Si, che è altamente idrofobico, idrofilico o rendendo idrofobica una superficie idrofilica come quella del ox-P-Si.

Ancora sono stati creati monostrati di idrofobine utilizzando la tecnica Languimir-Blodgett. Questi biofilm ordinati ed omogenei (caratterizzati per AFM) sono stati opportunamente trasferiti su superfici d'interesse che ci hanno permesso di verificare la presenza di rodlet idrofilici sul monostrato di idrofobine. Questo fenomeno è stato già mostrato per altre idrofobine di classe I, quale HGFI da *Grifola frondosa,* che forma, quando vengono più volte compressi i film di Languimir, strutture di tipo rodlets allineati all'interfaccia aria-acqua.

Biofilm di idrofobine auto-assemblati su superfici d'interesse per l'industria optoelettronica, sono in grado di indurre un allineamento controllato delle molecole di cristallo liquido (LC in fase nematica), sostituendo completamente gli strati allineanti di origine organica sintetica con enormi possibilità di riduzione dei costi e di impatto ambientale sul ciclo di produzione dei dispositivi.

È stata dimostrata la capacità del biofilm di idrofobine di immobilizzare peptidi, in questo caso il biofilm di idrofobine è stato depositato sulla piastrina porta-campione del MALDI-TOF, su cui, dopo numerosi lavaggi, sono stai immobilizzati dei peptidi. L'analisi MALDI-TOF-MS ha evidenziato che anche in seguito ai lavaggi, i peptidi restano legati al biofilm a fronte di una loro scarsa immobilizzazione verificata in assenza del biofilm di idrofobine. Questo risultato indica la possibilità di utilizzare i biofilm di idrofobine nella tecnologia SELDI-TOF.

Infine è stata dimostrata la capacità del biofilm di idrofobine di immobilizzare proteine ed enzimi. In particolare è stata verificata l'efficienza di immobilizzazione di BSA fluorescente su *chip* di Si ricoperti di idrofobine. È stato dimostrato come a partire da diverse concentrazioni di BSA marcata deposta su un chip di silicio, il segnale di fluorescenza risultante è omogeneo su tutta la superficie. Inoltre l'intensità della fluorescenza rimane stabile prima e dopo i diversi passaggi di lavaggio segno di immobilizzazione stabile della proteina sul biofilm di idrofobine. Questo risultato sottolinea la possibilità di utilizzare biofilm di idrofobine nel campo dei *microarray*.

Per quanto concerne gli enzimi, è stata dimostrata l'efficienza di immobilizzazione su *chip* di Si di un enzima, la laccasi, in forma attiva. Abbiamo deposto l'enzima su una superficie di silicio ricoperta da idrofobine, effettuati diversi lavaggi quindi saggiata l'attività enzimatica presente sul chip per immersione in una soluzione contenente il substrato L'attività rilevata sul chip è circa il 7 % della quantità totale di laccasi utilizzata, dello stesso ordine di grandezza delle laccasi immobilizzate su altri tipi di supporti (ad es. EUPERGIT C 250L©). Inoltre la superficie del chip a disposizione per l'immobilizzazione è dello stesso ordine di grandezza della superficie totale occupata dalle laccasi immobilizzate, considerando l'ingombro sterico di quest'ultima approssimabile ad una sfera. Ne deduciamo quindi che non solo l'immobilizzazione è avvenuta efficientemente su tutta la superficie, ma che anche tutte le laccasi immobilizzate sulla superficie sono attive. Abbiamo inoltre verificato che l'attività delle laccasi immobilizzate sul chip si dimezza dopo 24h ma rimane costante almeno per le successive 48h. Questi ultimi risultati indicano che il biofilm di idrofobine può essere utilizzato come interfaccia biocompatibile nella creazione di biosensori.

In conclusione questi studi possono contribuire all'analisi del comportamento di questa classe di proteine, sia in soluzione che come biofilm. Considerando che sono effettivamente molto poche le proteine studiate di questa classe, probabilmente a causa della difficoltà di manipolazione dovuta alla loro così alta tendenza all'aggregazione, questo contributo può essere fondamentale per una più approfondita conoscenza di queste proteine e per l'eventuale generalizzazione dei risultati ottenuti. Ciò può facilitarne l'applicazione nei diversi campi di interesse biotecnologico a cui si è fatto riferimento.

Abbreviations

AFM	Atomic force microscopy
BCA	Bicinchoninic acid
cDNA	complementary Deoxyribonucleic acid
CD	Circular Dichroism
DTT	Dithiothreitol
EM	Electron Microscopy
FFF	Field-Flow Fractionation
FTIR	Fourier Transform Infra-Red spectroscopy
GC-MS	Gas Chromatography-Mass Spectrometry
GrFFF	Gravitational Field-Flow Fractionation
GST	Glutathione S-transferase
HPLC	High Performance Liquid Chromatography
Hyd-a	Hydrophobin dissolved in ammonium bicarbonate
Hyd-et	Hydrophobin dissolved in 60% ethanol
Hyd-w	Hydrophobin dissolved in water
Hyd-20et	Hydrophobin dissolved in 20% ethanol
IPTG	Isopropyl β-D-1-thiogalactopyranoside
LB	Langmuir-Blodgett
LC	Liquid Crystals
LC-MS/MS	Liquid chromatography-mass spectrometry tandem
LS	Langmuir-Schaefer
MALDI-MS	matrix assisted laser desorption/ionization-mass spectrometry
ME	Malt Extract
ox-P-si	oxidized-Porous Silicon
ox-Si	oxidized-Silicon
NMR	Nuclear Magnetic Resonance
PAGE	Polyacrylamide gel electrophoresis
PCR	Polymerase Chain Reaction
PDY	Potato Dextrose and Yeast extract
P-Si	Porous Silicon
SAXS	Small Angle X-ray Scattering
SDS	Sodium Dodecyl Sulfate
Si	Silicon
TEV	Tobacco Etch Virus
TFA	Trifluoroacetic acid
ThT	Thioflavine T (dye)

1 Introduction

1.1 The hydrophobins

Hydrophobins are a large family of small cysteine rich proteins (about 100 amino acids) that appear to be ubiquitous in the Fungi kingdom. The name *hydrophobin* was originally introduced because of the high content of hydrophobic amino acids (1). They fulfil a broad spectrum of functions in fungal growth and development. They are ubiquitously present as a water-insoluble form on the surfaces of various fungal structures, such as aerial hyphae, spores, and fruiting bodies, etc and mediate attachment to hydrophobic surfaces. Hydrophobins are able to self-assemble at hydrophilic/hydrophobic interfaces into an amphipathic membrane, resulting in the change of nature of the target surfaces (e.g. between water and air, water and oil, or water and a hydrophobic solid like Teflon) making those surfaces hydrofobic or water-repellent.

Some fungi contain more than one hydrophobin gene and most of the hydrophobins are only known as gene sequences, and their important roles in fungal growth and development are mostly elucidated based on mutagenesis (gene deletion or disruption). Only a few hydrophobins have been isolated and studied at the protein level.

Interestingly, it is the structure specificity, rather than the sequence specificity, that determines their remarkable biophysical properties. The amino acid sequences of mature hydrophobins are highly diverse, but all have eight cysteine residues, including two pairs of adjacent cysteines and forming four disulfide bridges.

The distribution of the cysteines and the clustering of hydrophobic and hydrophilic residues allow hydrophobins to be grouped into two classes, I and II. The aggregates formed by these two classes can be distinguished on the basis of their solubility and morphology.

Class I hydrophobin genes have been isolated from ascomycetes and basidiomycetes, while the genes encoding class II hydrophobins have not been identified in basidiomycetes.

The assembled membrane formed by class I hydrophobins are highly insoluble (even resisting 2% SDS at 100℃) and can only be dissocia ted by high concentration acids (such as formic acid or pure trifluoroacetic acid). In contrast, assemblages formed by class II hydrophobins are less stable, in that they can be readily dissolved by 60% ethanol or 2% SDS. Most of class I hydrophobins form a microscopically identifiable rodlet structure outside the fungal cell wall (2,3,4). Class II hydrophobins form assemblies that lack a distinct rodlet morphology and can be dissolved in detergent and alcohol solutions. Despite these morphological differences, no obvious distinction between the functions of class I and class II hydrophobins within the fungal life cycle has yet emerged.

1.2 Hydrophobins in fungal physiology

Fungal hyphae need to produce specific and dedicated molecules in order to adapt to restraints in their living environment caused by interfacial forces. The molecules produced by filamentous fungi for this purpose are hydrophobins. It has been shown that hydrophobins are very efficient in lowering the surface tension of water. High surface tension is a consequence of water molecules situated on the water surface experiencing an unbalanced interaction between their neighbouring molecules; interactions with molecules in the neighbouring phase (e.g. air) are less favourable than interactions with bulk phase water molecules. This results in stronger cohesive

forces between the molecules at the interface than between the bulk molecules. The enhanced interaction between surface molecules is observable as surface tension.
The hydrophobin SC3 from S*chizophyllum commune* can lower water surface tension from 72 to 24 mN/m. (5) This reduction in surface tension has been shown to allow the hyphae to escape from the aqueous medium and grow into the air (fig. 1 A, B)

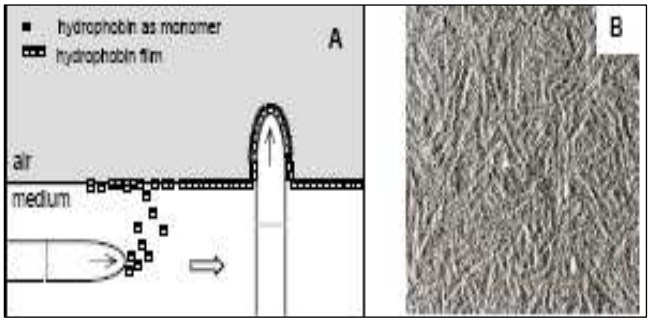

Figure 1.1 (A) A schematic model for formation of aerial hyphae (5,6). The hydrophobin secreted into the liquid culture medium form a hydrophobin film at the water-medium interface, allowing the hyphae to grow into the air. (B) An electron micrograph of hydrophobin film. (Image produced by H.A.B. Wösten and S. Askolin).

As the fungal hyphae grow through the air-water interface into the air, the hydrophobins at the interface are believed to coat the emerging hyphae as they penetrate through the interface (fig. 1.1A) (1). The class I hydrophobins are assembled at the surfaces of aerial hyphae and spores into a mosaic pattern of rod like structures, termed rodlets that are about 10 nm in width. This rodlet coating is very hydrophobic and it is believed to protect the fungal aerial structures from wetting. In addition, air channels in fungal aerial structures have been reported to be lined by hydrophobins (7,8). This hydrophobic coating has been proposed to protect the air channels from wetting and to ensure successful gas exchange. This mosaic of nanometer-sized parallel rods has been observed by electron microscopy (EM) (fig. 1.1B)and atomic force microscopy (AFM). Rodlet layers have been reported on aerial structures of fungi, and evidence for the role of hydrophobins in their formation has been obtained by studying hydrophobin deletion and disruption mutants (9,10,11). For example, the fungal hyphae of a hydrophobin deletion strain of *S*. *commune* cannot grow out from the water to produce aerial structures. Moreover deletion of RodA of *Aspergillus nidulans* resulted in spores which lacked the rodlet layer and were less hydrophobic (2). However, other proteins, e.g. chaplins in the *Streptomycetes*, also form rodlet-type-structures (12,13).
The hydrophobins also function as fungal adhesive molecules. Adsorption of fungal structures to surfaces has been shown to be mediated by hydrophobins in many cases. Hydrophobins have been shown for example to be involved in attachment of hyphae to solid substrates (6) and adsorption of pathogenic fungi to the surface of a host organism (14-17).
Furthermore, hydrophobins have been reported to be involved in fungi-plant interactions (18) and to be localized in mycorrhiza, the symbiotic structures between fungi and plants (19-21). In lichens (symbiotic relationships between fungi and algae or cyanobacteria), hydrophobins have also been observed at the interface between the two symbiotic partners (22,23). It has been proposed that a hydrophobic coating formed by the hydrophobins could protect the gas cavities in the repeated wetting and drying cycles occurring in the lichens harsh environments (12,13).
Hydrophobins have been found to be produced by filamentous fungi which use hydrophobins as their multitools for many different surface tasks. A single species expresses different hydrophobins at different developmental stages, so it is evident

that specialization has occurred. Current knowledge, however, on the functional differences between different hydrophobins is limited.
In summary, hydrophobins are important in the development of filamentous fungi. They are surface active and thus enable hyphae to grow out from aqueous medium; they form protective coatings, and they mediate attachment of fungal structures to various surfaces. Hydrophobins have been studied as isolated proteins in order to understand their role in fungi.

1.3 Structures of hydrophobins

The unifying feature among the amino acid sequences of different hydrophobins is a completely conserved pattern of eight Cys-residues (fig.1.2), where the second and third, and the sixth and seventh Cys residues are invariably adjacent. There are no other completely conserved amino acids among hydrophobins. Class II hydrophobins are generally smaller than class I proteins and display substantially more sequence similarity to one another (fig. 1.2) The length of the polypeptide segments between cysteines 3 and 4 (the Cys3–Cys4 loop) and that between cysteines 4 and 5 (the Cys4–Cys5 loop) are fully conserved in class II hydrophobins, and the other inter-cysteine regions are also well conserved. In contrast, class I hydrophobins display much greater sequence variation (24).

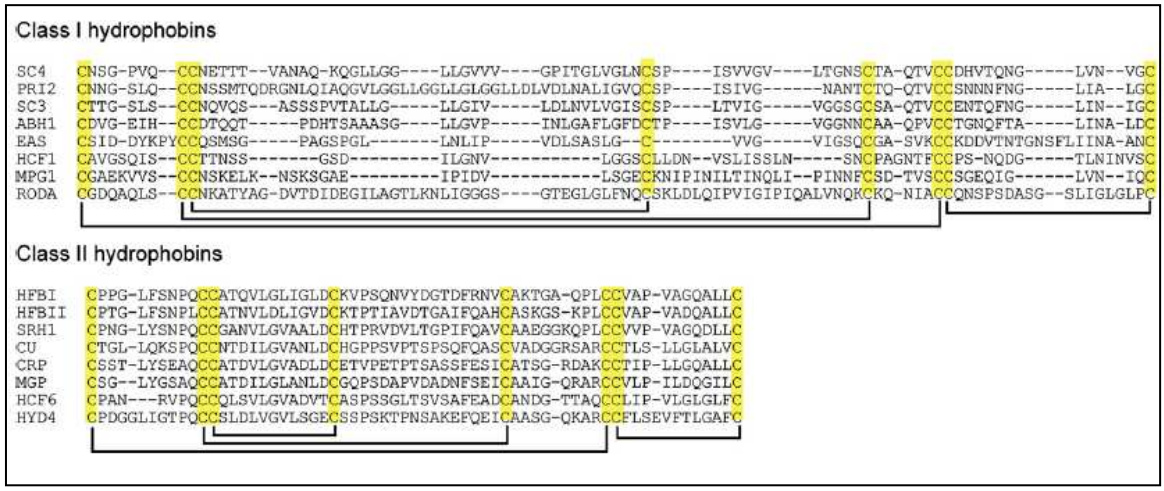

Figure 1.2 Amino acid sequence comparison of class I and II hydrophobins. Only amino acids between the first and last Cys residues are shown due to high sequence variations at the termini (24). The conserved Cys residues are highlighted in yellow with the conserved disulphide bonding pattern indicated with brackets. The abbreviations used are: SC3, S. commune (accession P16933); SC4, S. commune (accession P16934); EAS, N. crassa (accession Q04571); MPG1, M. grisea (accession P52751); HCF1, C. fulvum (accession Q00367); ABH1, A. bisporus (accession P49072); PRI2, A. aegerite(accession Q9Y8F0); RODA, A. fumigatus (accession P41746); HFBI, T. reesei (accession P52754); HFBII, T. reesei (accession P79073); CU, O. ulmi (accession Q06153); CRP, C. parasitica (accession P52753); HCF6, C. fulvum (accession Q9C2X0); MGP, M. grisea (accession O94196); HYD4, G. moniliformis (accession Q6YF29) and SRH1, T. harzianum (accession P79072).

The length of the inter-cysteine regions is highly variable. The Cys3–Cys4 loop varies from 4 residues (HYD3 from *Gibberella moniliformis*) to 44 residues (AaPRI2 from

Agrocybe aegerita), and the Cys4–Cys5 loop varies from 8 residues (EAS from *Neurospora crassa*) to 23 residues (DewA from *A. nidulans*). Across the entire hydrophobin family, the N-termini vary in sequence and length and do not appear to be critical for the structural integrity of the proteins or their surface activity.
Furthermore, class I hydrophobins tend to form rodlet structures at interfaces, whereas class II hydrophobins do not. Rodlets, with the width of about 10 nm each, could also be observed after drying down a purified hydrophobin solution on a hydrophilic surface (25). This division into two classes has had a very good predictive power with regard to hydrophobin properties.

Class I hydrophobins

Recently the structure of EAS from *N. crassa* has been resolved by NMR, in that its structure is similar (26,27) to those of the class II hydrophobin, HFBI and HFBII. The structure of EAS is centred on an irregular four-stranded β-barrel with an additional two stranded antiparallel β-sheet appended to one face. All of the β-sheet secondary structure is antiparallel. Two of the four disulfide bonds lie in the centre of the barrel, whereas the other two connect the outside surface of the barrel to an additional sheet and a nearby loop. However, the β-hairpin loop inter third and forth cysteine in EAS shows a considerable conformational freedom and a extremely hydrophobic nature (27) (fig. 1.3A). One of the features of the EAS sequence is the unusually low number of charged residues (≈10% of the sequence): five aspartates and three lysines. Of these eight residues, six are clustered on a single surface of the protein. The remainder of the surface of the well ordered core is essentially uncharged.

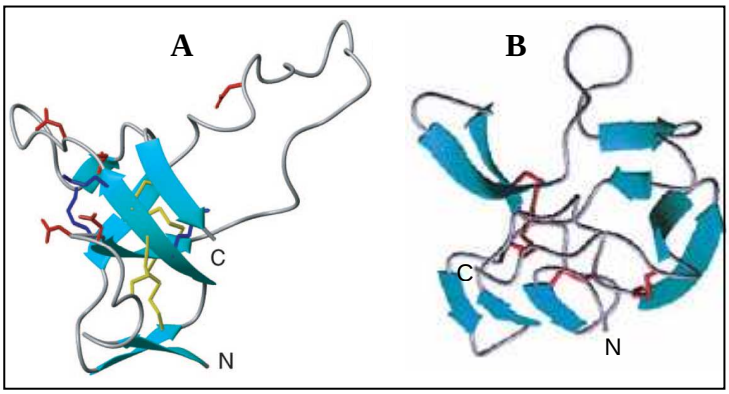

*Figure 1.3 (**A**) Ribbon diagram of solution structure of EAS. Cys side chains are shown as yellow sticks. Positively and negatively charged residues are shown as blue and red sticks, respectively. (**B**) One representative conformation of SC3 model, the disulphuric bridge are shown in red.*

This structure is consistent with its ability to form an amphipathic polymer. The disulfide bond network makes these proteins rigid and no major conformational changes appear to be possible The EAS monomer structure is essentially maintained in the protofilaments, and the ‘‘sticky’’ leading and trailing edges of the β-barrel core provide a means of linking monomers through backbone H-bonding. The Cys3–Cys4 loop might be added on to the barrel, forming additional β-structure that H-bonds to the next monomer in the formation of rodlets. Latest revise demonstrate that the Cys3–Cys4 loop does not have an integral role in the formation or structure of rodlets and that the major determinant of the unique properties of these proteins is the amphipathic core structure, which is likely to be preserved in all hydrophobins despite the high degree of sequence variation across the family (28).
One of the most studied Class I hydrophobin is SC3 from *S. commune*. Its secondary structure has been extensively studied using circular dichroism spectropolarimetry (CD) and attenuated total reflectance Fourier transform infra-red spectroscopy (ATR

FT-IR) (25). The CD spectrum of soluble SC3 is characteristic of a protein with elements of β-sheet structure together with some random coils. Moreover, drying SC3 on a germanium plate (under conditions that maintain its non-assembled state), an ATR FT-IR spectrum has been obtained, which is consistent with the presence of a mixture of secondary structure (25). Deconvolution and curve fitting analysis of the band estimated that soluble SC3 is composed of 23% α-helix, 41% β-sheet and 16% β-turn with the remaining 20% being random coil.
The percentage of β-sheet structure increases about two-fold on self-assembly. The β-sheet structure enhancement at the water/air interface plays an important role in the properties of hydrophobins, specifically in the ability to reduce surface tension and to organize itself into the characteristic rodlet structure.
Since SC3 is experimentally the best characterized of any of the class I hydrophobins in terms of structure/function relationships, it has been possible to validate the results of the modelling dynamics and simulation studies by comparison with a range of experimental data (26,27). The SC3 model structure in solution is compact, globular, and stabilized by the network of disulfide bridges. Two disulfide pairs link the N- and C-terminal regions of the protein limiting the flexibility of the entire molecule. The N- and C-termini and an amphiphilic β-hairpin are located on one face of the protein (fig. 1.3B). The hydrophobic loop is located on the other face, so the homology model predicts that the SC3 molecule is as amphipathic as EAS. Simulated in aqueous solution the protein as a whole adopted mainly β-sheet and coil conformations, nevertheless short regions of α helix did appear.

Class II hydrophobins

The crystal structures of two class II hydrophobins, HFBI and HFBII of *Thrichoderma reesei* have been determined by X-ray crystallography (29,30,31), and several other studies on these proteins have been performed. Of course, class II hydrophobins are more easily handled than class I proteins, because of their lower propensity to aggregate.
The hydrophobin fold is compact and globular and consists of a small antiparallel β-barrel formed by two β-hairpins connected by a stretch of α-helix (fig. 1.4.A, B). The α-helix is linked to the outside of the barrel via a disulphide bond, and another disulphide bond acts to cross-link the two strands within each of the two β-hairpins. These latter two disulphide bonds are completely enclosed by the barrel and are located on opposite ends, thereby giving high stability to the structure. The fourth disulphide bond connects the N-terminal loop to the core β-barrel.
The overall topology of HFBI and HFBII is the same, however, some flexibility was observed in the HFBI structure. The asymmetric unit of HFBI contains four molecules, and there is one seven-residue loop that takes up a different conformation in two of these molecules compared to the other two (fig. 1.4.C). This region includes some of the aliphatic residues in the hydrophobic patch, suggesting that while the β-barrel core of the hydrophobin fold is well-defined, the loop regions between the conserved cysteine residues are likely to have some flexibility.

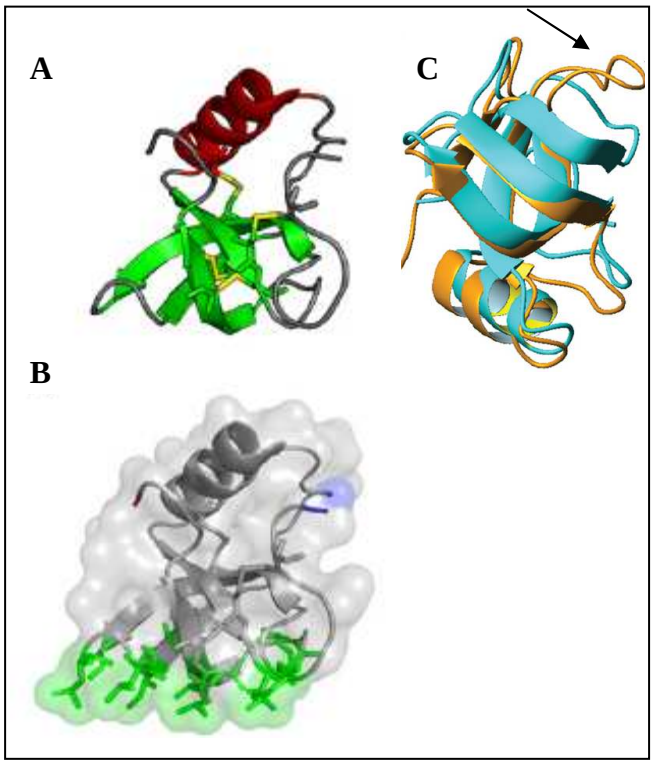

*Figure 1.4 X-ray crystal structure of HFBII (PDB ID 1R2M) (30). (**A**) Cartoon of the protein backbone structure showing the β-barrel formed by two β-hairpins (green) and the connecting α-helix (red). The disulfide bonds of Cys residues are shown in yellow. (**B**) Surface representation of HFBII in which the side chains of the conserved hydrophobic patch are shown and colored green. N- and C-termini are colored in blue and red, respectively (The images were produced using PyMol DeLano 2002). (**C**) Two conformations observed in the HFBI X-ray crystal structure(PDB ID 2FZ6).* A *superposition of two different HFBI molecules (shown in orange and cyan) in an asymmetric unit with the flexible loop indicated by a black arrow (24).*

The unique and surprising feature of the HFBII structure is that about 80% of the hydrophobic side chains are exposed at the protein surface instead of having its hydrophobic residues inside the protein. This structure is probably stabilized by the aforementioned disulfide bond network. Hydrophobic aliphatic amino acids at the protein surface form a planar hydrophobic area termed the hydrophobic patch (fig. 1.4 A, B). This hydrophobic patch constitutes 12 % of the total surface area of HFBII. The protein surface is otherwise mainly hydrophilic, and thus the surface is segregated into a hydrophobic and a hydrophilic part.
This amphiphilic structure governs the properties of both HFBI and HFBII, such as surface activity and surface adsorption. The residues forming the hydrophobic patch are conserved among class II hydrophobins, suggesting that they all share distinct hydrophilic and hydrophobic sides as a protein amphiphile (13,29).

1.4 Hydrophobin self-assembly

The characteristic property of hydrophobins is adsorption to hydrophobic-hydrophilic interfaces, at which they form amphiphilic films (32-34). The interface can occur between solid and liquid, liquid and liquid or liquid and vapour. Thus, hydrophobins are very surface active. In early studies, hydrophobins were found to self-assemble into aggregates and form various types of self-assembled structures (32). Aggregates formed by class II hydrophobins are more soluble than those of class I hydrophobins (32,35).
The ability to decrease the surface tension of water has been reported both for class I hydrophobins ABH3, SC3 and SC4 and class II hydrophobins CFTH1, CRP and HFBII, indicating that these proteins migrate into the water-air interface. Hydrophobins are capable of stabilizing oil droplets in water. For example SC3 has been shown to form a film around oil droplets in water (6,36). In addition, HFBII has been reported to stabilize polyunsaturated fatty acid oil-in-water emulsions (37).

Hydrophobin films can make hydrophilic surfaces hydrophobic and *vice versa* (27). The wettability of a solid surface can be estimated from the spreading of water droplets on it and by measuring their contact angles. A contact angle of 0° represents complete wetting. The hydrophilic (wettable) side of hydrophobin films has been reported to vary from moderate to highly hydrophilic (water contact angles between 22 and 64°). The hydrophobic sides of most hydrophobin films formed on a hydrophilic solid are highly water repellent.

The hydrophobic side of class I hydrophobin films has a characteristic pattern of rodlets (10,32,38). Purified class I hydrophobins have been shown to form rodlet patterned films *in vitro*. When a drop of aqueous class I hydrophobin solution has been allowed to dry down on solid support, rodlets have been observed (6,25,32,39,40,41). The diameter of these hydrophobin rodlets is around 10 nm. The length of rodlets is typically hundreds of nanometers, depending on the hydrophobin used and its concentration (38,42). A rodlet layer has also been seen on air vesicles coated with SC3 hydrophobin (4,43,44)

Interestingly, class I hydrophobin rodlets (41,45,46,47,48) and amyloid fibrils show similar spectroscopic changes in the presence of the dyes Thioflavine T (ThT) and Congo Red, confirming that the core structure of these rodlets consists of stacked β-sheets. The soluble form of SC3 does not bind Thioflavin T, a fluorescent dye that is commonly used to detect the stacked β-structure of amyloid fibrils, but SC3 assembled into rodlets by vortexing gives rise to enhanced fluorescence when stained with the dye (48,49). EAS rodlets display the green-gold birefringence that is diagnostic for amyloid fibrils when stained with Congo red (fig. 1.5) (50).

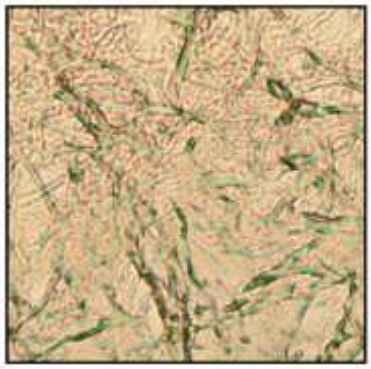

Figure 1.5 Amyloid characteristics of hydrophobin rodlets. Gold-green birefringence observed when EAS rodlets are stained with Congo red and viewed between cross-polarisers.

X-ray diffraction studies of EAS rodlets confirm that they have an ordered β-structure core (27). The diffraction pattern obtained from unaligned rodlets (produced by vortexing and then harvested by centrifugation) displays reflections, consistent with β-sheet structure.

The thickness of the SC3 monolayer has been reported several times. De Vocht et al. (25) used scanning force microscopy and estimated that the rodlets were 7– 8 nm thick. These results are in agreement with EM and other studies of class I hydrophobins, which generally report rodlet diameters for class I hydrophobins of about 10 nm (44) (fig. 1.6).

Figure 1.6 AFM topography image of HFBI films. Film produced by Langmuir–Schaefer method and transferred to highly oriented pyrolytic graphite results in hydrophilic surface presented to the AFM probe (Scale bars are 20 nm).

No rodlets have been observed analysing films formed by the purified class II hydrophobins, such as CRP (46), CU (51) and CFTH1 (52), even if Class II hydrophobin films have also shown ordered structures.
AFM studies of HFBI and HFBII films produced by the Langmuir–Blodgett technique show crystalline domains of the hydrophobins with regular features and a monolayer height of about 13 A° (53). These class II hydropho bin layers display a striking hexagonal repeating pattern that arises spontaneously at the air–water interface. HFBII aggregates have been examined by small and wide angle X-ray scattering (SAXS and WAXS) (53) and grazing incidence X-ray diffraction (54); the aggregates appear to have a monoclinic structure in solution and a hexagonal structure when dried, although the structural significance of these geometries is not currently clear.

The assembly process

CD and ATR FT-IR studies (25,55) both support the idea that SC3 undergoes a transition to a β-rich structure when polymerisation occurs at an interface. SC3 appears to initially populate α helix-rich conformation at the air–water interface, subsequently converting to the stable, β-rich rodlet form. Weak association of SC3 with Teflon can also induce a helix-rich state that is converted to the tightly bound β-form upon heating in the presence of detergents (43).
Interestingly, the presence of intact native disulfide bridges does not appear to be essential for rodlet formation (56). SC3 reduced and treated with iodoacetamide (to prevent re-formation of disulphides) underwent the same conformational changes detected for native SC3 and spontaneously formed native-like rodlets in water. These experiments suggest that the disulfide bridges are not directly involved in the assembly process (45).
Polarisation-modulated infrared reflectance adsorption spectroscopy (PM-IRRAS) has been used to study the self-assembly of SC3 directly at the air–water interface (44). SC3 accumulates rapidly at the air–water interface and is seen to undergo a conformational transition from a mixture of secondary structure elements to a mainly β-sheet form. PM-IRRAS is able to give information about the orientation of secondary structure elements, these analyses indicate that the β-sheets in the SC3 rodlets are parallel to the surface and therefore also co-planar with the long axis of the rodlets. Studies of SC3 oligomerisation, monitored by EM and PM-IRRAS (55), suggest that accumulation of the hydrophobin at the interface to a critical concentration is necessary to allow rodlet formation and that conversion to the β-form takes place at the interface.
The class II hydrophobins HFBI and HFBII also display some increase in helical conformation when bound to Teflon but they do not undergo the conformational changes seen in SC3 when they assemble at an air–water interface (57,58).
In fig. 1.8 the hydrophobins function at interfaces and in solution is summarized. Hydrophobins have been shown to be highly surface active molecules, self-assembled into a highly organized monolayer structure. Specific intermolecular interactions in the monolayer lead to a cohesive film which can be observed as the formation of a planar film. The unusual amphiphilic structure leads to unique properties at interfaces and in solution. Similarly to the formation of detergent micelles, the hydrophobins, in solutions, form multimers in which hydrophobic interactions are significant.

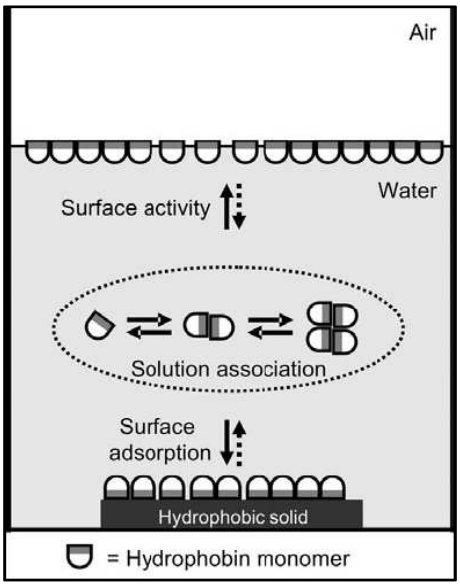

Figure 1.8 A cartoon representing the function of hydrophobin at interfaces and in solution. The hydrophobins are surface active, adsorb to interfaces, and associate in solution into multimers (59).

1.5 Production of hydrophobins

Hydrophobins have hitherto usually been produced and purified on a laboratory scale for analysis of their protein properties. However, for potential applications, larger quantities would be required. Production levels of hydrophobins secreted on the culture medium by wild-type fungi are usually rather low. For example wildtype *S. commune* strains secrete up to 60 mg SC3 per litre culture medium, which makes *S. commune* so far the best producer of SC3 (5,60).

In general, production of hydrophobins has not been widely studied, but some approaches to increase its production have been reported. For example, the production of the class II hydrophobin CU to the liquid culture medium by *O. novo-ulmi* was increased from 0.025 to 0.14 g l^{-1} by optimization of the medium composition (61,62).

Several attempts have been made to increase the production level of SC3 including both homologous and heterologous expression systems in fungi (60,63,64). The expressions of hydrophobin SC3 in filamentous fungus *Aspergillus niger* is also low. SC3 levels in the culture medium were less than 1% of that found in *S. commune*, even when it was fused to a well secreted homologous protein of *A. niger* (60,65). The most promising results have been obtained from heterologous expression in *T. reesei*, which is capable of secreting large amounts of proteins into the culture medium (60,64). Introduction of the gene encoding SC3 under regulation of the *hfb1* or *hfb2* promoter yielded similar or even higher production of SC3 to the culture medium than secreted by *S. commune* (approximately 0.06 g l-1) (5,64).

Heterologous hydrophobin production in bacteria, such as for example recombinant fusion proteins His-Tag sequence and *P. ostreatus* POH1 (65) in *E. coli*, has been reported to be very low (50 mg of pure recombinant protein per 100 ml of bacterial culture).

1.6 Purification of hydrophobins

Purification of hydrophobins has mostly been carried out in laboratory scale for analytical purposes. The amounts of hydrophobins purified have only rarely been reported, probably due to quantification problems. Purification of class I hydrophobins has usually been based on the low solubility of their aggregates in ethanol or hot

diluted SDS. For purification of the SC3 hydrophobin from the cell walls of *S. commune*, impurities were removed using hot 2% SDS followed by release of SC3 with TFA or formic acid (1,4,66,67). Soluble SC3 has been isolated from culture medium by precipitation, mixing the medium with air, dissolution in TFA and removal of the acid by evaporation (4). Several other class I hydrophobins have been purified essentially according to these methods (4,16,17,40,41,42,65,68,69,70,71,72,73). Chromatographic methods have been used for purification of class I hydrophobins such as EAS of *N. crassa* (74,75), RodB of *A. fumigatus* (73), RolA of *A. oryzaea* (76) and SC3 of *S. commune* (77,78).
Class II hydrophobins, such as CFTH1 of *Claviceps fusiformis*, CRP of *C. parasitica* and HFBI and HFBII of *T. reesei*, have been released from fungal cell walls using diluted solution of SDS or ethanol (77,78). Other purification methods, including high performance liquid chromatography (HPLC), have been used to further purify these proteins (79,80). For isolation of the soluble class II hydrophobins *O. ulmi* CU and HFBII from culture medium, a weak vacuum was applied or air was led to the medium and the hydrophobin was collected by generating foam (62,81). HFBI and HFBII have also been purified from liquid culture medium in aqueous two-phase systems (77,78).

1.7 Potential applications of hydrophobins

The ability of hydrophobins to spontaneously self-assemble at hydrophobic-hydrophilic interfaces gives rise to several potential applications.
The nature of a solid surface can be dramatically changed by the self-assembly of hydrophobins. A hydrophobic solid surface can be converted to a hydrophilic one with a hydrophobin coating, and hydrophilic solid surface can be converted to a hydrophobic one by drying down a hydrophobin solution on the top of it. These unique properties make hydrophobins ideal for many applications. For instance, the binding of hydrophobins to the surface of implants or catheters might prevent attachment of pathogenic bacteria and improve growth of human fibroblasts (for example SC3 fused with the cell-binding domain of fibronectin, RGD, supports the growth of human fibroblasts on a coated Teflon surface). Neither soluble-state nor assembled SC3 showed toxicity to the cultured cells, nor did they seem to be immunogenic (82). Such a hydrophobin coating might also be an intermediate to attach cells, proteins, or other type of molecules to hydrophobic surfaces, such as biosensors. For nanotechnological applications, hydrophobins, carrying different functional groups after certain modifications, might be used to pattern different molecules on a surface with nanometre accuracy, being the hydrophobin rodlets about 10-nm wide, and chemically highly stable.
In addition, the remarkably high surface activity of hydrophobins is at least similar to that of traditional biosurfactants, such as glycolipids, lipopeptides/lipoproteins, phospholipids, neutral lipids, substituted fatty acids, and lipopolysaccharides. Hydrophobins could be used as an alternative to surfactants in many applications such as emulsifiers or foaming agents in different branches of industry. For example HFBI has been shown to stabilize aqueous dispersion of Kevlar® nanopulp (37).
Hydrophobins have also been found to be useful as indicators of beer gushing. Hydrophobins produced by barley-contaminating fungi have been shown to cause gushing problems in beer, and a specific immunoassay has been developed (83). Besides that, hydrophobins might be able to substitute traditional surfactants to stabilize oil vesicles, or oil emulsions, in pharmaceutical applications (84). The surface activity of hydrophobins depends on a protein self-assembly process

accompanied by a conformational change of the molecules (β-sheet state) rather than on a diffusion-limited adsorption to the interface. Therefore, the hydrophobin layer may not only stabilize but also protect the oil vesicles from degradation during circulation in the body. Although various applications can be expected using native hydrophobins, future modification of hydrophobins may offer more possibilities. The modifications, either genetic or chemical, may change the biophysical properties of the hydrophobin coating and, therefore, make new applications possible. Some successful applications using hydrophobins have emerged recently and are introduced in the following sections.

Immobilization of cells and enzymes.

When the class II hydrophobin was fused to flocculin, followed by homologous expression in the yeast *S. s cerevisiae*, the fused protein could be targeted to the cell wall. The surface property of the engineered yeast appeared to be changed, as they became more apolar and slightly less negatively charged (85).

Fusing the same hydrophobin to the C-terminus of a hydrolytic enzyme, endoglucanase I, from *T. reesei*, enabled the protein to efficiently bind to hydrophobic surfaces, such as silanized glass and Teflon, forming a tightly bound, rigid layer. The enzyme activity remained unchanged after the immobilization (86).

Therefore, hydrophobin fusions can be used as a complement, or, alternative for the traditional approaches of immobilizing microbial cells and enzymes of industrial interest.

Hydrophobins purified from *P. ostreatus*, were first bound to a hydrophilic matrix, glyoxyl-agarose, forming an amphipathic membrane with the hydrophobic side facing the air. Subsequently, the lipases from *C. antarctica*, *H. lanuginose* and *P. fluorescens* were immobilized to the hydrophobins-coated glyoxyl-agarose via a hydrophobic interaction. The hydrophobin-immobilized lipases showed similar stability and catalytic properties to those of lipases interfacially immobilized on conventional hydrophobic supports (87). In another study, the class I hydrophobin, HYDPt-1, from fungus *P. tinctorius* heterologously expressed in *E.coli*, was used to modify electrode surfaces. The hydrophobin-coated electrodes were then functionalised and the electroactive reagents were stably attached for several weeks to the electrodes due to the hydrophobin layer. The adsorbed HYDPt- 1 layers were stable in solutions at a wide range of pH, and efficiently blocked the access of small hydrophilic electroactive probes from the solution to the electrode surface (88).

Purification of other proteins.

The amphipathic properties of hydrophobins might facilitate the large-scale purification of fusion proteins. The first example came from endoglucanase (EGI) of *T. reesei*, whose C-terminus was coupled to hydrophobin HFBI from the same fungus. The purification of this fusion protein using a two-phase system, appeared to be more efficient than that of EGI without the fusion. EGI-HFBI from the culture medium strongly partitioned into the micelle-rich phase and was separated from hydrophilic proteins, which preferably partitioned to the polymer phase. Subsequently, the EGI-HFBI could be back-extracted into a water phase by the addition of ethylene oxide-propylene oxide (EOPO) copolymers to the micelle-rich phase. The total recovery of EGI-HFBI was 90% after such a purification (89).

1.8 *P. ostreatus* hydrophobins

Pleurotus ostreatus is a commercially important edible mushroom commonly known as the oyster mushroom. This fungus is industrially produced as human food, and it accounts for nearly a quarter of the world mushroom production (90). It is also used for the bioconversion of agricultural, industrial, and lignocellulose wastes (91,92) as a source of enzymes and other chemicals for industrial and medical applications (93,94,95), as an agent for bioremediation (96), and as organic fertilizer (97). Several different *P. ostreatus* varieties are industrially produced. Commercial varieties *florida* and *ostreatus* differ in size, colour, and temperature tolerance. Both varieties have been used in previous studies about the hydrophobins present in this fungus (98,99).

The family of genes coding for *P. ostreatus* hydrophobins is large and complex, and the function of the encoded proteins is regulated by time or developmental stage (100). Different hydrophobin genes have been isolated from *P. ostreatus*: *vmh1*, *vmh2*, *vmh3*, *Fbh1* (100,65) *POH2*, *POH3* (101) and *Po.hyd* (102).

The genes coding for vegetative mycelium hydrophobins in *P. ostreatus var. florida* are single copy and encode three different hydrophobins *vmh1, vmh2* and *vmh3.* Two of them (*vmh1* and *vmh2*) are specific of vegetative mycelium, whereas *vmh3* expression also occurs in fruit bodies. The expression level of hydrophobin genes decays with culture time. The expression of the three hydrophobins genes is under the control of diverse regulatory elements and have different developmental roles necessary to fulfil the life cycle of the fungus. This decay is more pronounced in the case of *vmh1* and *vmh2*, as *vmh3* expression is detected in aged cultures. The fruit body-specific hydrophobin Fbh1 (or POH1, product of allele of the same gene) and Po.hyd (102) are not expressed during vegetative growth and their expression is spatially regulated in the fruit body.

The redundancy of gene coding for vegetative mycelia hydrophobins could suggest that they should play different roles during growth and differentiation.

1.9 Outline of this thesis

A deeper knowledge of the properties and behaviour of fungal hydrophobins, both in solution or assembled, is needed to spread the results obtained so far. As a matter of fact, notwithstanding the above mentioned studies, little is known about other Class I hydrophobins, their characteristics and the films they can form. This could be mainly due to the difficulties in extracting and handling these self-assembling proteins. We are contributing to this goal by shedding light on the properties of hydrophobins secreted by the basidiomycete fungus *Pleurotus ostreatus.*

Specific aims of this work were:

- production and characterization of soluble hydrophobin vmh2
- heterologous expression of vmh2
- stability study of hydrophobin in solution
- structural analysis of hydrophobin in solution
- optimization of conditions to make ordered biofilm
- characterization of vmh2 biofilm
- use of hydrophobin biofilm for biotechnological applications

2 Materials and Methods

2.1 Fungal growth and protein purification

White-rot fungus, *P. ostreatus* (Jacq.:Fr.) Kummer (type: Florida) (ATCC no. MYA-2306) was maintained through periodic transfer at 4 ℃ on potato dextrose agar (Difco) plates in the presence of 0.5 % yeast extract (Difco). Mycelia were inoculated (by adding six agar circles of 1 cm diameter) in 2 l flasks containing 500 ml of broth grown at 28 ℃ in static or in shaken (150 rpm) mod e. The used broths were:
PDY: potato-dextrose (24 g/l) supplemented with 0.5% yeast extract (PDY)
ME: 2% malt extract
Minimum broth (composition for litre of culture): glucose: 20 g; tartrate di sodio 0,288 g; KH_2PO_4 2 g; $(NH_4)SO_4$ 0,198 g; $MgSO_4 \cdot 7H_2O$: 0,5 g; $CaCl_2 \cdot 2H_2O$ 0,1 g; biotin 10 mg; tyrosol 0,069 g; 10 ml/l of mineral stock, (for 100 ml: Mn $SO_4 \cdot 5\ H_2O$ 0,05 g; NaCl: 0,1 g; Fe $SO_4 \cdot 7H_2O$: 0,01 g; $CoCl_2 \cdot 6H_2O$ 0,01 g; Zn $SO_4 \cdot 7H_2O$ 0,01 g; Cu $SO_4 \cdot 5H_2O$ 0,001 g; $AlK(SO_4)_2$ 0,001 g; H_3BO_3: 0,001 g; $NaMoO_4 \cdot 2H_2O$: 0,001 g).

After 10 days of fungal growth, hydrophobins released into the medium were aggregated by air bubbling using a Waring blender. Foam was then collected by centrifugation at 4,000 x *g*. The precipitate was freeze-dried, treated with TFA for 2hrs and sonicated for 30 min. After centrifugation at 3200 x *g* for 20 min, the supernatant was dried again in a stream of air, and then dissolved in water (Hyd-w), 50 mM ammonium bicarbonate pH8 (Hyd-a) or 60% ethanol (Hyd-et). In the latter case, the solution was kept at 4 ℃ overnight and t hen centrifuged at 3200 x *g* for 10 min.
Before use the protein was always disassembled using pure TFA, dried, and then the monomeric protein dissolved.

Hydrophobin from *P. ostreatus* mycelia were isolated using the protocol described by Peñas *et. al.* (98). The hydrophobins were isolated exploiting their properties: they are insoluble in a boiling solution containing sodium dodecyl sulphate (SDS) 1% and NaH_2PO_4 0,1M pH 7, for 15 minutes. After this procedure the insoluble hydrophobins were separated from other soluble proteins by centrifugation at 4000 x g and several washing steps with water. To further purify hydrophobins from hot SDS-extracted mycelia, the freeze-dried precipitate obtained was extracted five times with chloroform-methanol (2:1 v/v) at 65℃ for 10 min to remove non covalently bound lipids (4). The precipitate was then freeze-dried, treated with TFA for 2hr and sonicated for 30 min, as described for secreted hydrophobins. The hydrophobin was dissolved in 60% ethanol for further analysis.

Protein concentration was evaluated by bicinchoninic acid (BCA) assay (Pierce, Rockford, IL) using bovine serum albumin as standard or, when the hydrophobin was dissolved in ethanol solution, evaluated by measuring the absorbance band at 280 nm, using a value of ε=1.44 ml mg^{-1} cm^{-1}. This extinction coefficient has been estimated on the basis of the concentration determined by BCA assay on the protein in water.

2.2 Complex reconstitution

PDY broth was added to the dried, TFA treated Hyd-et, and the procedure used for hydrophobin purification (air bubbling, centrifugation, lyophilizing and TFA treatment) was performed. Alternatively Hyd-et (dissolved in 60% ethanol) has been diluted up

to 4% ethanol and then an aqueous solution of the glycans (previously separated) was added. The sample was then vortexed for 10 min, the aggregates centrifuged, lyophilized, TFA treated and solubilised in water.

2.3 Phenol-sulphuric acid test

The glycan solution (200µl) was mixed with 5% phenol (200ml) and sulphuric acid (1ml). This mixture was then incubated for 10 min at room temperature and 20 min at 37 ℃, and the absorbance at 485 nm was determined, using Beckman DU 7500 spectrophotometer (Beckman Instruments) (103). A standard curve was performed using from 2 to 200 µg of glucose.

2.4 HPLC

For chromatography separation an HPLC system (HP 1100 series Agilent Technologies) equipped with an analytical reverse phase Vydac C4 column (25×0.21 cm, 5 µm) (The Separation Group, Hesperia, CA, USA) was used. Solvent A was composed of 0.1% trifluoroacetic acid (Sigma-Aldrich) and 10% isopropanol; solvent B was composed of 0.1% trifluoroacetic acid in 90% acetonitrile and 10% isopropanol. A linear gradient of solvent B from 10 to 95% in 65 min at a flow rate of 1 ml/min was employed. UV absorbance of the eluent was monitored at 220 nm.

2.5 SDS-PAGE

SDS-polyacrylamide gel electrophoresis (SDS-PAGE) was performed using the Laemmli method (104) with the Bio-Rad Mini Protean III apparatus, using 15% polyacrilamide concentration.

ß-galactosidase (117 kDa), bovine serum albumine (85.0 kDa), ovalbumin (49 kDa), carbonic anidrase (34.0 KDa), b-lactoglobulin (25.0 kDa), lisozyme (19 kDa) were used as standards (Fermentas Inc., Glen Burnie, MD, USA) or PageRuler™ Prestained Protein Ladder (Fermentas SM0671).

The gels were stained by silver staining or by periodic acid staining (GelCode Glycoprotein Staning Kit 24562, Pierce).

2.6 Mass spectrometry

MALDI mass spectra were recorded on a Voyager DE Pro MALDI-TOF mass spectrometer (Applied Biosystems, Foster City, CA). The analyte solutions were mixed with sinapinic acid (20 mg/ml in 70% acetonitrile, TFA 0.1% v/v), or 2,5-Dihydroxybenzoic acid (DHB) (25 mg/ml in 70% acetonitrile) or α-cyano-4-hydroxycinnamic acid (10 mg/ml in 70% acetronitrile, TFA 0.1% (v/v) as matrixes, applied to the sample plate and air-dried. The spectrometer was used in the linear or reflectron mode. Spectra were calibrated externally.

In situ hydrolysis was carried out on the silver-stained protein bands excised from a 15% polyacrylamide gel run under denaturing conditions (104). Excised bands were extensively washed with acetonitrile and then with 0.1 M of ammonium bicarbonate. Protein samples were reduced by incubation in 10 mM dithiothreitol for 45 min at 56℃ and carboxamidomethylated by using 55 mM iodoa cetamide for 30 min, in the dark, at room temperature. The gel particles were then washed with ammonium bicarbonate and acetonitrile. Enzymatic digestion was carried out with 15 mg/ml trypsin (Sigma-Aldrich, St.Louis, MO, USA) in 10 mM of ammonium bicarbonate, at 4℃ for 2 h. The buffer solution was then removed a nd a new aliquot of buffer solution was added for 18 hours at 37℃. A minimum reaction volume, sufficient for complete rehydration of the gel was used. Peptides were then extracted washing the

gel particles with 20 mM of ammonium bicarbonate and 0.1% trifluoroacetic acid (Carlo Erba, Milan, Italy) in 50% acetonitrile at room temperature and then lyophilized. Aliquots of the digests were concentrated and directly analyzed by MALDI-MS.
Peptides from *in situ* hydrolysis were analyzed by LCQ ion trap (Finnigan Corp.) coupled to a 250 × 2.1-nm, 300 Å Phenomenex Jupiter C18 column on an HP 1100 HPLC (Agilent Technologies). Peptides were eluted at a flow rate of 0.5 ml/min with a 5%–65% gradient of 95% acetonitrile, 5% formic acid and 0.05% TFA in 60 min.
GLC and GLC-MS were all carried out for carbohydrate analysis as described (105,106). Monosaccharides were identified as acetylated O-methyl glycosides derivatives. After methanolysis (2M HCl/MeOH, 85°, 24 h) and acetylation with acetic anhydride in pyridine (85°, 30 min) the sample was analyzed by GLC-MS. Linkage analysis was carried out by methylation of the complete core region as described (107). The sample was hydrolyzed with 2 M trifluoroacetic acid (100℃, 2 h), carbonyl-reduced with $NaBD_4$, aetylated and analyzed by GLC-MS.

2.7 NMR spectroscopy
All spectra were recorded on a solution of 1 mg in 0.5 mL of D_2O, at 300 K, at pD 7. NMR experiments were carried out using a Bruker DRX-600 spectrometer. Chemical shifts are in ppm with respect to the 0 ppm point of the manufacturer's indirect referencing method. Nuclear Overhauser enhancement spectroscopy (NOESY) was measured using data sets (t1 × t2) of 2048 × 256 points, and 16 scans were acquired. A mixing time of 100 ms was used. Double quantum-filtered phase-sensitive correlation spectroscopy (DQF-COSY) experiment was performed with 0.258s acquisition time, using data sets of 2048 x 1024 points, and 64 scans were acquired. Total correlation spectroscopy experiments (TOCSY) were performed with a spinlock time of 120 ms, using data sets (t1 × t2) of 2048 × 256 points, and 16 scans were acquired.
In all homonuclear experiments the data matrix was zero-filled in the F1 dimension in order to give a matrix of 4096 x 2048 points which was then resolution enhanced in both dimensions by a shifted sine-bell function before Fourier transformation. Heteronuclear single quantum coherence (HSQC) was measured in the 1H-detected mode via single quantum coherence with proton decoupling in the ^{13}C domain, using data sets of 2048 × 256 points, and 64 scans were acquired for each t1 value. Experiments were carried out in the phase-sensitive mode in accordance with the States et al. method (108).

2.8 RNA Isolation
RNA was extracted from shaken cultures of *P. ostreatus* grown in PDY broth, using a RNAeasy kit as described by the manufacturer (Qiagen, Hilden, Germany). DNase I-treated total RNA was used as a template for RT-PCR using Superscript II (Invitrogen). cDNA was amplified with this template using the designed primers:

VMH1 fw	AAAGCTTATGCTCTTCAAACAAGCC
VMH1rev	AAAAAAGCTTTCAGAGATTGATATTGATAG
VMH2fw	AAAAAAGCTTATGTTCTCCCGAGTTATC
VMH2REV	AAAAAAGCTTCACAGGCTAATATTGATGGG
VMH3FW	AAAAAAGCTTATGTTCCAAACTACCATCG
VMH3REV	AAAAAAGCTTACAAGGCAACGTTGATGGG

PCR was carried out in 50 µl of solution containing:
2.5 µl cDNA, 5 µl Buffer Taq 10X, 5 µl $MgCl_2$ 25mM; 1 µl DNTP 10 mM, 5 µl OLIGO Vmh fw 100 µM, 5 µl OLIGO Vmh2 rev 100 µM, 1 µl *Taq* DNA Polimerasi 5 U/ µl, 25.5 µl H_2O.
The cycling program started with a 5-min denaturation step at 94°C, followed by 35 cycles of 45 sec of annealing at 54°C, 45 sec of extension at 72°C, and 1 min denaturation at 94°C. Double-stranded DNA fragments were sequenced by Primm s.r.l.

2.9 Production of the hydrophobin vmh2 in *E. coli.*
In order to produce the hydrophobin vmh2 in *E. coli* cells, the pET system (Novagen, Madison, Wis.) and pETM-30 (EMBL, kindly making available from Prof. Picone group) were used. The region coding for the mature vmh2 protein was amplified by PCR from the cDNA mixture synthesized above. The PCR was carried out by using as primers oligonucleotides which contain sequences corresponding to the N-terminal and C-terminal ends of mature vmh2 and *Bam*HI and *Hin*dIII restriction sites. The sequences of the used primers are:

OLIGO Vmh2-1 fw Nco:
5' CATGCCATGGATTCCCAGTTGCTCAAC 3'
OLIGO Vmh2-1 rv Xho stop
5' CCGCTCGAGTCACAGGCTAATATTGATGGG 3'

The amplified DNA was digested with *Nco*I and *Xho*I and cloned :

- in pET-22b(+) upstream the six histidine sequence (His-Tag sequence),

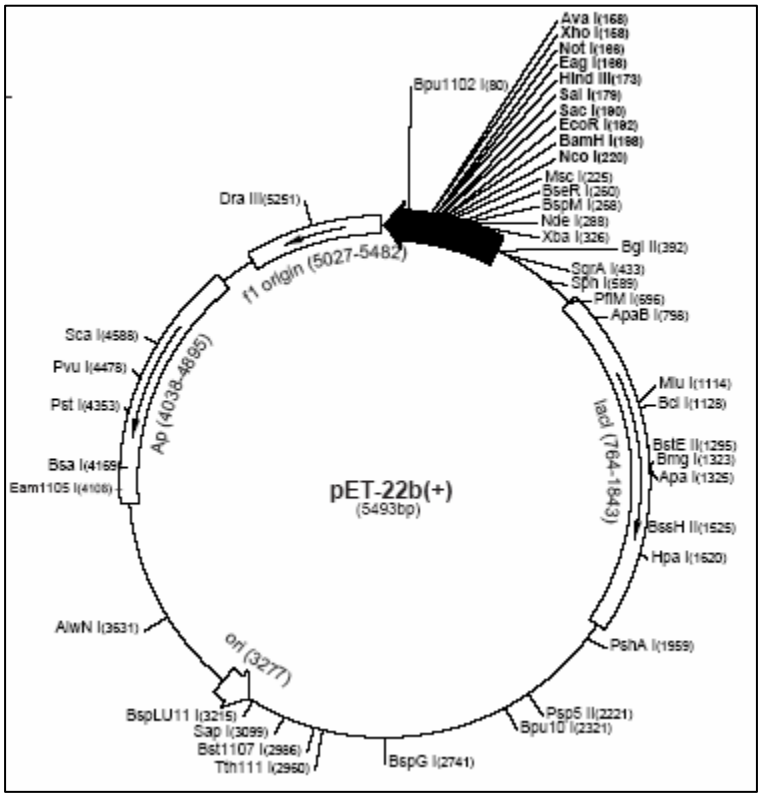

Figure 2.1 pET-22b(+) vector

- In pETM-30 downstream the six histidine sequence (His-Tag sequence) and the GST coding sequence

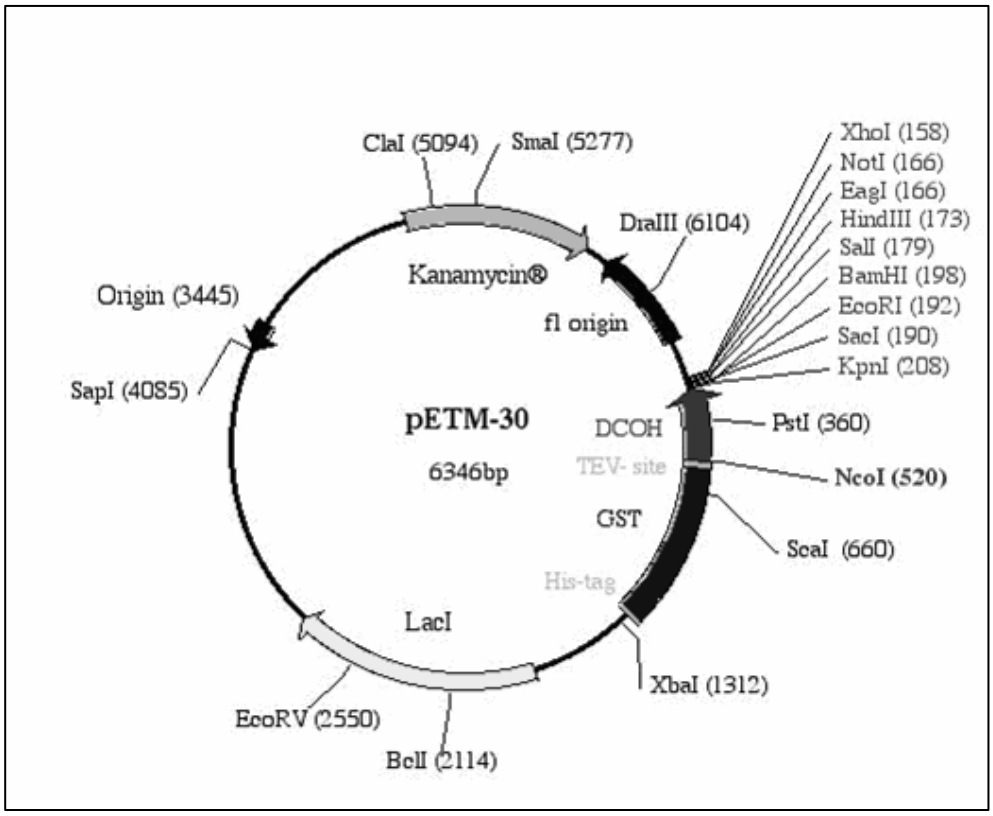

Figure 2.2 vector pETM-30.

The translation frame was kept in order to generate in pET-22b(+)a fusion protein vmh2-His-Tag and in pETM-30 a fusion protein His-Tag-GST-vmh2.
The resulting plasmids pET-ND2 (from pET-22b(+) and pETM-ND1 (from pETM-30) were transformed into the *E. coli* BL21 DE3 (Novagen).
Expression of the fusion protein was induced by adding isopropyl-b-D-thiogalactopyranoside (IPTG) (Sigma) to a final concentration of 1 mM to an early-exponential-phase culture of *E. coli* BL21(DE3) transformed with plasmids. After 3 hours of induction at 37℃, the bacteria were harve sted by centrifugation, resuspended in 50mM Tris-HCl buffer pH8.4, 5mM EDTA, and disrupted by sonication in Microson Ultrasonic Homogenizer XL2000, at 12 W, with 20 cycles (30" ON e 30" OFF). The soluble fraction was discarded, and the insoluble pellet with the inclusion bodies was washed in denaturing buffer containing 0,1 M Tris-HCl pH 8,4, 2%TRITON, 2M urea, 10 mM EDTA, sonicated and centrifugated three times at 24000 X g for 20 minutes. After that the pellet was further washed in 50mM Tris-HCl buffer pH 8.4, 5mM EDTA, sonicated for 10 minutes and centrifugated twice at 24000 X g for 20 minutes. Then the pellet was dissolved in 0.1 M Tris-HCl buffer pH 8.4, 10 mM EDTA, 8 M Urea, 10 mM DTT. The sample was dialysed to remove urea. Using the same buffer, the urea concentration was slowly decreased (1M each step till to 2M, then 0.2 M each step until 0,3 M).
The Ni-NTA affinity chromatography column was equilibrated with 100 mM NaH_2PO_4, pH 8,2, 10 mM Tris-Cl, 8 M urea, 5 mM 2-mercaptoethanol (buffer B). Inclusion bodies dissolved in the same buffer were loaded. Elution was performed using C, D and E buffers, containing the same components as buffer B but at pH 6,3, 5,9, and 4,5 respectively.

The fusion protein was cleaved by incubation with the enzyme TEV (tobacco etch virus, recombinant protein expressed in *E. coli* BL21PLYSS) 25mM at 30℃ for 24 hours. After hydrolysis by TEV the protein was refolded using 0.1M Tris-HCl buffer pH 8.4, 3 mM reduced glutathione, 0.6 mM oxidized glutathione for 20 hours at room temperature in a nitrogen atmosphere. The protein was then purified from the other proteins (GST e TEV) with 1 hour vortexing and centrifugation at 3200 X g for 15 minutes, in pellets. The recombinant hydrophobin was then purified as described for native vmh2. The precipitate was freeze-dried, treated with TFA for 2hrs and sonicated for 30 min. After centrifugation at 3200 x *g* for 20 min, the supernatant was dried again in a stream of air, and then dissolved in 60% ethanol.

2.10 Circular dichroism spectroscopy

Far-UV CD spectra were recorded on a Jasco J715 spectropolarimeter equipped with a Peltier thermostatic cell holder (Jasco model PTC-348), in a quartz cell (0.1-cm light path) from 190 to 250 nm. The temperature was kept at 20° C and the sample compartment was continuously flushed with nitrogen gas. The final spectra were obtained by averaging three scans, using a bandwidth of 1 nm, a step width of 0.5 nm, and a 4 sec averaging per point. The spectra were then corrected for the background signal using a reference solution without the protein.

CD spectra of the protein were also recorded changing temperatures at a rate of 1 ℃ /min with 10℃ steps, from 30℃ to 90℃.

2.11 Biofilm on silicon chip*.*

Single sided polished silicon samples, <100> oriented (chip size: 1cmx1cm), after standard cleaning procedures have been washed in hydrofluoridic acid solution for three minutes to remove the native oxide thin layer (1-2 nm) due to silicon oxidation. To obtain oxidized silicon the silicon samples have been thermally oxidized in an O_2 atmosphere, at 1100 ℃ for 1 hr, resulting in a oxi dized thickness of about 80 nm. Then samples have been incubated in hydrophobin solutions (0.1 mg/ml in 80% ethanol or in water) for 1 h, dried for 10 min on a hot plate (80℃), washed with the solvent solution, and then washed with 2% SDS at 100 ℃ for 10 min.

2.12 Peptide immobilization

The hydrophobin solutions (0.1 mg/ml in 80% ethanol) was deposited on a MALDI sample plate (stainless steel plate produced by Applied Biosystems, Foster City, CA) for 1 h, dried for 10 min on the hot plate (80℃), washed by dipping in the solvent solution (for 2 hours in 80% ethanol), then in water (for 1h) and in 50% acetonitrile (ACN) (for 15 minutes).

Trypsin (Sigma , Aldrich) was auto-hydrolyzed at 37℃ overnight and the peptides, which had been dissolved in water, were immobilized on a MALDI sample plate for deposition for 1 hour. After that the samples were washed three times with 50% ACN and analyzed by MALDI-MS.

For detection of the peptides, the Voyager DE Pro MALDI-TOF spectrometer was used in the reflectron mode and α-cyano-4-hydroxycinnamic acid (10mg/ml in 70% acetronitrile, TFA 0.1% v/v) was used as matrix.

3 Results

3 .1 Production of hydrophobins

A *P. ostreatus* hydrophobin was purified either from cultural broth and from mycelium, using different growth conditions (i.e. different media and static or shaken growth). The hydrophobin was identified by mass spectrometry analysis. Moreover it was expressed as heterologous protein in *Escherichia coli.*

3.1.1 Purification of the secreted hydrophobin

P. ostreatus was grown in static cultures using potato dextrose broth containing yeast extract (PDY) or malt extract broth (ME) until such time as the liquid surfaces were completely covered by mycelia (about 10 days for PDY and 14 days for ME). The hydrophobins were self-assembled into insoluble films at an air-water interface by air bubbling the liquid broths. The self-assembled form of hydrophobin is then collected, lyophilized and treated with 100% TFA to dissociate into water soluble monomers.
After this partial purification the amount of lyophilized material, ranged from 5 to 10 mg per litre of PDY cultural broth, whereas it was only 2-3 mg when samples were prepared from ME cultural broth. After the TFA treatment, the dried material obtained from the PDY broth was water soluble (Hyd-w); while all attempts aimed at dissolving samples prepared from ME cultural broth into water failed.
The amount of Hyd-w per litre of culture broth (determined by BCA protein assay) was about 0.5-1 mg. Hence non proteic components are present in the dried material obtained after bubbling of PDY culture broths.
When the dried material obtained from PDY broth, after the TFA treatment, was dissolved in 60% ethanol, an abundant precipitate was formed whereas the hydrophobin was left in the ethanol solution, as verified by SDS-PAGE (fig. 3.1a). The phenol-sulphuric acid test performed on the ethanol insoluble material indicated the presence of glycans. On the other hand, when the hydrophobin from ME cultural broth, was solubilized in 60% ethanol, no precipitate was formed, indicating the absence of glycans in these samples (Hyd-et). The SDS-PAGE of Hyd-w, stained by periodic acid (fig. 3.1b), showed the presence of glycans in Hyd from PDY but not in the Hyd from ME.

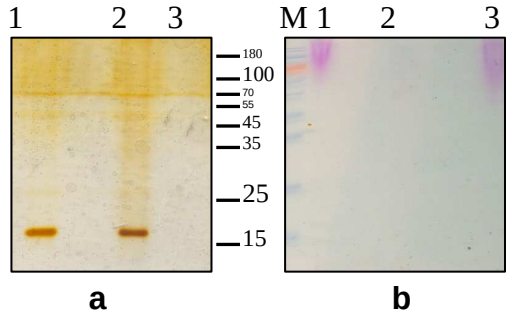

Figure 3.1 SDS-PAGE of: Hyd-w from PDY (lane 1); Hyd-et from ME (lane 2); ethanol precipitate of Hyd from PDY (lane 3); marker M; a) Silver staining b) staining with periodic acid.

After glycan separation by precipitation in 60% ethanol, the protein is only soluble in the presence of ethanol, not in pure water. In this condition its behaviour becomes similar to that of hydrophobin purified from an ME cultural broth. Therefore these glycans, when present, co-aggregate during air-bubbling with hydrophobins, giving a water soluble sample.
P. ostreatus was grown in PDY shaken cultures for 10 days, in this case the lyophilized material was about 1.5 mg for litre of culture.

To investigate the interactions between the hydrophobin and glycans, an analytical reverse phase chromatography procedure has been set up. Elution of the proteins from the C4 column was only obtained in conditions less polar than the standard (in the presence of 10% isopropanol) and with very low yield. Very different elution volumes of Hyd-w and Hyd-et (before and after glycans removal) were observed. As shown in fig. 3.2, a single peak eluting at about 10 min was detected, when Hyd-w was loaded on the column, whereas a heterogeneous peak centred at 57 min was eluted when Hyd-et was loaded. The presence of the hydrophobin in these peaks has been confirmed by SDS-PAGE, whereas the simultaneous presence of glycans in the peak eluting at 10 min was confirmed by the phenol-sulphuric acid test. These results indicate that a complex, stable in the conditions used for the chromatography, is formed between the hydrophobin and glycans.

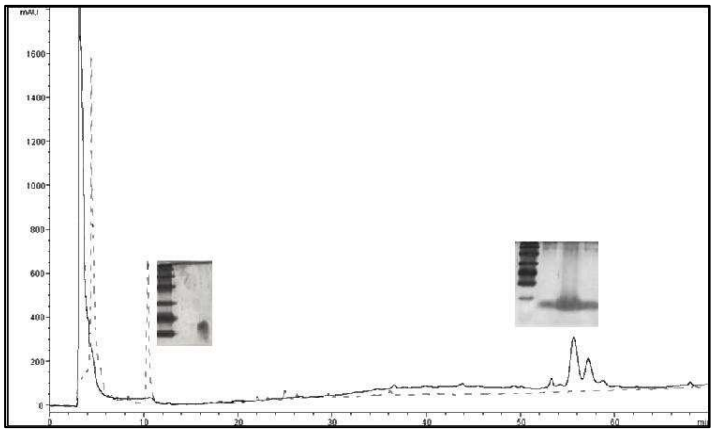

Figure 3.2 A reverse phase chromatography of Hyd-w (solid line) and Hyd-et (dotted line) is showed and SDS-PAGE of the peaks.

Several attempts have been performed to reconstitute the hydrophobin-glycan complex starting from the Hyd-et, in order to re-obtain a water soluble protein:

- aqueous solution of the glycans was added to dried Hyd-et inducing or not aggregation by vortexing
- dried Hyd-et TFA treated, and dissolved in water was added to dried glycans
- PDY broth was added to dried Hyd-et and then the sample was treated as for purification (bubbling, centrifugation, lyophilizing, TFA treatment and water dissolution)
- water was added to Hyd-et (dissolved in 60% ethanol) up to 6% of ethanol and then an aqueous solution of the glycans was added.

In all cases the samples of hydrophobin and glycans were vortexed, lyophilized, TFA treated and dissolved in water, but only in the latter case a water soluble protein-glycan complex has been re-obtained. As a result, only when co-aggregation of the two components is induced, the protein-glycan complex is formed, leading to the water soluble hydrophobin.

3.1.2 Hydrophobin extraction from *P. ostreatus* mycelium

Pleurotus ostreatus was grown in PDY medium for 10 days in static or shaken cultures and hydrophobins were extracted by the vegetative mycelia.

The amount of dried mycelia obtained from shaken cultures was higher than that obtained from static cultures grown for the same time (tab 1). Using the procedure set up and described in the Material and Methods section, the presence of a unique band was observed by SDS-PAGE analysis of the obtained samples (fig. 3.2 a). The

amounts of hydrophobin purified in the two cases is proportional to the amounts of the mycelia obtained.
The hydrophobin was also purified from *P. ostreatus* mycelia grown in minimum medium. These experiments were aimed at verifying the possibility of labelling the native protein by growing the fungus in minimum medium containing heavy isotopes suitable for NMR structural analysis (^{15}N). In this case the hydrophobin was soluble in 60% ethanol (not in water) and the amount obtained was higher than that obtained in the other conditions (tab. 1) probably because of an increased production of hydrophobin in conditions of nutrient starvation. SDS-PAGE showed a unique protein band present also in these samples (fig. 3.3 b)

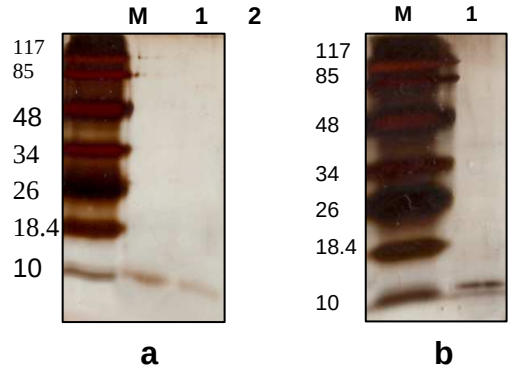

*Figure 3.3 SDS-PAGE Silver staining M: marker **a**). Hydrophobin from mycelium growth in static PDY culture (lane 1), hydrophobin from mycelium growth in shaken PDY culture (lane 2) **b**) hydrophobin from mycelium growth in shaken minimum medium culture (lane 1).*

	Hydrophobin amount (mg/l of culture)
static PDY culture	14.5
shaken PDY culture	29.1
static culture in minimum medium	62,4
shaken culture in minimum medium	32,2

Tab. 1 Amounts of hydrophobin from mycelia obtained in different growth conditions.

3.1.3 Structural analysis

MALDI MS spectra of the samples (Hyd-w and Hyd-et) show two peaks at 8463 and 8564 m/z (fig. 3.4), with the relative intensity of the latter always higher than the former.

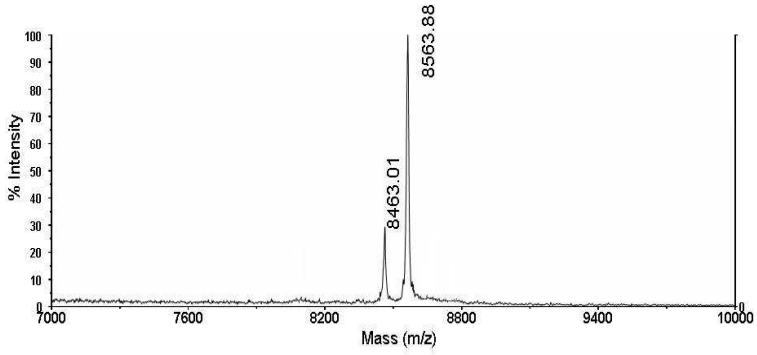

Figure 3.4 MALDI-MS spectrum of Hyd-w performed in linear mode using sinapinic acid as matrix.

According to Penãs et al. (97), *P. ostreatus* hydrophobins undergo a proteolytic processing after signal peptide removal. The peak at 8564 m/z can be attributed to vmh2-1 (TrEMBL accession number Q8WZI2) starting from T25 with eight cysteines linked by four disulphide bridges, and the peak at 8463 m/z to the same protein after further removal of the N terminal threonine residue. Analysis of the MALDI-MS spectrum (fig. 3.5) of the tryptic peptides, obtained by *in situ* hydrolysis, showed the presence of the expected peaks at 2001.9 m/z (D26-K44) and 2102.9 m/z (T25-K44), whereas the other expected peak at 6938.6 m/z (corresponding to the peptide A45-L113) was not detected. The absence of this peak could be due to the difficult extraction of such a large peptide from the polyacrylamide gel.

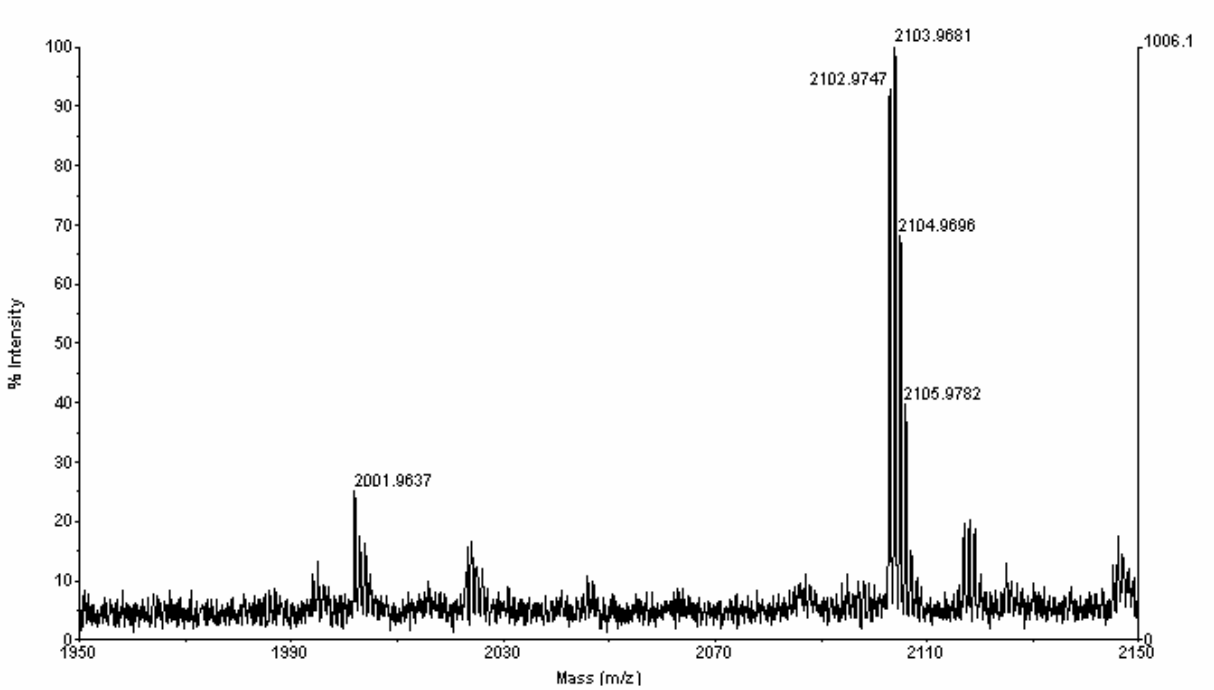

Figure 3.5 MALDI-MS spectra (in reflectron mode) of the triptic peptides of the hydrolyzed protein

The identity of the protein and its N-terminal processing was confirmed by LC-MS-MS analysis. Fragmentation of the 2102.9 and 2001.9 m/z peak led to the sequences SCSTGSLQC (S29-C37) and CSTGSLQCCSSV (C30-V41) respectively (fig 3.6 a b).

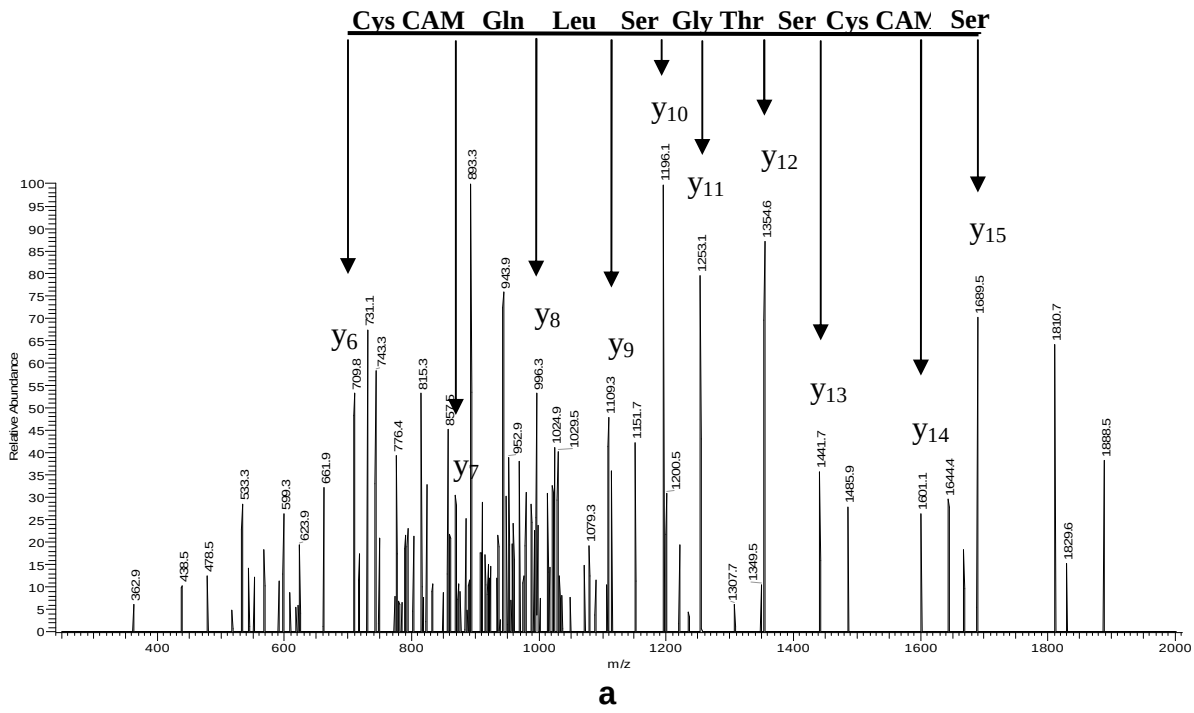

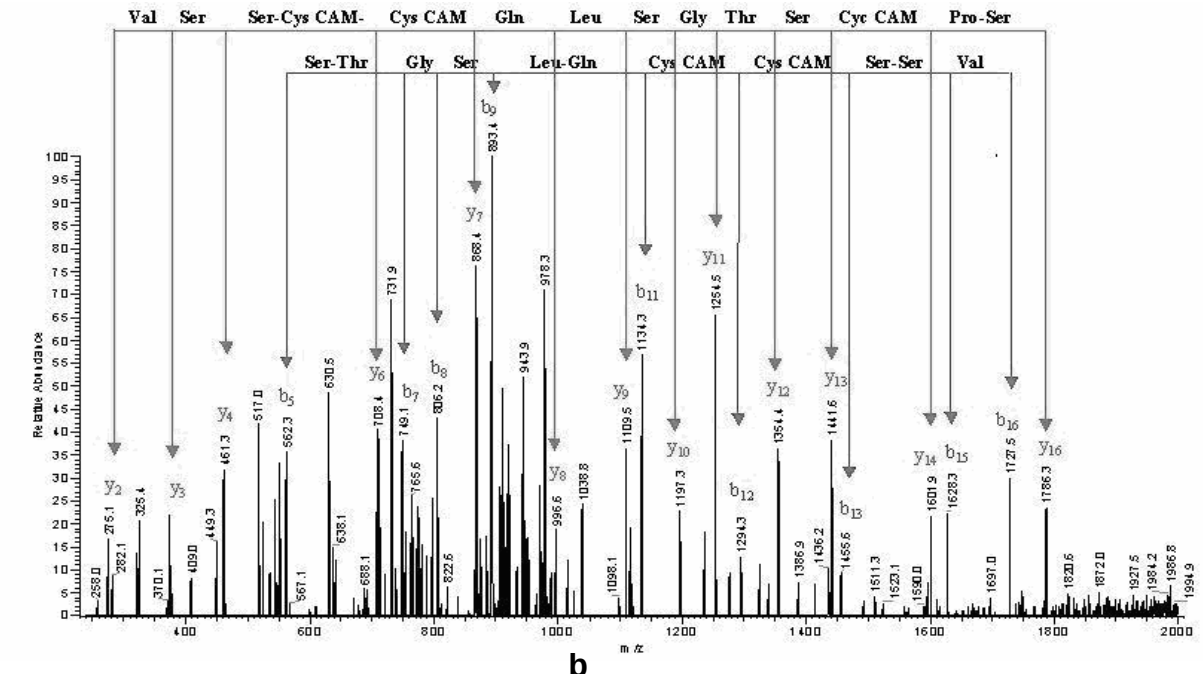

*Figure 3.6 Triptic peptides analysis LC-MS-MS of the 2102.9 m/z peak (**a**) and of the 2001. 9 m/z peak (**b**)*

The protein was purified from fungal cultures grown at different times (5, 10, 15 or 20 days), and a relative increase of the intensity of the peak corresponding to the form D26-L113, in respect to that corresponding to T25-L113, was observed in older cultures. Furthermore a peak at 8349.5 m/z probably corresponding to the form lacking also D26, was detected in the preparation from 15 and 20 days old cultures.

Several other experiments were carried out to further analyse the hydrophobin structure in solution:

- hydrolysis of the protein with pepsin in acidic condition;
- hydrolysis of the protein with chimotrypsin at different reaction times;
- hydrolysis of the protein with pepsin after oxidation by performic acid at different time (109);
- hydrolysis of the protein reduced by phosphine and modified by cianylation (27);
- hydrolysis of the protein at high temperature (108°C) in the presence of formic acid 12% with or without a reducing agent (DTT) (110);
- microwave hydrolysis with pepsin or trypsin or chimitrypsin with or without reducing agent (DTT) (111);
- microwave hydrolysis in the presence of 12% formic acid (112,113) with or without a reducing agent (DTT).

In every case no result has been obtained, since no peptide was detected by MALDI-MS analysis. This could be due to the adhesion of the hydrophobin on hydrophobic surfaces, i.e. during chromatography elution (needed to eliminate salts by the samples) or to the low solubility and high aggregation tendency of both the hydrophobin and its peptides.

The glycan component of Hyd-w was also subjected to chemical and spectroscopic analyses after purification by ethanol precipitation. Carbohydrate analysis by GLC-MS revealed exclusively the presence of 4-linked D-Glucose in pyranose form (4-D-Glcp), no terminal residues were detected, neither reducing nor non-reducing. The ^{1}H NMR spectum of this glucan showed proton signals in the anomeric and ring sugar regions. The water dissolved precipitate was fully assigned by 2D NMR spectroscopy that confirmed the presence of a single component, the α-(1$\rightarrow$4) glucan. It is worth to note that reducing ends were undetectable in NMR spectra.
Analysis of MALDI MS spectra of such glucan showed the presence of several peaks whose molecular masses agreed with the theoretical values for cyclic glucans with degree of polymerization from 6 to 16. As a matter of fact, a cyclodextrin blend should have a mass of 162n, whereas glucans in any non-cyclic structure should have a molecular mass of 162n + 18 (fig. 3.7a).
Incubation of the cyclic glucan at 110°C for two hours at pH 3 led to partial hydrolysis of the cyclic glucans (peaks corresponding to molecular masses of 162n + 18), as shown in the MS spectrum reported in Fig. 4A. In agreement, in the ^{1}H NMR spectrum of this sample (fig. 3.7b) the presence of anomeric reducing signals was detectable.

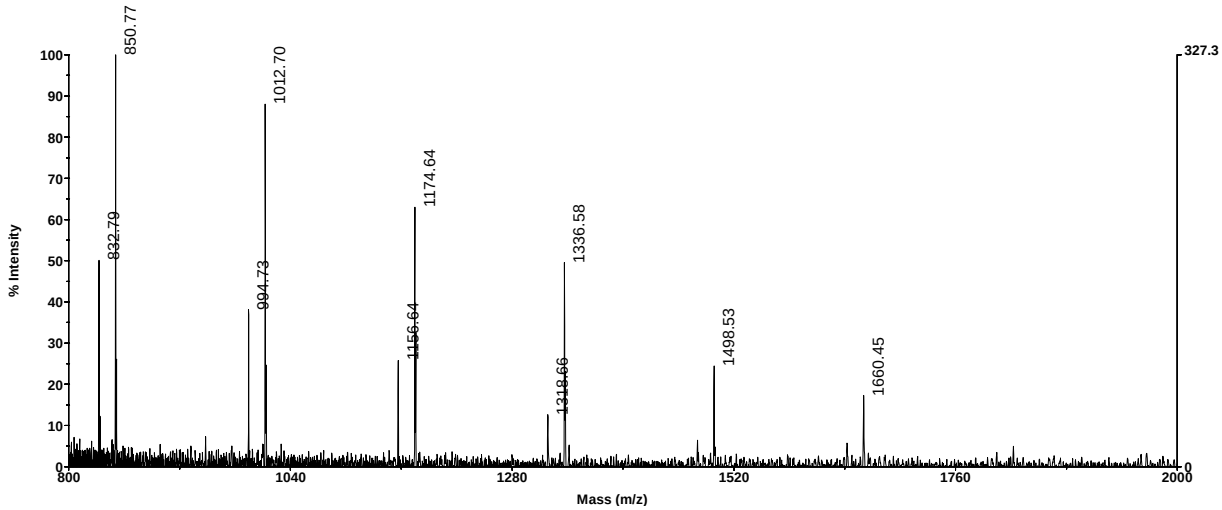

a

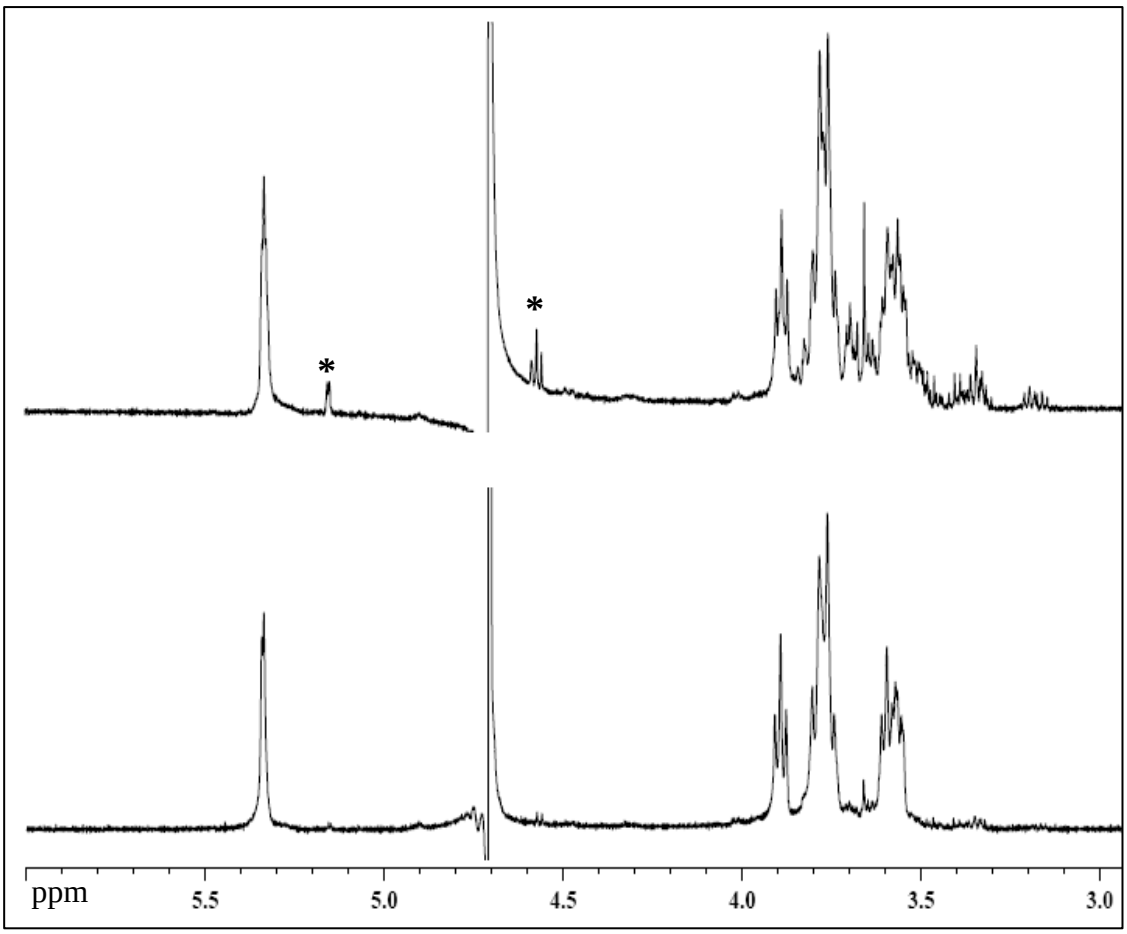

b

*Figure 3.7 Panel **a**: MALDI MS analysis of glycans after incubation at 110 ℃ for two hours at pH 3. Peaks corresponding to cyclic structures (162n), and peaks corresponding to linear structures (162n + 18) are shown. Panel **b**: Comparison of the ^{1}H NMR spectrum of the α-(1→4) glucan before (bottom) and after (up) the acid hydrolysis. The anomeric signals of the reducing units are labelled.*

It is worth noting that amylose ((α-(1→4)-Glc)$_n$glucan), a component of the PDY cultural broth coming from potato infusion, is absent in the ME culture broth. The lack of glycans in the hydrophobin preparation from the latter cultural broth indicated that the cyclodextrins are produced by the fungus when grown in the presence of amylose.

3.1.4 Alignment

Sequence analysis has been performed comparing vmh2 with several others class I hydrophobins. vmh2 shows 46% of identity on the whole sequence with the often-used example of class I hydrophobin SC3, raising to 62% if the fragment starting from the first C is considered (fig. 3.8 a). The main difference between the two sequences lies in the T stretch upstream the first C of SC3, that is absent in vmh2.
Comparison with some class II hydrophobins, showed in Fig.3.8 b, reveals a very low percentage of identity of vmh2 with these proteins, also starting from the first C. The highest percentage of identity is with HYD4 but it is only 18%. These analyses confirm that vmh2 belongs to Class I hydrophobins.

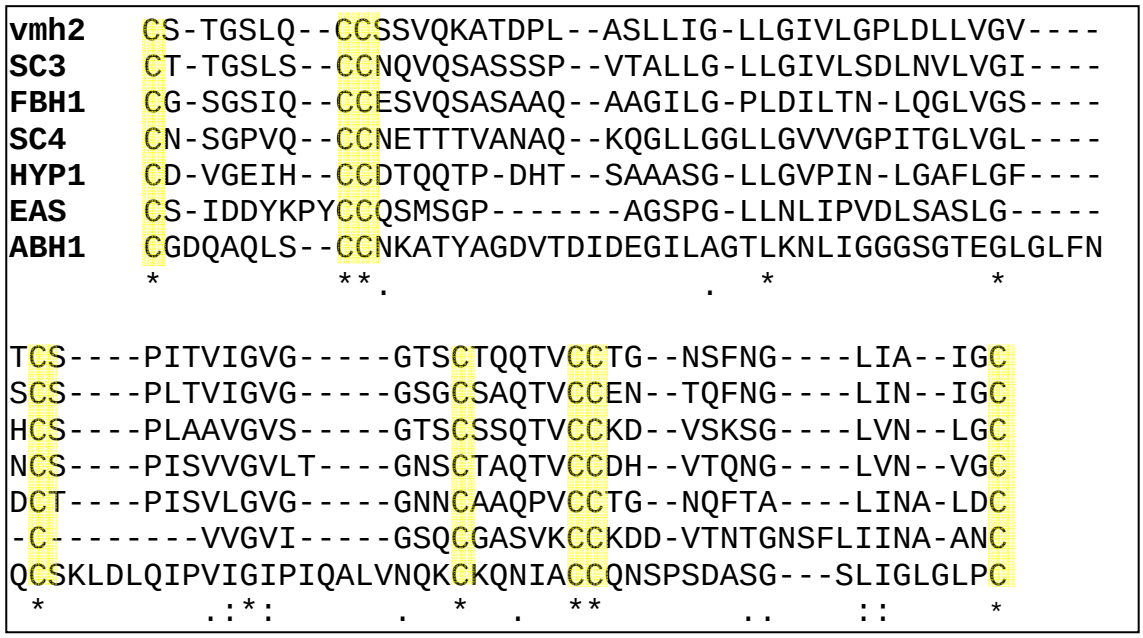

a

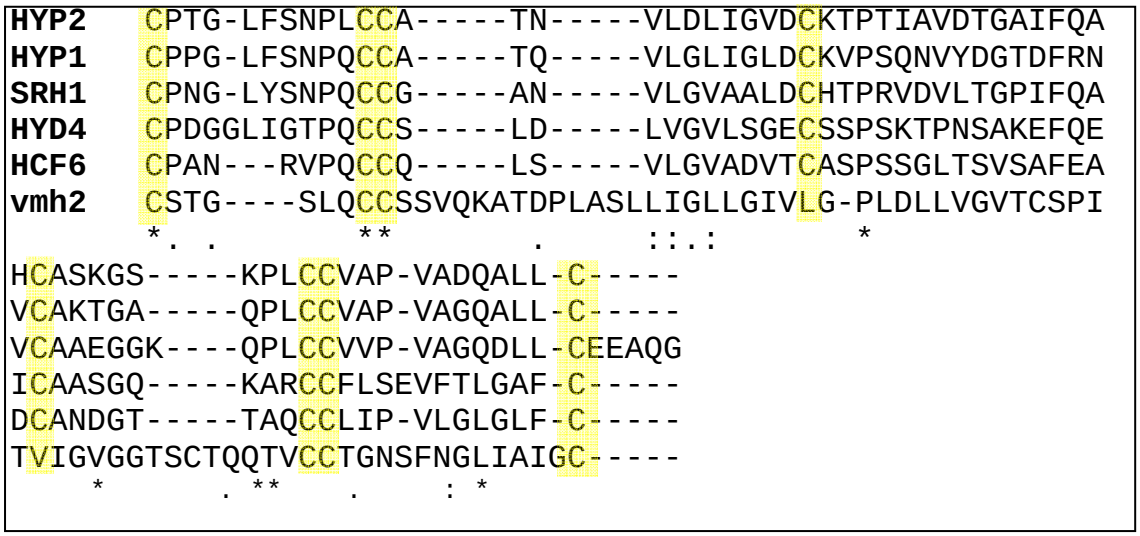

b

*Figure 3.8 Amino acid sequence comparison of vmh2 with class I (**a**) and II hydrophobins (**b**). Only amino acids between the first and last Cys residues are shown due to high sequence variations at the termini. The conserved Cys residues are highlighted in yellow The abbreviations used are: SC3, S. commune (accession P16933); SC4, S. commune (accession P16934); EAS, N. crassa (accession Q04571); ABH1, A. bisporus (accession P49072); HFBI, T. reesei (accession P52754); HFBII, T. reesei (accession P79073); HCF6, C. fulvum (accession Q9C2X0); HYD4, G. moniliformis (accessionQ6YF29) and SRH1, T. harzianum (accession P79072).*

Hydropathy plot of vmh2 shows a typical profile of class I hydrophobins. In fig. 3.9 the vmh2 hydropathy profile is shown in comparison with that of the other class I hydrophobin SC3. The amino acid sequence of vmh2 is slightly more hydrophobic with respect to SC3, mainly in the C-terminal part of the sequence.

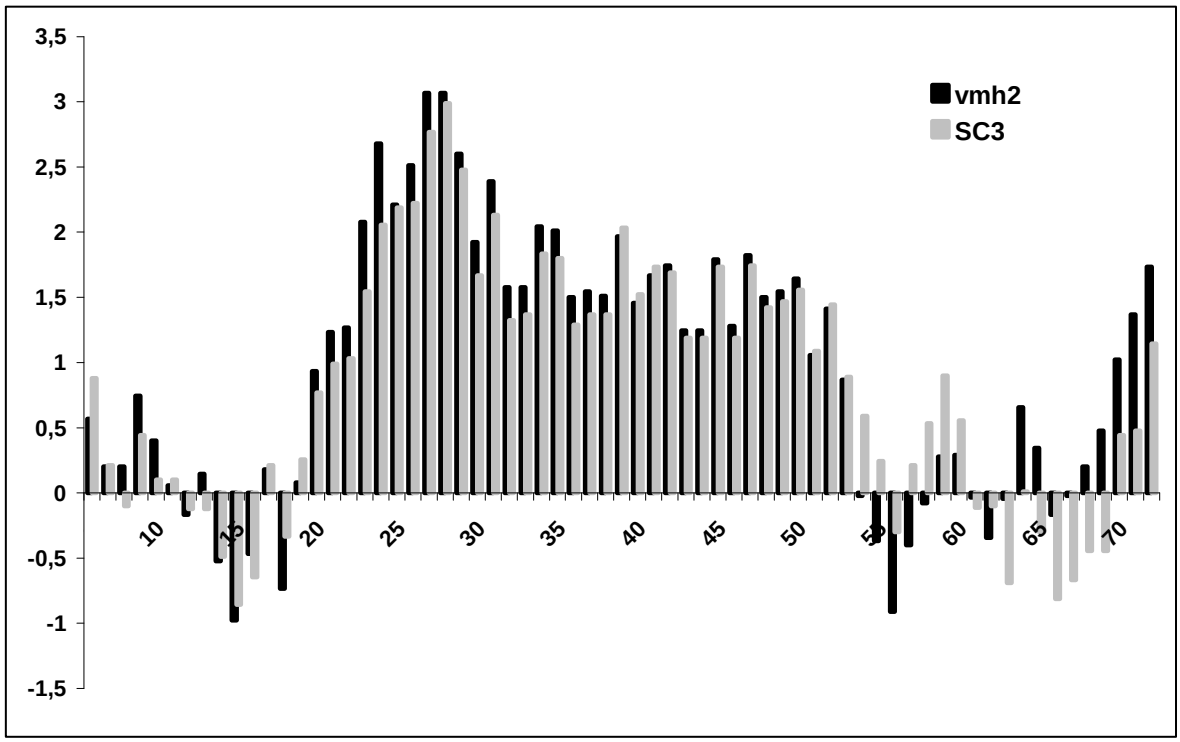

Figure 3.9 Hydropathy pattern of vmh2 and SC3 (starting from the first Cysteine) determined using the parameters of Kyte and Doolittle (114). Hydrophilic regions (- hydropathy index) are shown below the horizontal line; hydrophobic regions (+ hydropathy index) are shown above the horizontal line. Numbering represents the vmh2 and SC3 linear amino acid sequence.

3.1.5 Expression analysis

The expression of the hydrophobin in mycelia grown on PDY was studied using RNA samples extracted from mycelia withdrawn at various growth times (7, 10 and 16 days) from shaken cultures and used as template for RT-PCR. Specific hydrophobin cDNAs were amplified on this template under standard PCR conditions using primers designed on the 5' and 3' ends of the *vmh1, vmh2, vmh3* genes. These primers were designed using the TrEMBL sequences (accession number Q8WZI5(6); Q8WZI2(1); Q8WZI4(3)) of the three *P. ostreatus* hydrophobins from the vegetative mycelium.

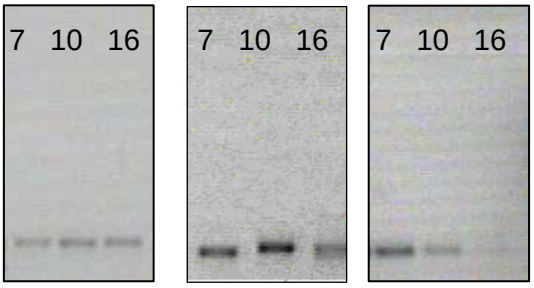

*Figure 3.10 Analysis of amplification at 7, 10 and 16 days of vmh1 cDNA (**a**), of vmh2 cDNA (**b**), of vmh3 cDNA (**c**) of grown in PDY broth.*

The cDNA coding for the hydrophobin, purified from vegetative mycelium, was amplified by PCR (fig. 3.10). This approach yielded a single DNA band at approximately 450 bp, for all primers used. In particular the level of *vmh2* expression was higher at 10 days culture time and *vmh3* became undetectable at longer culture times.

3.1.6 Heterologous expression

Recombinant expression of vmh2 from *P. ostreatus* has been performed using two different strains of *E. coli* as hosts (BL21PLYSS and BL21DE3) and two vectors with different proprieties. The vector pET-22b(+) produces the protein with an additional His-6 tag at the C-terminus while using the vector pETM-30 it is possible to produce the recombinant protein fused to glutathione S-transferase (GST) and an additional His-6 tag at the N-terminus. This construct should increase the solubility of the protein and should make for easy protein purification. Cleavage of the GST by means of the appropriate protease (TEV) can then give the recombinant protein. .
The *vmh2* cDNA was cloned into the two different vectors giving the plasmids pETM-ND1 e pET-ND2 in pETM-30 and pET-22b(+), respectively. Expression of the recombinant protein starts only after induction by IPTG, in this way it is also possible to express proteins toxic for the host microrganism.
Using the strain BL21PLYSS as host, no expression of heterologous protein for both the vector pETM-ND1 and pET-ND2 was observed. On the other hand using the strain BL21DE3, the SDS-PAGE analysis showed (fig. 3.11) the presence of the expressed protein at about 35 kDa (corresponding to the sum of 8.5 kDa for the mature hydrophobin, 26 kDa of GST and 822 Da of His-tag) when the vector pETM-ND1 was used and 3 hours after the induction, whilst the same band was not detected in any conditions using pET-ND2.

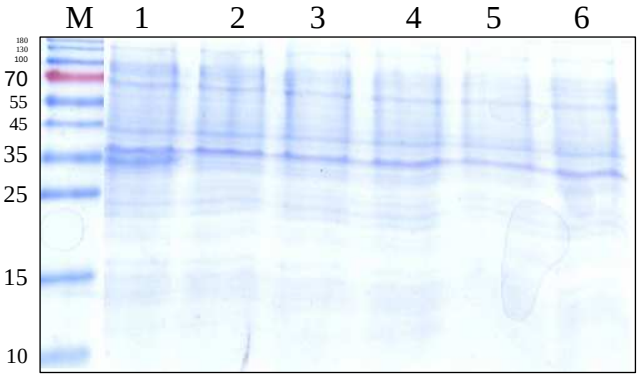

*Figure 3.11 SDS-PAGE analysis of the proteins extracted from BL21DE3 transformed with: pETM-ND1 (lanes 1-3) or pET-ND2 (lanes 4-6); lane 1 and 4: after 3 h of induction; lane 2 and 5 time zero; lane 3 and 6: without induction; M**:** marker.*

Different incubation temperatures (28℃ e 37℃), in duction times and concentrations of inductor (IPTG) have been analyzed to maximize the hydrophobin expression using pETM-ND1 and the strain BL21DE3 as host. SDS-PAGE analyses (Fig.3.12 a and b) show that the highest hydrophobin expression was obtained at 1mM IPTG and 37℃, without any difference between 3 hours or overnight incubations.

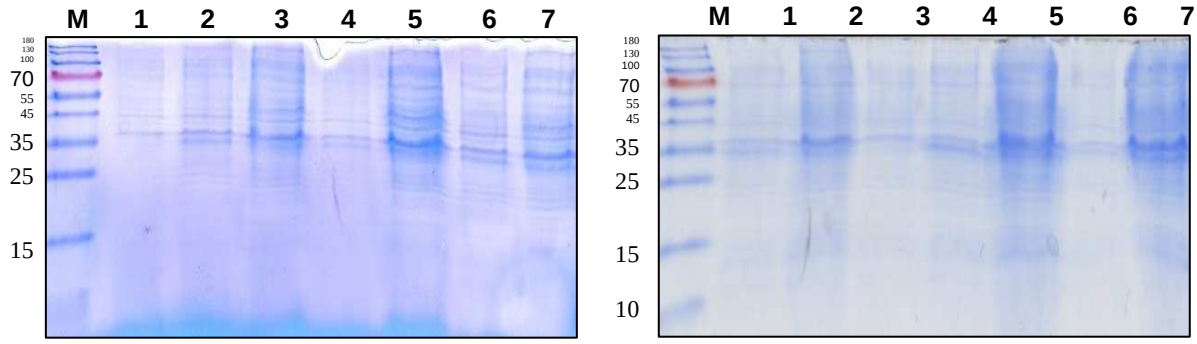

a **b**

Figure 3.12 SDS-PAGE analysis of the proteins expressed in different conditions ***a)*** *Induction at 37 ℃. M: marker; lane 1 : without induction; lane 2: induced with IPTG 0,4 mM, 3 h or overnight (lane 3); lane 4: induced with IPTG 0,7 mM, 3 h or overnight (lane 5); lane 6: induced with IPTG 1 mM, 3 h or overnight (lane 7);* ***b)*** *Induction at 28 ℃. M: marker; lane 1 : induced with IPTG 0,4 mM 3 h or overnight (lane 2); lane 3: without induction; lane 4: induced with IPTG 0,7 mM, 3 h or overnight (lane 5); lane 6: induced with IPTG 1 mM, 3 h or overnight (lane 7).*

The heterologous protein has then been extracted by bacteria grown in the conditions set up and its localization analysed by SDS-PAGE. This analysis showed that the heterologous protein is present in the inclusion bodies even if expressed as fusion protein with GST to increase its solubility (fig. 3.13).

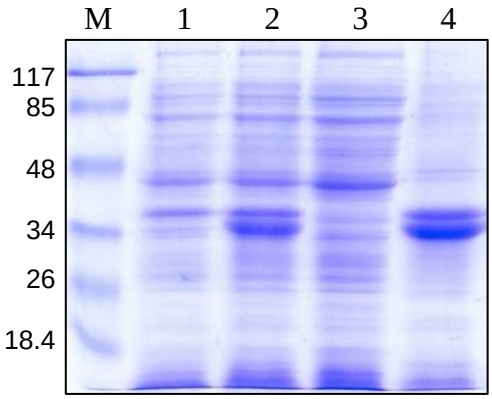

Figure 3.13 SDS-PAGE analysis of the heterologous protein samples. M: marker; lane 1: without induction; lane 2: induced with IPTG 1 mM, 3 h; lane 3: soluble part; lane 4: inclusion bodies.

The inclusion bodies have been dissolved in 8M urea. All the attempts aimed at purifying the protein by affinity chromatography using its His tag were unsuccessful because of the absence of interaction of the protein with the stationary phase (fig. 3.14).

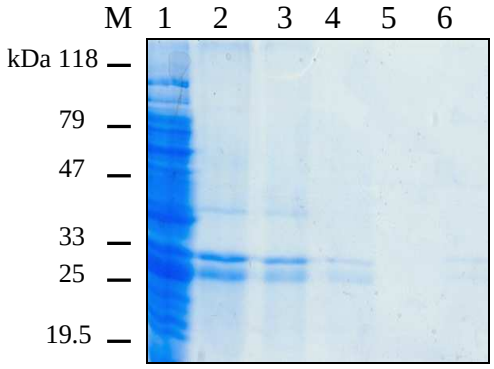

Figure 3.14 SDS-PAGE analysis of protein purification by affinity chromatography. lane 1: induced with IPTG 1 mM, 3 h; lane 2: loaded sample; lane 3: elution with loading buffer; lane 4: elution with washing buffer; lane 5: elution with D buffer; lane 6: elution with E buffer.

Therefore a protocol to purify inclusion bodies and extract the recombinant protein in 8M urea has been performed. Suitable buffers have been used to separate the recombinant protein from cellular debris and from other more soluble proteins. As it is shown in fig 3.15 this procedure allows a significant enrichment of the protein sample.

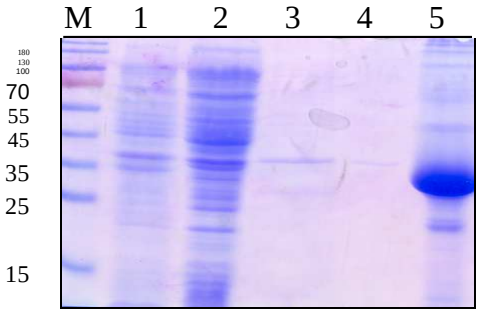

Figure 3.15 SDS-PAGE of the purification of inclusion body. M: marker; lane 1: induction with IPTG 1 mM, 3 h; lane 2: soluble of cellular lysis; lane 3: washing of soluble; lane 4: washing of soluble with buffer cellular lysis; lane 5: purified inclusion bodies.

However precipitation of the protein always occurred when the urea concentration was quickly reduced. A procedure leading to a soluble protein at 0.3M urea has been set up, slowly reducing urea concentration step by step and dialysing the sample versus buffer at decreasing urea concentration. Furthermore it has been demonstrated that the TEV protease is active in 0.3M urea. Therefore the soluble protein in 0.3M urea has been hydrolyzed by TEV. Different temperatures, enzyme concentrations and hydrolysis times were examined. The best conditions tested were to use 12,5 µM of enzyme, incubated at 30℃ for 24 hours. In the se conditions SDS-PAGE analysis shows the presence of a band at about 10 kDa (Fig. 3.16 lane 3) whilst the intensity of the band at 35 kDa corresponding to the fusion protein decreased.

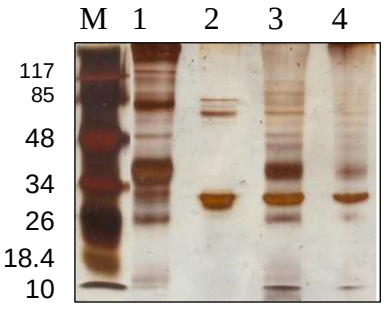

Figure 3.16. Silver stained SDS-PAGE analysis of the fusion protein hydrolysis. M: marker; lane 1: fusion protein; lane 2 TEV; lane 3: hydrolysis with 12,5 µM TEV, 30℃; lane 4 : hydrolysis with 12,5 µM TEV, 4 ℃.

Refolding of the protein was induced by incubation in the presence of the redox couple, reduced and oxidized glutathione. To purify the protein we thought to use its peculiar properties (owed to the properly refolded protein) in a similar way to that used for the purification of the native protein. Aggregation was induced by bubbling, then the protein was treated with TFA, dried and dissolved in 60% ethanol. This treatment has been repeated 3 times to improve the purification. SDS-PAGE of this sample shows an intense band at about 8000 Da (fig. 3.17).
The total amount of recombinant protein obtained from this expression system was estimated about 12 mg/litre of culture. This amount is slightly higher than that obtained from the *P. ostreatus* cultural broth (about 10 mg/litre) and very much lower than that extracted from *P. ostreatus* vegetative mycelium (60 mg/litre).

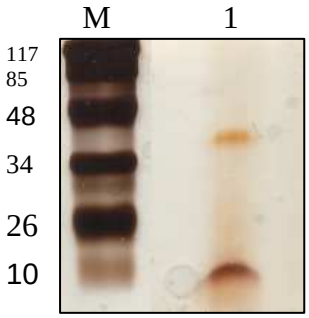

Figure 3.17. Purification of heterologous hydrophobin. M: marker; lane 1: purified protein.

3.2 Analysis of vmh2

Since hydrophobins are prone to interfacial self assembly during time or in response to external stimuli such as agitation of the solution, we have studied vmh2 behaviour in different conditions using different techniques.

3.2.1Analysis of vmh2 in ethanol solution

The pure protein was dissolved in 60% ethanol (Hyd-et). In this case, the protein concentration was estimated by absorbance at 280nm, because of the interference of ethanol in the BCA assay. No variation of this values as well as band intensities on SDS-PAGE was observed inducing aggregation by vortexing (fig 3.18) Protein concentration did not change, even up 20 days after sample dissolution (fig 3.18 and 3.20).

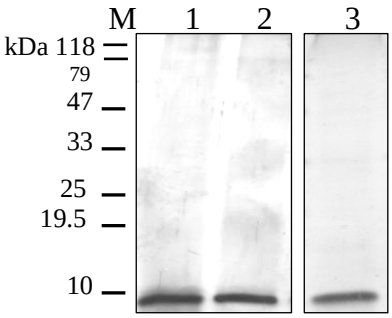

Figure 3.18 Silver stained SDS-page of Hyd-et (line 1) , after vortexing (line 2) and after 20 days (line 3).

The same amounts of pure hydrophobin (after glycans removal) were dissolved at different concentrations of ethanol (ranging from 20 to 80%) and protein concentration determined by measuring the absorbance at 280nm. As it is shown in fig. 3.19 a 70% reduction of the amount of the dissolved hydrophobin was observed at 20% ethanol, whereas lower solubility differences were observed in the range from 40 to 80% ethanol.

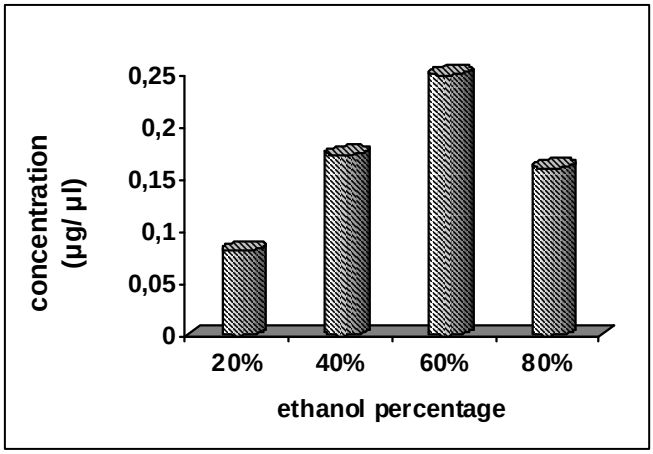

Figure 3.19 Hydrophobin concentration at different percentage of ethanol

Moreover, it is worth noting that, as shown in fig 3.20, the concentration of hydrophobin dissolved in 20% ethanol, (Hyd-20et) decreases over time, differently from that one dissolved in 60% ethanol,

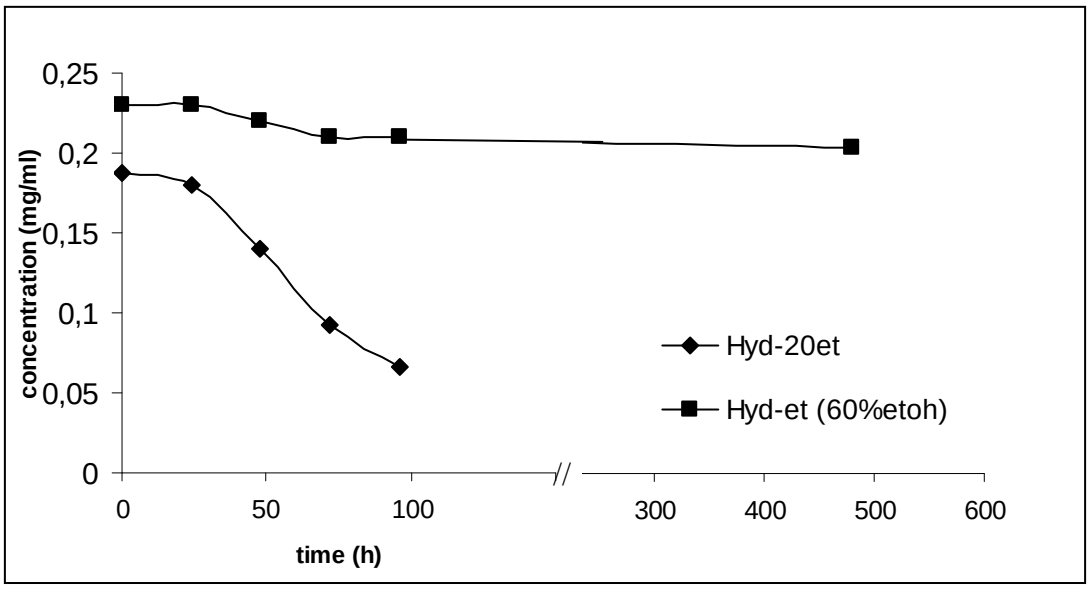

Figure 3.20 Analysis of hydrophobin concentration in aqueous solutions during time

3.2.2 Analysis of vmh2 in aqueous solution

Samples, prepared from PDY cultural broth (in the presence of glycans), were dissolved in water (Hyd-w) or in 50 mM ammonium bicarbonate pH 8 (Hyd-a). Protein concentration was tested by BCA assay and monitored during a 7 day period (fig. 3.21). Complete dissolution of Hyd-w needs at least one day, after that the protein concentration remains almost nearly constant. In the case of Hyd-a protein concentration decreased just after dissolution, indicating a main bias towards aggregation under this condition.

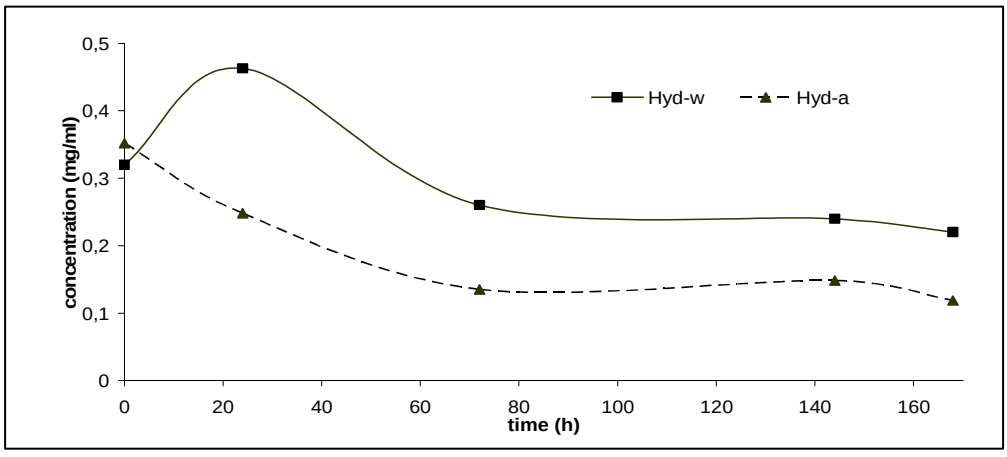

Figure 3.21 Analysis of hydrophobi concentra-tion in aqueous solutions over during time.

Hyd-w and Hyd-a concentrations were also evaluated during three days just after removal of the aggregates by centrifugation (fig. 3.22 a and b). After centrifugation, the protein concentration always decreased indicating the presence of aggregates in both these solutions. However the Hyd-a concentration decreased more quickly than Hyd-w.

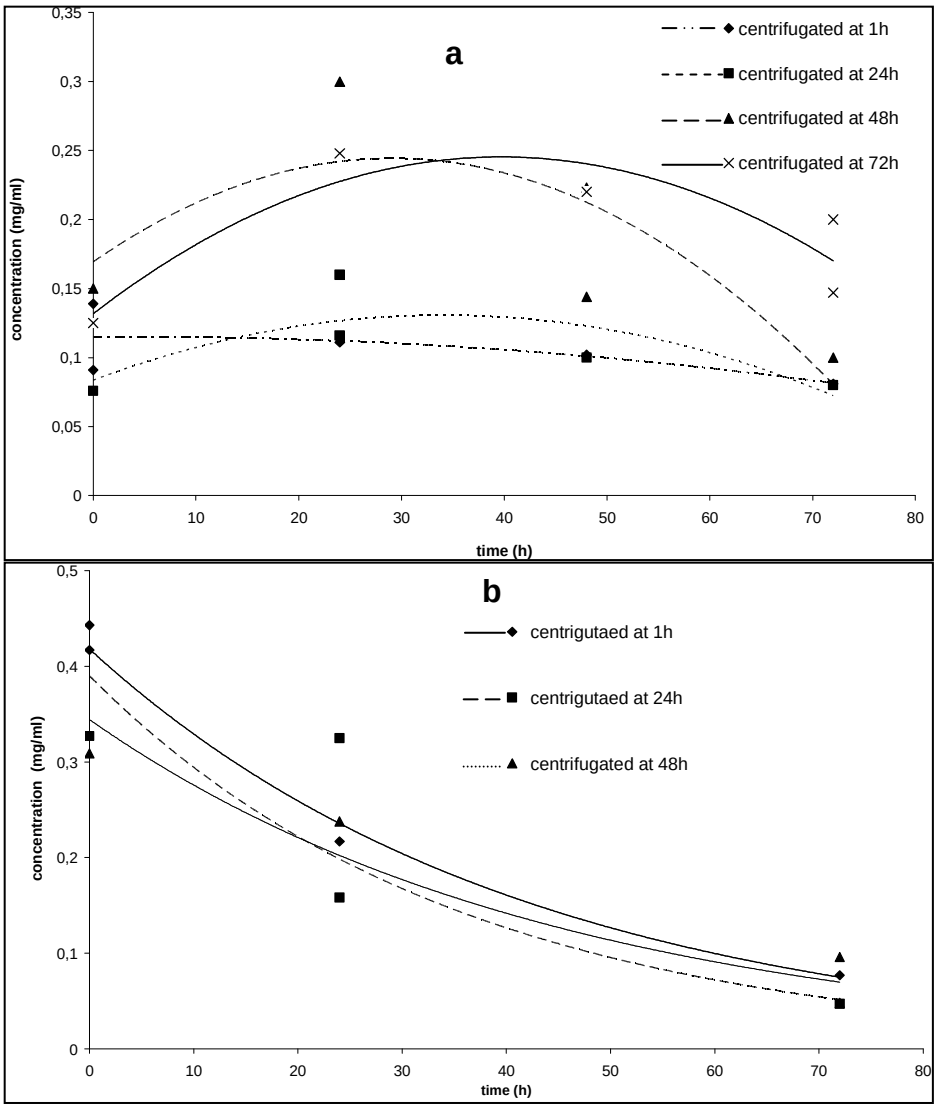

*Figure 3.22 (**a**) Analysis of concentration of hydrophobin dissolve in water after removal of aggregates by centrifugation over time (**b**) Analysis of concentration of hydrophobin dissolve in ambic after removal of aggregates by centrifugation over time.*

SDS-PAGE analysis of Hyd-w and Hyd-a after one and three days has been performed. A remarkable appearance of multimers was shown in the Hyd-a, whereas just a decrease of the intensity of the Hyd-w band was observed (fig. 3.23).

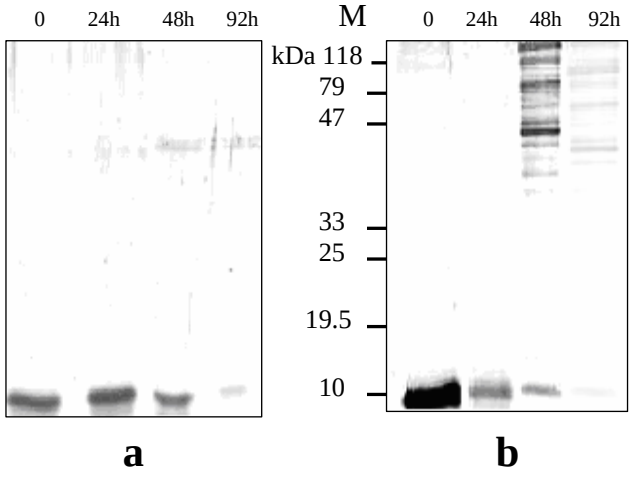

*Figure 3.23 Silver stained SDS-PAGE of Hyd-w (**a**) and of Hyd-a (**b**) at different time after dissolution.*

3.2.3 CD analyses

CD spectra of Hyd-et were recorded showing a significant contribution of α helixes to the structure of the protein. It is worth noting that no change of the spectrum was detectable after vortexing of these samples (fig 3.24).

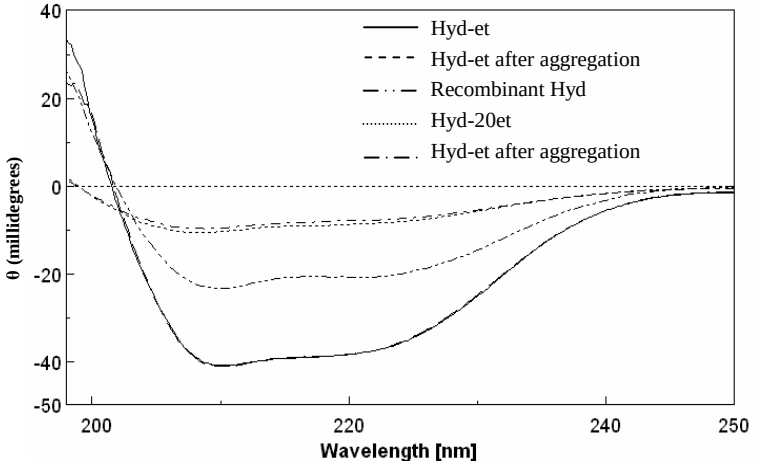

Figure 3.24 CD analysis of Hyd-et and of Hyd-20et before and after induction of aggregation (by vortexing). CD spectrum of recombinant hydrophobin is also shown.

A similar spectrum was also obtained for the recombinant hydrophobin dissolved in 60 % ethanol (fig. 3.24), thus confirming the occurrence of the proper folding of this protein.

The CD spectrum of hydrophobin in 20% ethanol (Hyd-20et) showed a profile similar to that of Hyd-et but at lower intensity. No variation of these parameters was observed after vortexing, as for Hyd-et in 60% ethanol (fig. 3.24).

Distinct spectra were observed for hydrophobin solubilised in water. CD spectra of Hyd-w and Hyd-a slightly varied from sample to sample (fig. 3.25) even when the same dried sample was apparently suspended in the same conditions. These differences could be due to the diverse amounts of glucans present in the powder withdrawn to prepare each sample. In all the samples, however, a significant contribution of random structure was noticed. Conformational changes with large shift towards β structure were observed after vortexing (fig. 3.25).

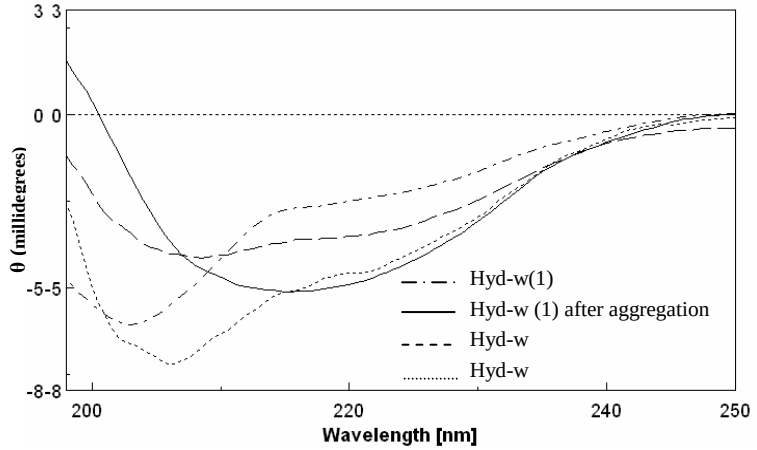

Figure 3.25 CD spectra of several samples of and one sample after vortexing (Hyd-w 1).

CD spectra of Hyd-w were also registered increasing temperature in the range from 30 to 90 ℃. A change of the secondary structure was observed between 80 and 90 ℃, similar to that observed when the aggregation process was induced by vortexing (fig. 3.26).

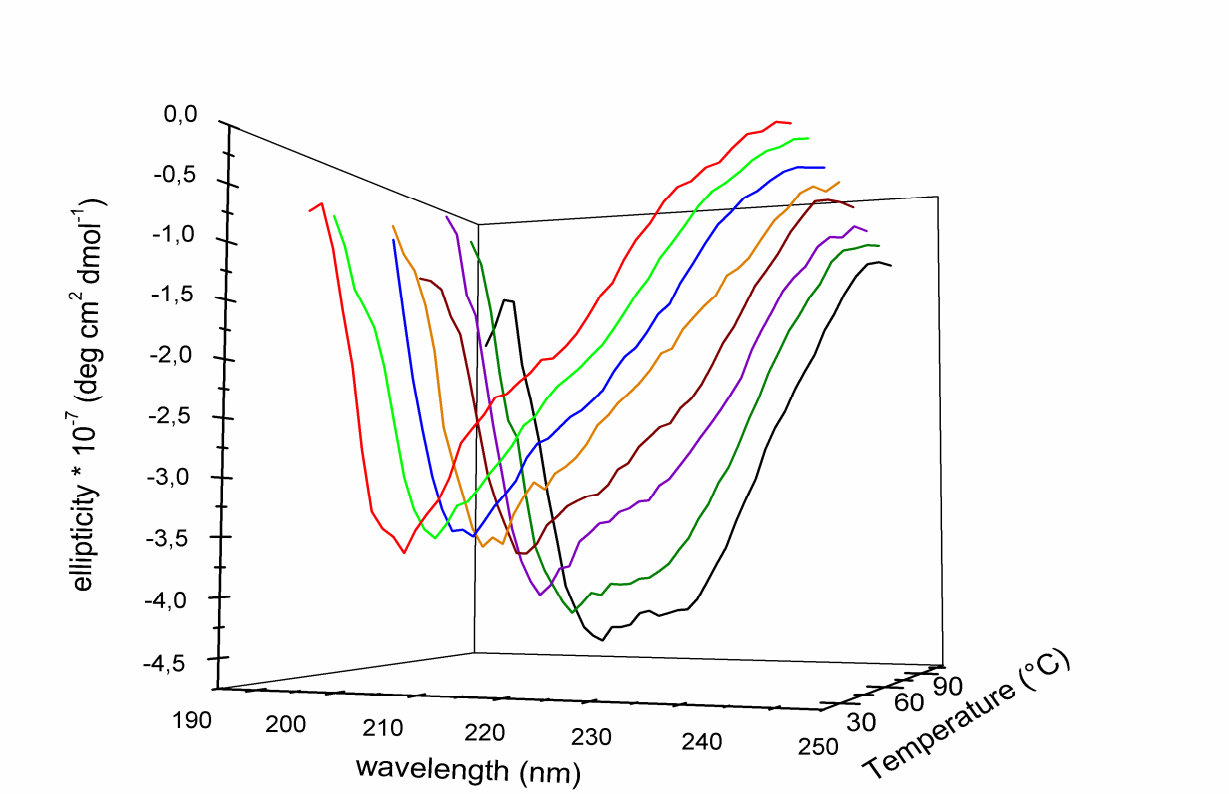

Figure 3.26 CD spectra of Hyd-w at different temperature.

3.2.4 FFF analysis

Field-flow fractionation (FFF) is a family of selective flow-assisted techniques suitable for the separation of nanometer-sized and micrometer-sized analytes of any origin (115,116). In FFF the absence of a stationary phase ensures there is no mechanical stress on macromolecular and particulate analytes, which could induce their degradation. In the last two decades many applications of FFF to biological samples have been reported, covering a variety of biomedical fields such as hematology, bacteriology, virology, molecular biology and cancer research, including the neurosciences 117).

Gravitational field-flow fractionation (GrFFF) is an analytical technique that belongs to the field-flow fractionation (FFF) family. It employs the Earth's gravitational field, applied perpendicularly to the mobile phase flow stream inside the channel, to fractionate a wide variety of particulate analytes in the micrometer size range. This technique is particularly suitable for protein, like hydrophobins, with high tendency toward aggregation. The absence of stationary phase make possible elution of the protein, avoiding the problems encountered and above reported when this protein is loaded on chromatography supports (118).

Preliminary analyses of the hydrophobin have been performed using GrFFF under different conditions, four days after sample dissolutions (fig. 3.27). These experiments have been performed in collaboration with prof. Pierluigi Reschiglian, Dept. Chemistry "G. Ciamician" University of Bologna, Italy.

The fractogram obtained for Hyd-et shows a band at low retention time, typical of species with hydrodynamic dimensions of about 3-4 nm, as the monomeric hydrophobin. The band present after the field release could be due to the presence of multimeric hydrophobin. As a matter of fact elution after the field release should be due to species of at least 30 nm of hydrodynamic dimensions.

The Hyd-w fractogram is similar to that of Hyd-et. The unique difference is the intensity of the bands: Hyd-et bands are more intense than that of Hyd-w, even if the same quantities of samples were used. This difference can be due to the lower solubility of the protein in water.
The fractogram of Hyd–a (Hyd in the presence of glycans dissolved in ambic) is really more interesting that the previous ones. This fractogram shows a more intense and larger band at an elution time higher than those observed for the other samples, The main band is typical of species with hydrodynamic dimensions of about 8 nm, corresponding to the dimension of hydrophobin oligomers. This result confirms those obtained from other analyses as protein concentrations and SDS-PAGE. As a fact the hydrophobins dissolved in ambic form aggregates during time as shown in fig. 3.22b and 3.23b.

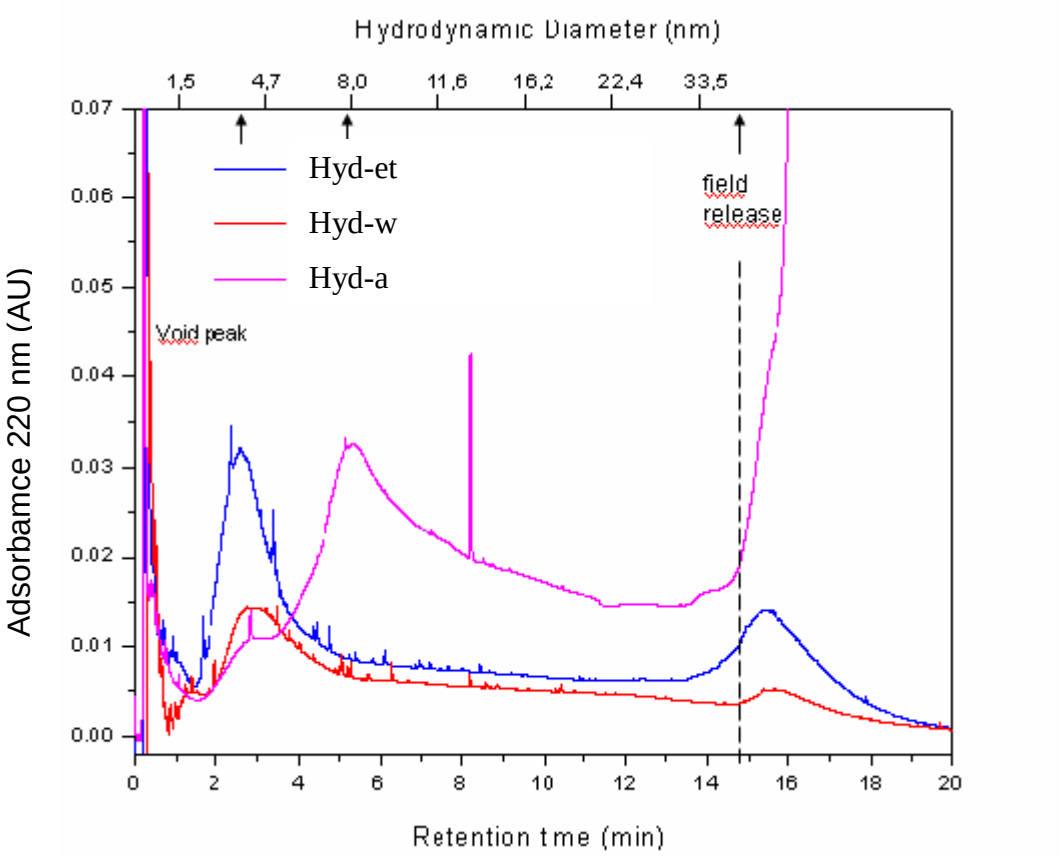

Figure 3.27 GrFFF of hydrophobin in different solutions (Mobile phase: water, pH 5.5).

3.3 Hydrophobin biofilm characterization

3.3.1 Biofilm on silicon

Silicon is the mostly used material in the world since it is at the basis of the microelectronic industry: all the integrated circuits in computers or in any electronic instrument are made of silicon based device (119). The commercial market requires more and more performances, mainly in terms of low cost and miniaturization, so that a continuous evolution of the technologies in micro and nanofabrication is assured. For these reasons, silicon is a very interesting platform due in all the devices that can be needed in medicine, security, defence and more. The new scientific revolution will be assured by the development of silicon based nanodevices which can be actually fabricated due to the deep degree of control in silicon machining. The integration of sensors, actuators and any other electronic or mechanical component together with the integrated circuit which can record, analyse and store data is a very attractive and fascinating field so that, in recent years both the industrial and academic fields have looked up to silicon as the natural platform on which develop the next generation of scientific instruments. A more futuristic approach is the integration of silicon with the organic world, not only from the polymers point of view but also in the case of biomolecules. Biosensors, i.e. sensors in which the active probe is a biological one (a DNA single strand, a protein, an enzyme, and so on), are a classical example where a biomolecule must be integrated in a silicon based microsystem (120,121). Another emerging field is that of molecular electronics, where molecules with specific electronic properties must be bound to the silicon surface. Lot of studies have been published in the past year (122) about the chemical functionalization of silicon in order to make it compatible with organic chemistry and only recently can be found in literature some attempts to use biological probes directly on silicon surface.
In this research perspective, we have studied the behaviour of a hydrophobin biofilm when deposited on a silicon surface. In our experiment the silicon acts as a substrate for non-covalent binding of hydrophobin.The hydrophobin biofilm has been studied by optical methods such as variable angle spectroscopic ellipsometry, a widely used optical technique to characterize thin films, and water contact angle technique, which defines the wettability of a surface. The conditions of hydrophobin deposition have been optimized as function of protein concentration, time and temperature of deposition. We found that the proteins biofilm is highly resistant to alkaline environment that are very corrosive for the silicon surface.
The details of these experiments are reported in

*<De Stefano L., Rea I., **Armenante A.**, Giardina P., Giocondo M., Rendina I., "Self-Assembled Biofilm of Hydrophobins Protects the Silicon Surface in the KOH Wet Etch Process" Langmuir 2007; 23(15): 7920-7922>*

These experiments were performed using Hyd-et, the pure protein dissolved in ethanol. Hyd-et forms a very stable biofilm on silicon whose thickness is 3.1±0.7 nm, whereas it did not stably interact with oxidized silicon, thus the biofilm was not detectable Moreover, the same kind of experiments were carried out with Hyd-w (the hydrophobin in the presence of glucans). In this case, the thickness of the biofilms were more variable and sometimes significantly higher than Hyd-et biofilm on crystalline silicon. These experiments are reported in "Armenante et al 2008". The Hyd-w biofilms thickness ranged from 3.5 to 30 nm on the silicon surface and from 6 to 38 nm on the oxidized silicon surface.

Self-Assembled Biofilm of Hydrophobins Protects the Silicon Surface in the KOH Wet Etch Process

Luca De Stefano,*[,†] Ilaria Rea,[†,‡] Annunziata Armenante,[§] Paola Giardina,[§] Michele Giocondo,[||] and Ivo Rendina[†]

Unit of Naples-Institute for Microelectronics and Microsystems, Via P. Castellino 111, 80131 Naples, Italy, Department of Physical Sciences and Department of Organic Chemistry and Biochemistry, University of Naples "Federico II", Via Cinthia 4, 80126, Naples, Italy, and LYCRIL − INFM-CNR, Via P. Bucci, Cubo 33/B, 87036 Arcavacata di Rende, Cosenza, Italy

Received April 24, 2007

The anisotropic wet micromachining of silicon, based on a water solution of potassium hydroxide (KOH), is a standard fabrication process that is extensively exploited in the realization of very complex microsystems, which comprise cantilevers, membranes, and bridges. A nanostructured self-assembled biofilm of amphiphilic proteins, the hydrophobins, was deposited on crystalline silicon by solution deposition and characterized by variable-angle spectroscopic ellipsometry (VASE). This procedure formed chemically and mechanically stable mono- and multilayers of self-assembled proteins. The biomolecular membrane has been tested as masking material in the KOH wet etch of the crystalline silicon. The process has been monitored by VASE and atomic force microscopy measurements. Because of the high persistence of the protein biofilm, the hydrophobin-coated silicon surface is perfectly protected during the standard KOH micromachining process.

Introduction

Recently, in the microelectronic and nanodevice fabrication field, increasing interest has been devoted to the utilization of nanostructured biological molecules purified by living organisms or synthesized in the laboratory. Hybrid organic−inorganic devices that exploit the best features of both worlds can be designed and realized, as in the case of biosensors, which are devices that use biological molecules as highly selective probes for target analytes.[1] Among all of the biological molecules that nature has optimized during life's history on earth, hydrophobins are particularly attractive because of their biophysical features. Hydrophobins are small proteins, constituted of 100−125 amino acids residues, which can be purified by filamentous fungi. These amphiphilic proteins can strongly adhere to hydrophobic or hydrophilic surfaces, have high surface activity, and self-assemble in membranes and biofilms.[2] Because of their very peculiar characteristics, hydrophobins have been recently proposed for many practical applications, ranging from antifouling to the fabrication of new biomaterials.[3] Hydrophobins are divided in two classes on the basis of the stability of the assembled biofilm: the class I hydrophobins form highly insoluble assemblies, which can be dissolved in strong acids, whereas class II biofilms can be dissolved in ethanol or in sodium dodecyl sulfate. The most studied hydrophobins are the SC3 hydrophobin from *Schizophyllum commune* (class I) and the HFBI and HFBII (class II) from *Trichoderma reesei*.[4] The biophysical properties of these proteins are also of interest in technological processes. In this work, we present the results of a specific technological application of the class I hydrophobin from the fungus *Pleurotus ostreatus* in the wet etch micromachining process of crystalline silicon based on potassium hydroxide (KOH), which could be of straightforward interest to the microelectronics industry.

Experimental Section

Protein Purification. White-rot fungus, *P. ostreatus* (Jacq.:Fr.) Kummer (type: Florida) (ATCC no. MYA-2306), was maintained through periodic transfer at 4 °C on potato dextrose agar (Difco) plates in the presence of a 0.5% yeast extract (Difco). Mycelia were grown at 28 °C in static cultures in 2 L flasks containing 500 mL of potato dextrose (24 g/l) broth with 0.5% yeast extract. After 10 days of fungal growth, hydrophobins released into the medium were aggregated by air bubbling using a Waring blender. Foam was then collected by centrifugation at 4000*g*. The precipitate was freeze dried, treated with trifluoroacetic acid (TFA) for 2 h, and sonicated for 30 min. The sample was dried again in a stream of air and then dissolved in 60% ethanol. After centrifugation, the supernatant was dried in a vacuum centrifuge (Speed-Vac Concentrator, Savant), treated with TFA again, and dissolved in water. The purity of the sample was ascertained by SDS-PAGE by using a silver staining method. Ethanol−deionized water (80/20% v/v) solutions containing 0.11 mg/mL of hydrophobins were used to rinse silicon and silicon oxide samples both by immersion and by drop covering. The two rinsing methods give the same results. Each sample has been rinsed for 1 h, dried for 10 min on the hot plate, and then washed by the same solution used for the deposition.

Analysis Techniques. Ellipsometric characterization of the hydrophobin biofilm deposited on the silicon substrate has been performed by a variable-angle spectroscopic ellipsometry (model UVISEL, Horiba-Jobin-Yvon). Ellipsometric parameters Ψ and Δ have been measured at an angle of incidence of 65° over the range of 360−1600 nm with a resolution of 5 nm. Fourier transform infrared spectroscopy (FTIR) spectra have been recorded by a Nicolet Continuμm XL (Thermo Scientific) equipped with a microscope. The depth of the KOH etch has been measured by a profilometer (KLA - Tencor P15) with a resolution of 1 nm. Optical images have been recorded by an optical microscope (Leica DM 6000 M) equipped with a 1.25× objective. Atomic force microscopy (Nanoscope, Digital Instruments) measurements have been performed in tapping mode over different areas of the treated samples.

* Corresponding author. E-mail: luca.destefano@na.imm.cnr.it. Tel: +390816132375. Fax: +390816132598.

† Institute for Microelectronics and Microsystems.

‡ Department of Physical Sciences, University of Naples "Federico II".

§ Department of Organic Chemistry and Biochemistry, University of Naples "Federico II".

|| LYCRIL − INFM-CNR.

(1) Craighead, H. *Nature* **2006**, *442*, 12.

(2) Hektor, H. J.; Scholtmeijer, K. *Curr. Opin. Biotechnol.* **2005**, *16*, 434.

(3) Wosten, H. A. B.; de Vocht, M. L. *Biochim. Biophys. Acta* **2000**, *1469*, 79.

(4) Szilvay, G. R.; Paananen, A.; Laurikainen, K.; Vuorimaa, E.; Lemmetyinen, H.; Peltonen, J.; Linder, M. B. *Biochemistry* **2007**, *46*, 2345.

10.1021/la701189b CCC: $37.00
Published on Web 06/20/2007 PAGE EST: 2.5

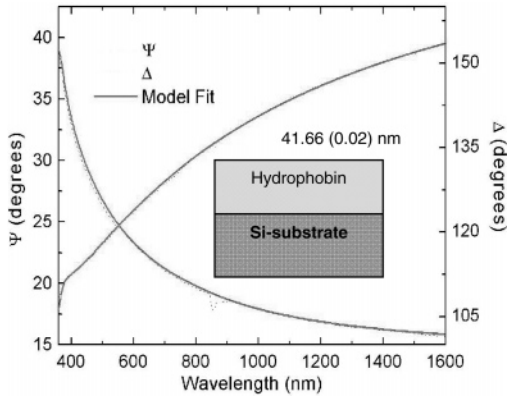

Figure 1. Optical model and fit of ellipsometric parameters Ψ and Δ used in the biofilm thickness determination.

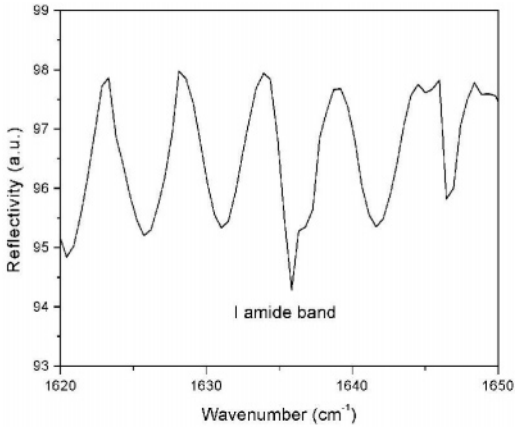

Figure 2. FTIR spectrum of the hydrophobins after assembling on the intrinsic crystalline silicon surface.

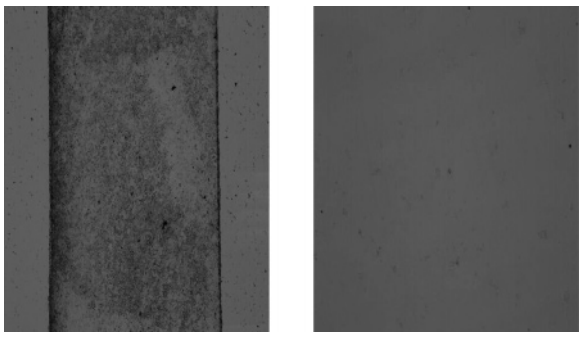

Figure 3. Optical photographs of the silicon chips after the KOH wet etch: (left) a 700 nm etched dig on unprotected crystalline silicon; (right) an unetched silicon surface protected by the hydrophobin biofilm.

Results and Discussions

It is well known that the amphipathic biofilm of hydrophobins that self-assembled at a hydrophobic/hydrophilic interface can be disassembled only by treatment with a strong acid such as trifluoroacetic acid.[5] In our experiment, thin films of *P. ostreatus* hydrophobin were prepared from aqueous solutions using adsorption followed by a drying stage on a hot plate at 80 °C. The biofilm was deposited on two different surfaces: crystalline silicon and oxidized silicon. The first one, after being rinsed in pure hydrofluoridic acid, exhibits hydrophobic behavior, whereas the second one is completely hydrophilic. The thickness of the self-assembled hydrophobin biofilms was determined by variable-angle spectroscopic ellipsometry, which can estimate with high precision the physical parameters of thin organic and inorganic layers.[6] We have verified that step-by-step deposition allows the assembling of biofilms of increasing thicknesses: after three consecutive depositions, for a total time of 3 h, we have obtained biofilms assembled on crystalline silicon of up to 40 nm thick, that is, thicker than those reported in literature.[7] In Figure 1, we show the measured value of the ellipsometric parameters and the optical model used to fit them: in the inset, the estimated thickness values of the biofilm are also reported.

By optical characterization, we discovered that the same deposition procedure of hydrophobins on silicon oxide also produces an assembled biofilm that is thinner than in the case of crystalline silicon. In the case of thermal silicon dioxide (72 nm), the biofilm reached a maximum thickness of about 20 nm. This different behavior can be ascribed to the greater number of hydrophobic residues present on the outer portion of the protein that better promotes the hydrophobic interaction. The adhesion characteristics of the hydrophobin biofilm have been studied by washing the samples in 2% sodium dodecyl sulfate (SDS) at 100 °C for 10 min and in 0.1 M sodium hydroxide (NaOH) solution for 10 min.[5] Rinsing in the SDS solvent removes on average 85% of the biofilm, whereas the basic solution removes only 42% of the hydrophobin layer. The hydrophobin film is formed via strong noncovalent interactions among these small proteins. Therefore, peculiar properties of their assembly can be ascribed solely to hydrophobin amino acid sequences and consequently to their 3D structures. The high persistence of the hydrophobin film on the silicon surface is due to its characteristic assembly in β-sheet structures, as confirmed by the presence of the amide I band at 1636 cm^{-1} in the FTIR spectrum[5] reported in Figure 2. The sinusoidal modulation in the FTIR spectrum is due to the reflections from the bottom of the intrinsic silicon wafer, which is 400 μm thick.

Because the protein biofilm is not removed from the silicon surface on exposure to the basic solution, we started to study the protection grade against the standard chemical etch solution for crystalline silicon, KOH. We have found that the hydrophobin biofilm, even if thinned, perfectly protects the silicon surface. To this aim, we have thermally oxidized a silicon wafer because silicon dioxide is a good masking material for KOH wet etches. Then, we removed the oxide (130 nm thick) in a controlled area by highly concentrated HF and exposed the wafer to KOH (water solution 1:2 w/w) at 80 °C in a thermostated bath for 30 s. Under this condition, the KOH etch rate is 1400 nm/min. A twin sample, with the crystalline silicon area covered by the hydrophobin self-assembled biofilm, has been immersed in the KOH bath under the same conditions.

In Figure 3, the optical photos of the two silicon samples after this treatment are shown: on the left the etched surface is clearly visible whereas in the right image the surface is perfectly homogeneous.

This qualitative result is quantitatively confirmed by ellipsometric and profilometric measurements: an 8.40 (0.05) nm biofilm of hydrophobins is still optically detected by the ellipsometer and the profilometer cannot detect any dig into the hydrophobins shielded sample, as can be seen in Figure 4. We

(5) de Vocht, M. L.; Scholtmeijer, K.; van der Vegte, E. W.; de Vries, O. M. H.; Sonveaux, N.; Wösten, H. A. B.; Ruysschaert, J.; Hadziioannou, G.; Wessels, J. G. H.; Robillard, G. T. *Biophys. J.* **1998**, *74*, 2059.

(6) Azzam, R. M. A.; Bashara, N. M. *Ellipsometry and Polarized Light*; Elsevier Science Publishers B.V.: Amsterdam, 1988.

(7) Misra, R.; Li, J.; Cannon, G. C.; Morgan, S. E. *Biomacromolecules* **2006**, *7*, 1463.

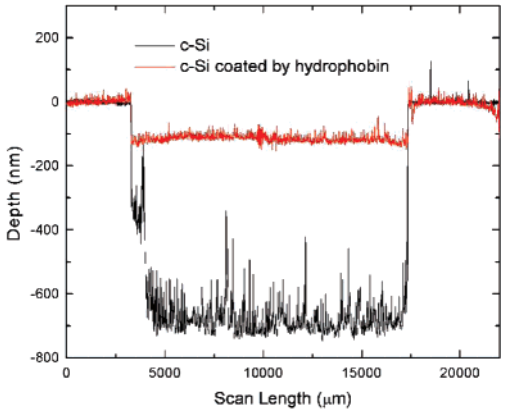

Figure 4. Thickness profiles measured by the profilometer for both samples.

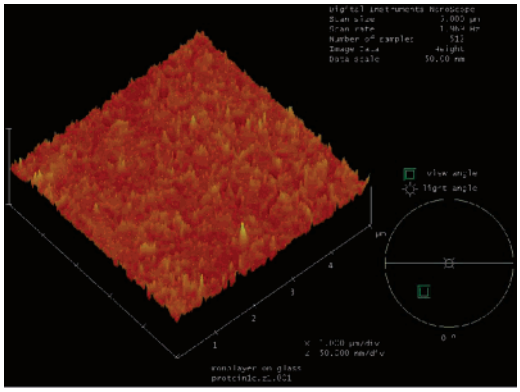

Figure 5. AFM height image of a hydrophobin-coated sample.

have also verified how long the self-assembled biofilm defends the silicon surface against the KOH wet etch: prolonged exposure of the protein-coated wafer decreases the biofilm thickness down to 5 nm, and then the film is stable, at least on the time scale of 20 min.

We believe that this value is probably the one corresponding to a monolayer of proteins assembled as a film on the silicon surface. The homogeneity of the residual surface is also confirmed by AFM measurement, as reported in Figure 5.

In all the explored areas, the protein layer is compact, and no hole in the layer can be observed. Because of the simplicity of the hydrophobin deposition, effective shielding against prolonged exposure to KOH can be obtained by spotting the protein solution over the masked areas before continuing the etching process.

Following the same experimental procedure, we have also studied whether the hydrophobin film could protect the silicon dioxide against the HF wet etch. In this case, the proteins are only partially successful: a 72 nm layer of silicon dioxide is completely removed in 5 min by a 1:10 HF−water solution at room temperature, whereas 21 nm of silicon dioxide is still present on a protein-masked sample.

Conclusions

We have demonstrated that biological matter can be fruitfully used in a relevant fabrication process, such as the KOH wet etch, which is the basis of the silicon micromachining techniques. Furthermore, the heterologous expression of these biomolecules will allow us to describe the basis for the achievements of modified proteins with improved characteristics in terms of surface interaction.

LA701189B

3.3.2 Infiltration of Biofilm on porous silicon

Porous silicon (P-Si) is a silicon-related material which can be produced from doped crystalline silicon by the electrochemical dissolution in a water solution of fluoridic acid and ethanol (122). Porous silicon can be used as smart transducer material in sensing application, and in particular in the detection of vapors, liquids and biochemical molecules (123). In fact, on exposure at chemical substances, several physical quantities, such as refractive index, photoluminescence, and electrical conductivity, change drastically. A key feature of a physical transducer, being sensitive to organic and biological molecules, either in vapor and liquid state, is a large surface area: PSi has a porous sponge-like structure with a specific area of the order of 200 - 500 m^2 cm^{-3}, so that it can assure a very effective interaction with several adsorbates. Moreover, porous silicon is an available, low cost material, compatible with standard integrated circuits processes, so that it could usefully be employed in the realization of smart sensors and microsystems. A scanning electron microscope image of a cross-sectioned sample of porous silicon is shown in figure 3.28. Unfortunately, the surface of the porous silicon as it has produced is highly hydrophobic so that aqueous solution can not infiltrate the sponge like matrix. A proper passivation process must be applied to stabilise the surface and to covalently link the bioprobe. Another important drawback of porous silicon as optical biosensor transducer is that porous silicon is rapidly dissolved in basic environment which are typical of biological solution.

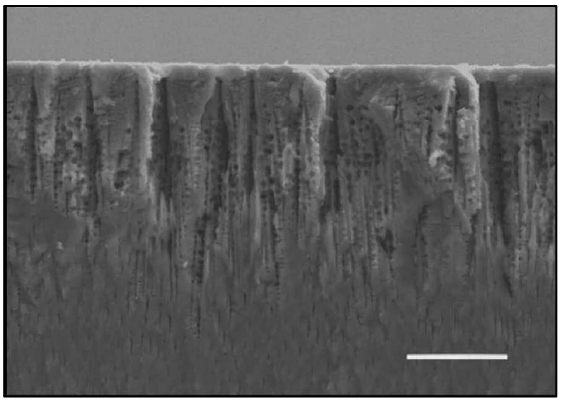

Figure 3.28 Scanning electron microscopy image 27of a cross section of porous silicon which shows the high porosity of the sample. The scale bar is 1 mm.

We have studied the infiltration by adsorption of Hyd-et in PSi monolayers and multilayers and on oxidized P-Si. The condition of hydrophobin deposition optimized on cSi were also used for P-Si. We have found that P-Si can be efficiently protected against NaOH by the hydrophobin biofilm penetrated into the nanometric pores. The details of these experiments are reported in:

*<De Stefano L., Rea I., Giardina P., **Armenante A.**, Rendina I., "Protein-Modified Porous Silicon Nanostructures" Advanced Materials 2008; 20(8): 1529-1533>*

DOI: 10.1002/adma.200702454

Protein-Modified Porous Silicon Nanostructures

By *Luca De Stefano,* Ilaria Rea, Paola Giardina, Annunziata Armenante,* and *Ivo Rendina*

Porous silicon (PSi) is really a very versatile material owing to its peculiar morphological, physical, and chemical properties: evidence of this is the huge number of papers about PSi features and devices based on this nanostructured material that appear in the literature every year. One reason for this clear success is the easy fabrication of sophisticated optical multilayers, such as one-dimensional (1D) photonic crystals, by a simple, but not trivial, computer-controlled electrochemical etching process.[1,2] The reflectivity spectrum of the photonic crystals shows single or multiple resonances,[3] band-gap and other characteristic shapes, depending on the spatial arrangement of the porous layers,[4] which are very useful in a great many applications, from biochemical sensing to medical imaging. The major drawback of the ''as etched'' PSi is its chemical instability: it is well known that the hydrogen-terminated PSi surface is slowly oxidized at room temperature by atmospheric oxygen, resulting in a blue shift of the optical spectrum because the oxide has a lower refractive index than the silicon.[5] Moreover, it has been shown that a PSi wafer can be dissolved under the physiological conditions that are very often used in biological experiments.[6] A large number of chemical and technological methods for the passivation of the PSi surface have been proposed to overcome the spontaneous thermodynamic oxidation and to obtain small particles with the same properties as the photonic crystal but with improved chemical and mechanical stability.[7,8] In the work reported here, we have covered the PSi surface with a highly stable and resistant biofilm resulting from the self-assembly of hydrophobins (HFBs).[9–11] HFBs are a family of small and cysteine-rich fungal proteins produced in the hyphal cell walls that can be purified by the culture medium. The HFBs self-assemble into thin, amphiphilic membranes at hydrophilic/hydrophobic interfaces. If the membrane is transferred onto a substrate, the wettability of this surface can be controlled and hydrophobic behavior can be converted into hydrophilic behavior, and vice versa.[12–14] A general classification of HFBs is made on the basis of the biofilm resistance: class I HFBs form highly insoluble assemblies, which can be dissolved only in strong acids, whereas class II biofilms can be dissolved in ethanol or in sodium dodecyl sulfate (SDS).[9] We have studied the infiltration by adsorption of the class I HFB from the fungus *Pleurotus ostreatus* in PSi monolayers and multilayers. Solutions with various concentrations of HFB have been used at different temperatures and the process has been monitored by variable angle spectroscopic ellipsometry (VASE) measurements.[15] Once this process has been optimized, the protein-coated surface of the PSi takes advantage of the HFB properties, gaining chemical stability and variable wettability. In Figure 1 is reported the VASE characterization of a 514 nm PSi monolayer of about 76 % porosity as etched (A) and after HFB infiltration (B). Because of the hydrophobic interaction, the HFBs penetrate the whole stack, accumulating at the bottom, where the hydrogen concentration is higher since the hydrostatic pressure stops air penetration. The HFB biofilm, when self-assembled on planar crystalline silicon, measures about 2–3 nm after the standard washing procedure with sodium hydroxide and SDS.[16] These values are compatible with the size dimension of the mesoporous material, ranging from 5 to 30 nm.[17]

This nanometer-scale organic layer is able to modify strongly the wettability of the PSi surface: after the electrochemical etching process, the PSi is highly hydrophobic (see Fig. 2a), resulting in a water contact angle value of 131 °, while after HFB infiltration the same surface shows a hydrophilic behavior and the water contact angle is reduced to 62 ° (Fig. 2b).

Following the same procedure, it is possible to turn the highly hydrophilic surface of the oxidized PSi into a slightly hydrophobic one, as demonstrated by the images in Figure 3a and b. The ability to switch between two different wettability regimes could be a key feature in designing bioactive interfaces for miniaturization not only of biosensors but also of medical devices.[13]

We have recently demonstrated that a nanometric biofilm of HFB, self-assembled on planar crystalline silicon, acts as a perfect mask material during a standard wet etching process based on potassium hydroxide (KOH).[16] Encouraged by these results, we have tested the shielding ability of the HFB biofilm against the etching ability of NaOH, when self-assembled on the internal surface of PSi monolayers and multilayers.

In Figure 4 we report the results of ellipsometric measurements to compare the dissolution rate of two PSi twin monolayers (thickness 465 nm, porosity 72 %), one protein coated and

[*] Dr. L. De Stefano, I. Rea, Dr. I. Rendina
Naples Department, Institute for Microelectronics and Microsystems, CNR Via P. Castellino 111, 80131 Napoli (Italy)
E-mail: luca.destefano@na.imm.cnr.it

I. Rea
Department of Physical Sciences
University of Naples ''Federico II''
Via Cinthia 4, 80126 Naples (Italy)

Prof. P. Giardina, A. Armenante
Department of Organic Chemistry and Biochemistry University of Naples ''Federico II''
Via Cinthia 4, 80126 Napoli (Italy)

ADVANCED MATERIALS

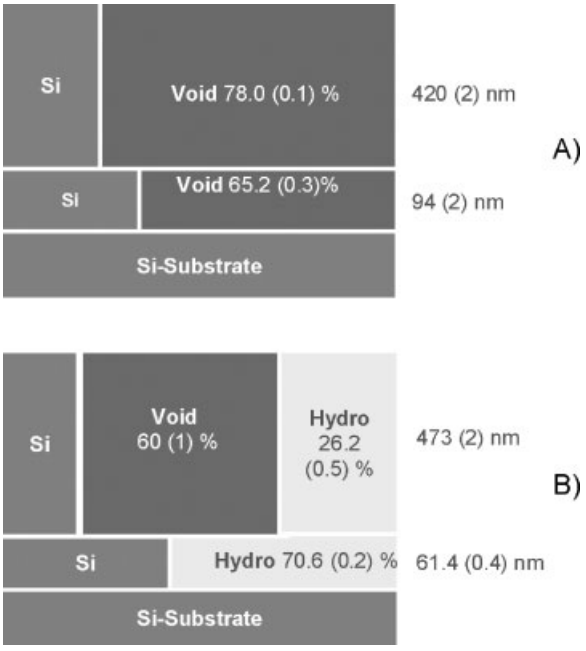

Figure 1. The ellipsometric model of HFB infiltration in a PSi monolayer. A) The PSi monolayer as etched is characterized by a vertical void distribution. B) Also in the protein-modified PSi monolayer the biological matter shows a nonuniform distribution throughout the sample.

the other bare, on exposure to a NaOH 0.1 M (pH 12.5) water solution for equal times. We characterized both the samples by VASE at the same time intervals, so that we can directly assess the competition between the oxidation and the dissolution processes. We have never witnessed the formation of an oxide layer on either sample, but only a reduction of the film thickness together with an increase of porosity. In particular, the thickness of the coated sample (black curve) changes by about 4%, while in the case of the bare sample (red curve) the change is about 81% in the same time interval. The possibility of imparting strong chemical stability to the PSi without modifying its intimate structure is even more intriguing in the case of PSi-based photonic crystals, which are almost ideal transducers in chemical and biological sensing experiments. Furthermore, the protein nanometer-scale biofilm is completely transparent from ultraviolet to near-infrared wavelengths (data not shown here) so that it is perfectly compatible with optical applications. We have thus infiltrated a PSi optical microcavity (PSMC), which is constituted by a Fabry-Perot interferometer between two Bragg mirrors (details in the Experimental section), with HFB solution.

In this case, as ellipsometry is not well suited to analyzing such thick, multilayered samples,[15] we used spectroscopic reflectometry.[18] The reflectivity spectra of two PSMCs, one coated by the HFB protein, and the other bare, have been recorded by an optical spectrum analyzer. In Figure 5 we report the optical spectra of the two samples for a rapid comparison. On exposure to a 0.1 M aqueous solution of sodium hydroxide, the protein-coated microcavity undergoes a blue shift of about 329 nm, due to the removal by NaOH dissolution of some unprotected silicon nanocrystallites, while in the same time interval the uncoated sample is completely dissolved: the unmodulated continuous line at the bottom of panel A reproduces the source spectrum; in contrast, the plot in panel B retains the initial characteristic shape of the microcavity. Even if blue-shifted, the optical spectrum still shows a reflectivity stop band of about 50 nm with a well-defined transmission defect inside. We also exposed the coated PSMC to sodium phosphate (20 mM, pH 8) and Hepes (pH 7.5) buffer solutions, which are often used in biological experiments, to test the chemical stability of the PSi structure in these standard environments. The PSMC was immersed in the solutions for 1 h and was analyzed every 10 min: the optical spectrum of the PSMC remained unchanged in all tests.

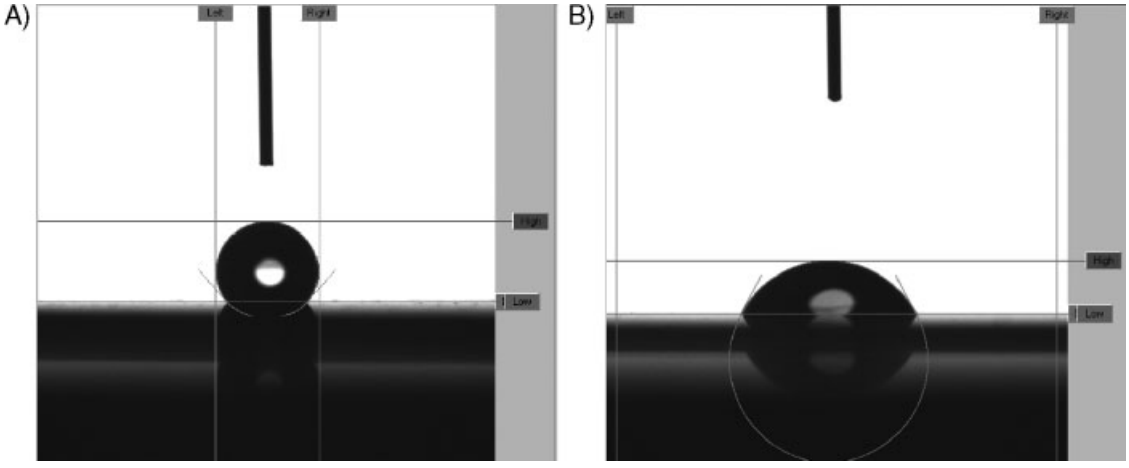

Figure 2. Changing the wettability of PSi. The HFB nanolayer turns the hydrophobic surface of PSi into a hydrophilic one. A) A water drop on the as-etched PSi has a contact angle of 131°. B) After HFB infiltration a water drop has a contact angle of 62°.

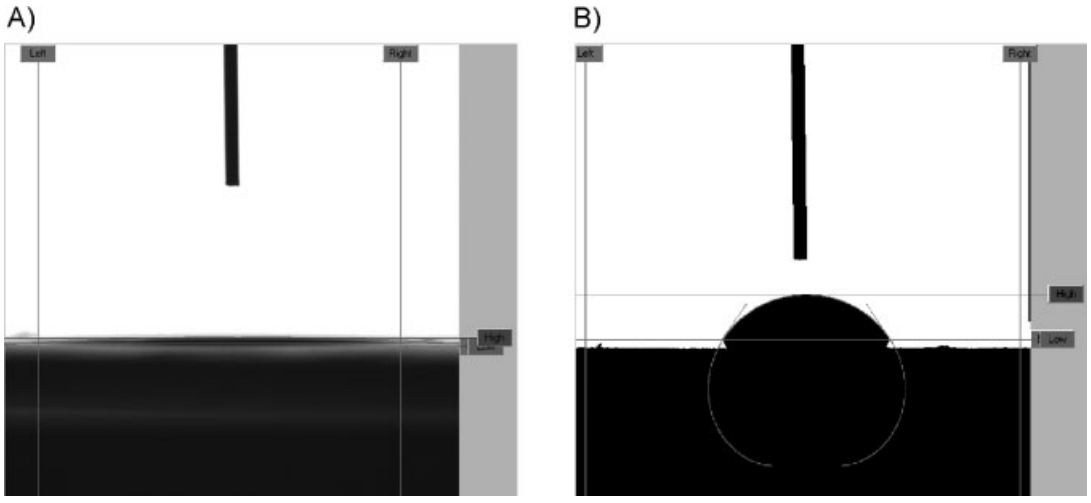

Figure 3. Changing the wettability of oxidized PSi. The HFB nanolayer turns the hydrophilic surface of oxidized PSi into a hydrophobic one. A) A water drop on oxidized PSi has a contact angle of 6°. B) After HFB infiltration a water drop has a contact angle of 57°.

After the basic etching process the hybrid organic/inorganic device still works as a chemical optical transducer: we have proved its ability to sense vapors of different volatile substances. In Figure 6a, we report the characteristic red shifts due to the capillary condensation of the vapors inside the nanometric pores of the PSMC. The red shift, due to the presence of a single gas, is completely reversible when the gas is replaced by air, and the protein-coated microcavity can be used for at least a month (we checked it before and after August 2007) with different substances giving highly reproducible results. We have also calculated the sensitivity of this optical transducer to refractive index changes by exposing it to substances having different refractive index. Assuming that the four solvents equally penetrate the nanostructured spongy multilayer, we estimated a sensitivity of 459(3) nm expressed in refractive index units.[4]

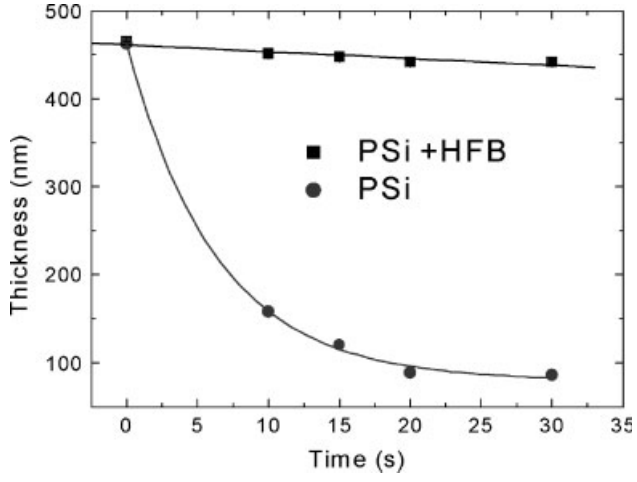

Figure 4. The HFBs protect the PSi against dissolution in basic solutions. A layer of a protein-modified PSi sample is very slowly etched, while the noninfiltrated PSi layer is greatly reduced on the same time scale.

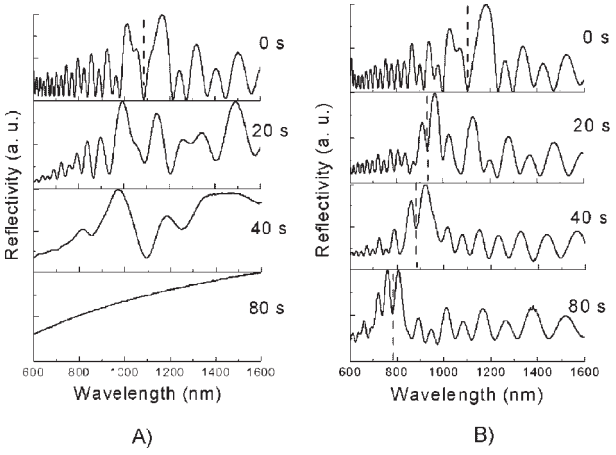

Figure 5. Owing to the nanometer dimensions of the HFB layer, these proteins can self-assemble also inside the pores of a thick PSi vertical structure such as a microcavity, which protects the microcavity from etching by NaOH solution. A) Noninfiltrated PSi microcavity. B) Protein-modified PSi microcavity.

In conclusion, we have demonstrated the biological passivation of some optical devices based on PSi technology when infiltrated by fungal proteins called HFBs. The self-assembled protein biofilm changes the wettability of the PSi structures. Moreover, this protein membrane not only protects the nanocrystalline material from basic dissolution in NaOH, but also leaves unaltered the sensing ability of such an optical

ADVANCED MATERIALS

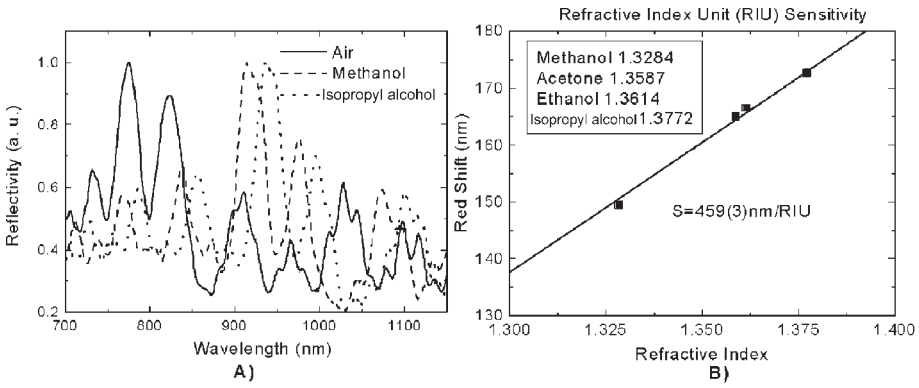

Figure 6. The protein-modified PSi microcavity still works as an optical transducer for vapor and liquid detection. A) The characteristic red shifts of the optical spectrum on exposure to methanol and isopropanol. B) Determination of the sensitivity of the optical transducer to refractive index changes.

transducer, adding chemical stability, which can be key in biomolecular experiments.

Experimental

Protein Purification and Deposition: White-rot fungus, *Pleurotus ostreatus* (Jacq.:Fr.) Kummer (type: Florida) (ATCC no. MYA-2306) was maintained through periodic transfer at 4 °C on potato dextrose agar (Difco) plates in the presence of 0.5% yeast extract (Difco). Mycelia were grown at 28 °C in static cultures in 2 L flasks containing 500 mL potato dextrose (24 g L^{-1}) broth with 0.5% yeast extract. After 10 d of fungal growth, HFBs released into the medium were aggregated by air bubbling using a Waring blender. Foam was then collected by centrifugation at 4000*g*. The precipitate was freeze-dried, treated with trifluoroacetic acid (TFA) for 2 h, and sonicated for 30 min. The sample was dried again in a stream of air, and then dissolved in 60% ethanol. The purity of the sample was ascertained by SDS polyacrylamide gel electrophoresis (SDS-PAGE), using a silver-staining method. Ethanol/deionized water (20%/60% V/V) solutions containing 0.11 mg mL^{-1} of HFBs were used to rinse PSi and oxidized PSi samples both by immersion and by drop covering. In the latter case, a high ethanol concentration assures the HFB solution penetration in the hydrophobic PSi. Even though the two rinsing methods give the same results, having available a sufficient quantity of proteins we adopted the immersion procedure as standard. Each sample was rinsed for 1 h then dried for 10 min on a hotplate at 80 °C and washed in the same solution as used for the deposition.

Fabrication of PSi Structures: The PSi Fabry–Pérot film, which acts optically as an interferometer, was fabricated by the electrochemical etching of p^+-type (100) crystalline silicon (resistivity 8–12 mΩ cm) in HF/EtOH (30:70) solution. The etching current had a value of 62 mA cm^{-2} and was applied for 2.6 s. The multilayer structure fabricated for this study was a PSi optical microcavity constituted by a $\lambda/2$ Fabry–Pérot optical resonator sandwiched between two Bragg reflectors of nine periods, each one realized by alternating layers with high and low refractive indices. The PSMC was obtained by electrochemical etching in a HF-based solution (50 wt % HF/ethanol, 3:7) in the dark at room temperature. A current density of 39 mA cm^{-2} was applied for 1.1 s to a highly doped p^+-type standard silicon wafer, ⟨100⟩ oriented, 10 mΩ cm resistivity, 400 μm thick, to produce the high refractive index layer (with a porosity of 69%), while a current density of 94 mA cm^{-2} was applied for 1 s in the case of the low index layer (with a porosity of 76%). The $\lambda/2$ layer is a high refractive index one. This structure has a characteristic resonance peak at 1024 nm in the middle of a 207 nm broad stop band.

Analysis Techniques: Ellipsometric characterization of the HFB biofilm deposited in the PSi monolayer was performed on a variable angle spectroscopic ellipsometer (model UVISEL from Horiba–Jobin–Yvon). The ellipsometric parameters Ψ and δ were measured at an incident angle of 65 ° over the range 360–1600 nm with a resolution of 5 nm.

Optical spectra were recorded by an optical spectrum analyzer (Ando, AQ6315A). The light source was a tungsten lamp (400 nm $< \lambda <$ 1800 nm). The reflectivity spectra were measured with a resolution of 1 nm.

Water contact angle measurements were made on a CAM200, KSV Instruments Ltd.

Hepes solution was bought from Promega Italia srl, Italy.

Received: September 28, 2007
Revised: November 30, 2007
Published online:

[1] F. Müller, A. Birner, U. Gösele, V. Lehmann, S. Ottow, H. Föll, *J. Porous Mater.* **2000**, *7*, 201.
[2] H. F. Arrand, T. M. Benson, A. Loni, R. Arens-Fischer, M. Kruger, M. Thonissen, H. Luth, S. Kershaw, *IEEE Photon. Technol. Lett.* **1998**, *10*, 1467.
[3] V. Mulloni, L. Pavesi, *Appl. Phys. Lett.* **2000**, *76*, 2523.
[4] L. Moretti, L. De Stefano, I. Rea, I. Rendina, *Appl. Phys. Lett.* **2007**, *90*, 191112.
[5] L. T. Canham, in: *Properties of Porous Silicon*, Vol. 18, (Ed: L. T. Canham), INSPEC, London **1997**, p. 154.
[6] S. H. C. Anderson, H. Elliot, D. J. Wallis, L. T. Canham, J. J. Powell, *Phys. Status Solidi A* **2003**, *197*, 331.
[7] M. M. Orosco, C. Pacholski, G. M. Miskelly, M. J. Sailor, *Adv. Mater.* **2006**, *18*, 1393.
[8] Y. Y. Li, V. S. Kollengode, M. J. Sailor, *Adv. Mater.* **2005**, *17*, 1249.
[9] H. J. Hektor, K. Scholtmeijer, *Curr. Opin. Biotechnol.* **2005**, *16*, 434.
[10] H. A. B. Wosten, M. L. de Vocht, *Biochem. Biophys. Acta* **2000**, *79*, 1469.

[11] G. R. Szilvay, A. Paananen, K. Laurikainen, E. Vuorimaa, H. Lemmetyinen, J. Peltonen, M. B. Linder, *Biochemistry* **2007**, *46*, 2345.
[12] J. T. Han, S. Kim, A. Karim, *Langmuir* **2007**, *23*, 2608.0.
[13] R. Wang, Y. Yang, M. Qin, L. Wang, L. Yu, B. Shao, M. Qiao, C. Wang, X. Feng, *Chem. Mater.* **2007**, *19*, 3227.
[14] R. Wang, Y. Yang, M. Qin, L. Wang, L. Yu, B. Shao, M. Qiao, C. Wang, X. Feng, *Langmuir* **2007**, *23*, 4465.
[15] R. M. A. Azzam, N. M. Bashara, *Ellipsometry and Polarized Light* Elsevier Science, Amsterdam **1986**.
[16] L. De Stefano, I. Rea, P. Giardina, A. Armenante, M. Giocondo, I. Rendina, *Langmuir* **2007**, *23*, 7920.
[17] L. De Stefano, I. Rendina, L. Moretti, S. Tundo, A. M. Rossi, *Appl. Opt.* **2004**, *43*, 167.
[18] L. De Stefano, I. Rendina, L. Moretti, A. M. Rossi, *Mater. Sci. Eng. B* **2003**, *100/3*, 271.

3.3.3 Hydrophobin Languimir-Blodgett Film

In the Langmuir-Blodgett (LB) method a film formed by surface active molecules is compressed in a LB tub by moving barriers that reduce the available water surface area, as it is shown in figure 3.29. The film is transferred to a solid substrate by lifting an immersed flat substrate through the film so that simultaneous compression deposits the film onto the substrate (124,125). In the case of Langmuir-Schaefer (LS) deposition, an analogous method is used: in this case the film is adsorbed to the surface which has been previously brought in contact with the LB tub (fig. 3.29 B). The films transferred to solid supports were imaged using AFM.

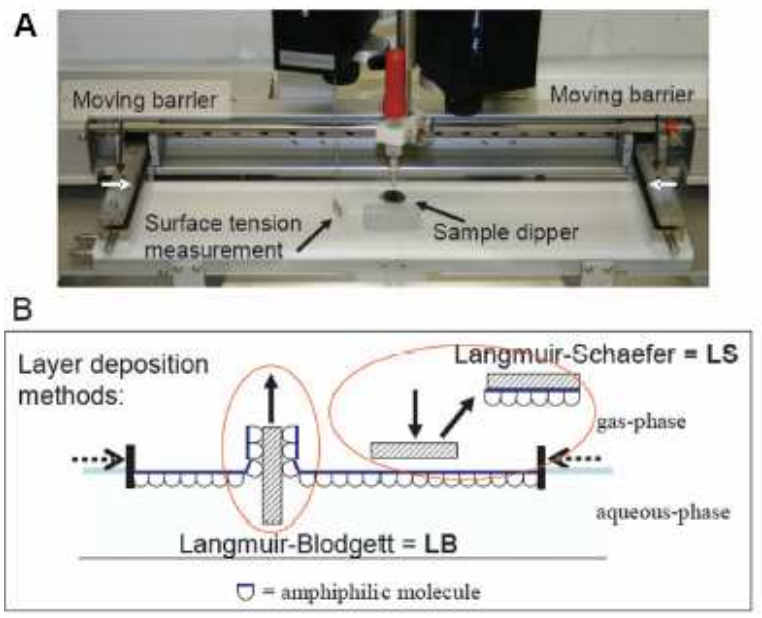

*Figure 3.29 The Langmuir-trough and film deposition methods (126). (**A**) The trough is filled with aqueous buffer and the surface tension is measured The moving barriers are used to compress the film formed by surface active molecules. The sample dipper is used to deposit the film to solid supports. (**B**) In the LB-technique, i.e. vertical deposition, a solid substrate is lifted out from the liquid and simultaneously the film is compressed onto the surface. In the Langmuir-Schaefer (LS) technique, i.e. horizontal deposition, a solid substrate is brought in contact with the film whereby the molecules on the surface can adsorb to the surface.*

The Langmuir-Blodgett (LB) films formed by Hyd-et, after assembling at the air-water interface (LB) and the AFM observations of these films deposited onto hydrophilic silicon substrates were analyzed and reported in:

*<Houmadi S., Ciuchi F., De Santo M., De Stefano L., Rea I., Giardina P., **Armenante A.,** Lacaze E., Giocondo M., "Langmuir Blodgett film of hydrophobin protein from Pleurotus ostreatus at the air-water interface" Langmuir 2008 DOI:10.1021/la802306r>*

Langmuir−Blodgett Film of Hydrophobin Protein from *Pleurotus ostreatus* at the Air−Water Interface

S. Houmadi,[†,||] F. Ciuchi,[†] M. P. De Santo,[†] L. De Stefano,[‡] I. Rea,[‡] P. Giardina,[§] A. Armenante,[§] E. Lacaze,[||] and M. Giocondo*,[†]

CNR-INFM LICRYL−Liquid Crystals Laboratory c/o Dipartimento di Fisica, Università della Calabria, 87036 Rende, Italy, CNR-IMM−Istituto per la Microelettronica e i Microsistemi, Unità di Napoli, Via P. Castellino 111, 80131 Napoli, Italy, Dipartimento di Chimica Organica e Biochimica, Università di Napoli Federico II, Via Cintia 4, 80126 Napoli, Italy, and Institut des NanoSciences de Paris (INSP, CNRS UMR 7588, Université Pierre et Marie Curie-Paris r), Campus Boucicaut, 140 Rue de Lourmel, 75015 Paris, France

Received July 18, 2008. Revised Manuscript Received September 10, 2008

We present results concerning the formation of Langmuir−Blodgett (LB) films of a class I hydrophobin from *Pleurotus ostreatus* at the air−water interface, and their structure as Langmuir−Blodgett (LB) films when deposited on silicon substrates. LB films of the hydrophobin were investigated by atomic force microscopy (AFM). We observed that the compressed film at the air−water interface exhibits a molecular depletion even at low surface pressure. In order to estimate the surface molecular concentration, we fit the experimental isotherm with Volmer's equation describing the equation of state for molecular monolayers. We found that about $^1/_{10}$ of the molecules contribute to the surface film formation. When transferred on silicon substrates, compact and uniform monomolecular layers about 2.5 nm thick, comparable to a typical molecular size, were observed. The monolayers coexist with protein aggregates, under the typical rodlet form with a uniform thickness of about 5.0 nm. The observed rodlets appear to be a hydrophilic bilayer and can then be responsible for the surface molecular depletion.

Introduction

Hydrophobins are amphiphilic proteins produced by filamentous fungi.[1] They function in a variety of roles that involve interfacial interactions, such as in growth through the air−water interface, adhesion to surfaces, and formation of coatings on various fungal structures.[2] They contribute to surface hydrophobicity, which is important for processes such as adhesion of hyphae in reproductive structures, dispersal of aerial spores, and adhesion of pathogenic fungi to host structures.[3] Hydrophobins are divided in two classes: Class I hydrophobin biofilms are not disrupted when treated with surfactants, solvents, and denaturing agents.[4,5] They appear as very stable and strongly interact with hydrophobic solids. Only trifluoroacetic acid (TFA) has been found to dissociate the corresponding supramolecular structures.[5] On the other hand, films formed by class II hydrophobins are easily disrupted with surfactants or solvent mixtures such as 60% ethanol/water.[6] The SC3 from *Schizophyllum commune* (class I) is the most extensively studied hydrophobin to date.[4,7] Hydrophobins present a biological and biotechnological interest. Due to their amphiphilic nature and their self-assembling properties, the proposed applications range from using hydrophobins as surfactants, emulsifiers in food processing, and surface coating; they appear interesting for immobilization applications and nanotechnology and even as indicators for beer gushing.[1,8] The strong and stable assembly of class I hydrophobins makes them attractive candidate molecules for surface coating of biomaterials such as surgical instruments and medical implants. The biocompatibility of hydrophobic surfaces could be enhanced by increasing their wettability with an hydrophobin layer. Hydrophobin coating could prevent nonspecific protein binding in the body and bacterial adhesion.[1] On the other hand, hydrophobin coating could increase the attachment of cells and fibroblasts, and be useful in tissue engineering.[9−11] Our investigation in this work is focused on the study of self-assemblies of the class I hydrophobin from the fungus *Pleurotus ostreatus*. *Pleurotus ostreatus* is a commercially important edible mushroom commonly known as the oyster mushroom.[12] This fungus is industrially produced as human food, and it accounts for nearly a quarter of the world mushroom production.[13] It is also used for the bioconversion of agricultural, industrial, and lignocellulose wastes,[14,15] as a source of enzymes and other chemicals for

* To whom correspondence should be addressed. E-mail: giocondo@fis.unical.it. Telephone: +390984496125. Fax: +390984494401.

[†] CNR-INFM LICRYL.

[‡] CNR-IMM Unità di Napoli.

[§] Università di Napoli Federico II.

[||] Institut des NanoSciences de Paris.

(1) Linder, M. B.; Szilvay, G. R.; Nakari-Setälä, T.; Penttilä, M. E. *FEMS Microbiol. Rev.* **2005**, *29*, 877–896.

(2) Szilvay, G. R.; Paananen, A.; Laurikainen, K.; Vuorimaa, E.; Lemmetyinen, H.; Peltonen, J.; Linder, M. B. *Biochemistry* **2007**, *46*, 2345–2354.

(3) Wösten, H. A. B.; Ruardy, T. G.; Van der Mei, H. C.; Busscher, H. J.; Wessels, J. G. H. *Colloids Surf., B* **1995**, *5*, 189.

(4) Wösten, H. A. *Annu. Rev. Microbiol.* **2001**, *55*, 625–646.

(5) Wösten, H. A. B.; de Vries, O. M. H.; Wessels, J. G. H. *Plant Cell* **1993**, *5*, 1567–1574.

(6) Russo, P. S.; Blum, F. D.; Ipsen, J. D.; Yusuf, J. A.; Miller, W. G. *Can. J. Bot.* **1982**, *60*, 1414–1422.

(7) Zangi, R.; de Vocht, M. L.; Robillard, G. T.; Mark, A. E. *Biophys. J.* **2002**, *83*(1), 112–124.

(8) Wessels, J. G. H. *Adv. Microb. Physiol.* **1997**, *38*, 1–45.

(9) Scholtmeijer, K.; Janssen, M. I.; Gerssen, B.; de Vocht, M. L.; van Leeuwen, B. M.; van Kooten, T. G.; Wösten, H. A.; Wessels, J. G. *Appl. Environ. Microbiol.* **2002**, *68*, 1367–1373.

(10) Janssen, M. I.; van Leeuwen, M. B.; van Kooten, T. G.; de Vries, J.; Dijkhuizen, L.; Wösten, H. A. *Biomaterials* **2004**, *25*, 2731–2739.

(11) Janssen, M. I.; van Leeuwen, M. B.; Scholtmeijer, K.; van Kooten, T. G.; Dijkhuizen, L.; Wösten, H. A. *Biomaterials* **2002**, *23*, 4847–4854.

(12) Penas, M. M.; Rust, B.; Larraya, L. M.; Ramirez, L.; Pisabarro, A. G. *Appl. Environ. Microbiol.* **2002**, *68*, 3891–3898.

(13) Chang, R. *Nutr. Rev.* **1996**, *54*, 91–93.

(14) Ballero, M.; Mascia, E.; Rescigno, A.; di Teulada, E. S. *Micol. Ital.* **1990**, *19*, 39–41.

(15) Puniya, A. K.; Shah, K. G.; Hire, S. A.; Ahire, R. N.; Rathod, M. P.; Mali, R. S. *Indian J. Microbiol.* **1996**, *36*, 177–178.

10.1021/la802306r CCC: $40.75

Published on Web 10/17/2008

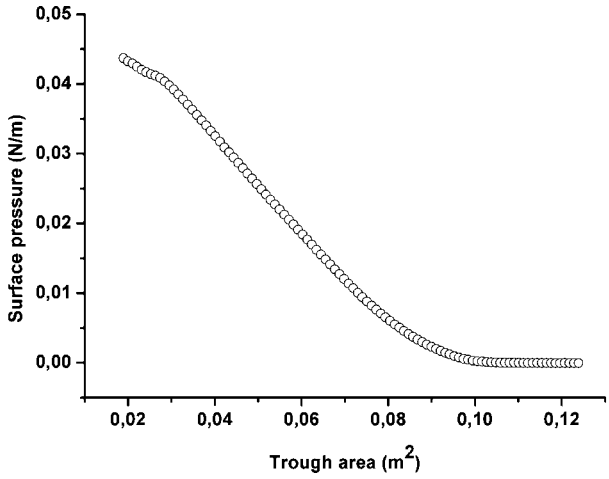

Figure 1. Surface pressure versus area isotherm of the class I hydrophobin at the air−water interface at pH 5.5. Note that the surface pressure is plotted as function of the trough area instead of the usual molecular area because of the film solubility in the subphase.

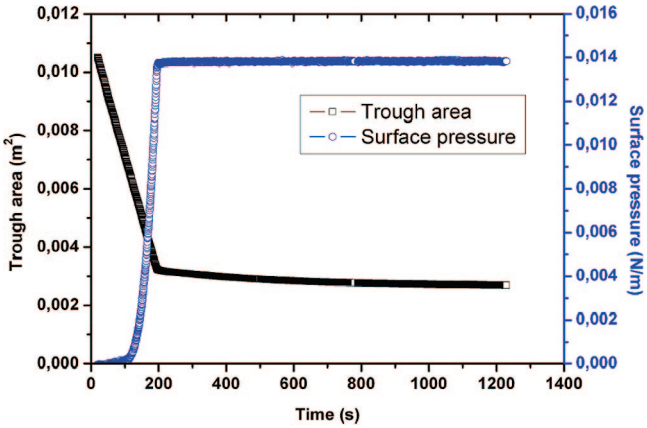

Figure 2. Area versus time curve to keep constant a given surface pressure value. In this case, the surface pressure is set at 14 mN/m. This plot points out the molecular depletion from the interface toward the subphase bulk. From this plot, we estimate the characteristic time of the process to be of the order of a few 10^2 s.

industrial and medical applications,[16−18] as an agent for bioremediation,[19] and as an organic fertilizer.[20] In a recent work, we have exploited the coating properties of a *P. ostreatus* hydrophobin biofilm when self-assembled on a silicon surface by the drop deposition technique.[21] We found that, due to the high persistence of the protein biofilm, the hydrophobin coated silicon surface is perfectly protected during the standard KOH micromachining process.

In this paper, we present results about films of the class I hydrophobin from *Pleurotus ostreatus*, both at the air−water interface (Langmuir films) and when deposited on a silicon substrate (Langmuir−Blodgett (LB) films). The experimental isotherm curves obtained at the air−water interface were interpreted using the equation of state proposed by Volmer,[22] and the deposited films were analyzed by atomic force microscopy (AFM).

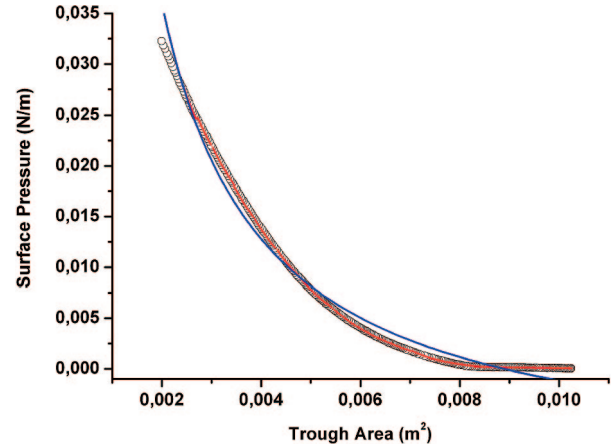

Figure 3. Experimental (open circles) and best fit from Volmer's equation (red and blue solid lines) isotherms for hydrophobin films. The blue solid line corresponds to the fit curve performed over all the experimental points. The red solid line corresponds to the fit performed on subsets of the experimental data (see the text for details). The values of the model parameters of eq 2 are listed in Table 1.

Table 1. Parameter Values of eq 2 as Calculated from the Best Fit of the Experimental Isotherm for Hydrophobin Films at 18 °C[a]

parameter	whole curve fitting	subsets fitting (range)
m	60	10−40
ω (nm^2)	10^{-2}	1−5
Π_{coh} (N/m)	10^{-2}	10^{-3} −10^{-2}
n	1.5×10^{14}	4×10^{14}−6×10^{14}
χ^2	1.1×10^{-6}	1.25×10^{-10}−4×10^{-8}

[a] In the second column are listed the obtained fitting parameters related to the whole isotherm fitting, whereas in the third column are reported the ranges of the same parameters obtained by fitting the isotherm part by part.

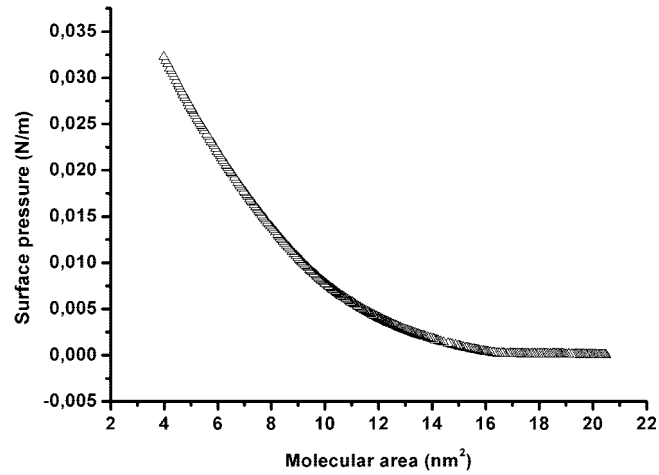

Figure 4. Experimental isotherm for the hydrophobin film as a function of the area per molecule, calculated as S/n, where S is the trough area and $n = 5 \times 10^{14}$ is the estimated number of hydrophobin molecules existing on the air−water interface as deduced from the experimental data fit.

Materials and Methods

Protein Purification. White-rot fungus, *P. ostreatus* (Jacq.:Fr.) Kummer (type: Florida) (ATCC no. MYA-2306), was maintained through periodic transfer at 4 °C on potato dextrose agar (Difco)

(16) Giardina, P.; Aurilia, V.; Cannio, R.; Marzullo, L.; Amoresano, A.; Siciliano, R.; Pucci, P.; Sannia, G. *Eur. J. Biochem.* **1996**, *235*, 508–515.
(17) Gunde-Cimerman, N. *Intl. J. Med. Mushrooms* **1999**, *1*, 69–80.
(18) Marzullo, L.; Cannio, R.; Giardina, P.; Santini, M. T.; Sannia, G. *J. Biol. Chem.* **1995**, *270*, 3823–3827.
(19) Axtell, C.; Johnston, C. G.; Bumpus, J. A. *Soil Sediment Contam.* **2000**, *9*, 537–548.
(20) Abdellah, M. M. F.; Emara, M. F. Z.; Mohammady, T. F. *Ann. Hortic. Sci. (Cairo)* **2000**, *45*, 281–293.
(21) De Stefano, L.; Rea, I.; Giardina, P.; Armenante, A.; Giocondo, M.; Rendina, I. *Langmuir* **2007**, *23*, 7920.
(22) Volmer, M. *Z. Phys. Chem. (Leipzig)* **1925**, *115*, 253.

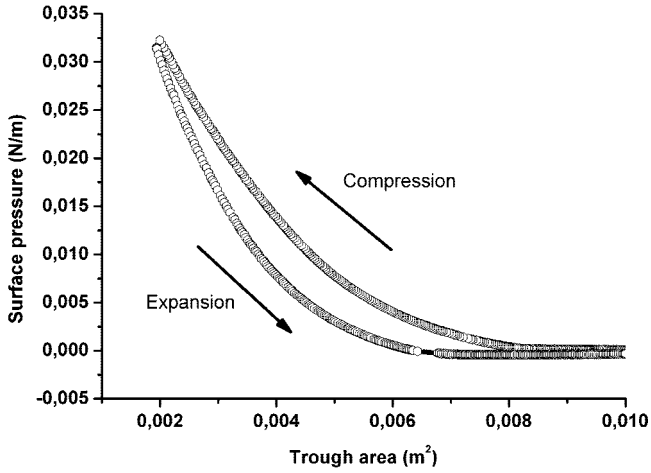

Figure 5. Experimental compression−expansion isotherm. The shift between the two branches is due to the molecular depletion occurring through the formation of hydrophilic rodlets.

plates in the presence of 0.5% yeast extract (Difco). Mycelia were grown at 28 °C in static cultures in 2 L flasks containing 500 mL of potato dextrose (24 g/L) broth with 0.5% yeast extract. After 10 days of fungal growth, hydrophobins released into the medium were aggregated by air bubbling using a Waring blender. Foam was then collected by centrifugation at 4000*g*. The precipitate was freeze-dried, treated with 100% trifluoroacetic acid (TFA) for 2 h, and sonicated for 30 min. The sample was dried again in a stream of air, dissolved in 60% ethanol, and centrifugated. The purity of the sample was ascertained by SDS-PAGE by using a silver staining method. Protein concentration was determined using absorbance at 280 nm and $\varepsilon = 1.44$ mL mg^{-1} cm^{-1}. The molecular mass of the protein (8568 Da) was determined by matrix-assisted laser desorption ionization time-of-flight (MALDI TOF; Voyager-DE STR, Applied Biosystems) analysis.

Sample Preparation. The Langmuir films were prepared in a Nima Tech 632D1D2 LB system trough using ultrapure water, at pH 5.5 and $T = 18.0 \pm 0.5$ °C for the subphase. The required pH of the solutions was obtained by adding a suitable amount of HCl. The dried protein, as obtained from the purification procedure, was dissolved in 60% ethanol in ultrapure water in order to get a protein concentration of 0.15 mg/mL. This solution was then spread on the subphase by the usual microsyringe technique; small droplets were deposited at different places distributed over the whole trough area in order to get a uniform distribution on the subphase. To monitor the interfacial film formation, the surface pressure was recorded at constant trough area as a function of time after 2000 μL of the protein solution was spread at the air−water interface on a 1200 cm^2 trough. Surface pressure was measured using a Wilhelmy plate attached to a sensitive balance with an accuracy of $\pm$0.01 mN/m. Compression of the monolayer was started after the surface pressure had stabilized, about 3 h after spreading. The monolayer was compressed to the deposition pressure of 36 mN/m. The films were then transferred at constant pressure onto silicon substrates by the vertical lifting method at a rate of 10 mm/min. In order to optimize the use of the available hydrophobin sample, we modified our trough by considerably reducing its size down to 102 cm^2. This allowed us to save material and then to have available fresh solution for each experiment. In this case, 250 μL of the protein solution was spread at the air−water interface.

Theoretical Basis. The experimental data were analyzed using a simplified form of Volmer's equation[22] that describes the equation of state for amphiphilic monolayers.[23−25] In the cited references, the authors show that, for monolayers in the gaseous or liquid expanded phase, in the case $A > A_c$ (where A is the actual area per molecule and A_c is the area per molecule corresponding to the onset of the phase transition, that is, when $\Pi = \Pi_c$), the equation of state is

$$\Pi = \frac{mkT}{A - \omega} - \Pi_{coh} \quad (1)$$

where Π ¨is the surface pressure, k is the Boltzmann constant, T is the temperature, ω is the limiting area of a molecule in the gaseous state, A is the area per molecule, Π_{coh} is the cohesion pressure, accounting for the intermolecular interactions, and m is a parameter accounting for the number of kinetically independent units (fragments or ions). As reported in ref 26, eq 1 can be used to analyze protein surface films.

Atomic Force Microscopy (AFM). The hydrophobin film was transferred from the water subphase to crystalline silicon substrates covered by the native SiO_2 layer. The different areas of the samples were imaged by AFM operating in the tapping mode using a silicon cantilever. The AFM observations were carried out in air at atmospheric pressure with a Nanoscope 3100 Veeco microscope equipped with an Extender Electronics module.

Results and Discussion

Formation of Hydrophobin Films. The surface pressure versus area isotherm is shown in Figure 1. The isotherm features a smooth rise of the surface pressure, characteristic for a liquid-expanded phase, and a collapse point close to 40 mN/m.

With reference to Figures 1, 3, and 5, we want to point out that the surface pressure is plotted as function of the trough area instead of the usual molecular area. In fact, we noticed that the film at the interface exhibits a molecular depletion in the subphase. This feature becomes evident in Figure 2 where the area change versus time, in order to keep constant a given surface pressure value, is plotted.

From this plot, we estimate the surface molecular depletion characteristic time to be in the order of a few hundreds of seconds. We want to stress that, in such cases, that is, when the surface molecule number depletes, experiments should be performed in a time much shorter than the characteristic time ruling the depletion process, in order to consider constant the surface molecular concentration during the whole experiment. Nevertheless, this condition cannot be always fulfilled, as the compression rate cannot be made arbitrarily high because of possible instabilities in the Langmuir film structure. As a consequence, the actual surface molecular concentration is generally unknown. In order to estimate the number of hydrophobin molecules present at the air−water interface, we compared the experimental isotherms to the equation of state expressed by eq 1. To do this, we express the parameter A, that is, the area per molecule, as the ratio between the trough area S and the number n of molecules present at the interface. Therefore eq 1 is modified as follows:

$$\Pi = \frac{mkT}{(S/n) - \omega} - \Pi_{coh} \quad (2)$$

Equation 2 was then used to fit the experimental isotherm. Figure 3 shows the experimental (open circles) and the calculated (blue solid line) isotherms of the hydrophobin film. As one can see, this curve does not fit very well all the experimental points. We believe that the reason is associated with the surface molecular depletion, making their numbers not constant during the compression process. In order to validate this hypothesis, we performed a further fit over 10 subsets of the experimental points obtained by dividing the whole isotherm in 10 parts, providing that at least a few tens of points are considered for each data set. This allowed us to virtually make faster the experiment by

(23) Fainerman, V. B.; Vollhardt, D. *J. Phys. Chem. B* **1999**, *103*, 145.
(24) Vollhardt, D.; Fainerman, V. B.; Siegel, S. *J. Phys. Chem. B* **2000**, *104*, 4115.
(25) Fainerman, V. B.; Vollhardt, D. *J Phys. Chem. B* **2003**, *107*, 3107–3098.

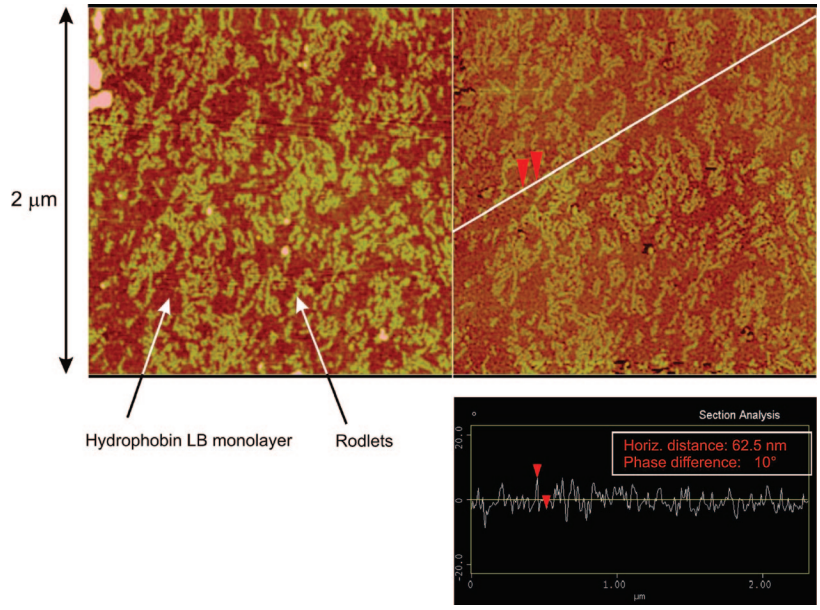

Figure 6. Tapping mode AFM images of a hydrophobin LB film on a silicon wafer. Topography image (left) and phase image (right); the image size is $2 \times 2\ \mu m^2$, and height scale 7 nm. The section analysis refers to the phase image.

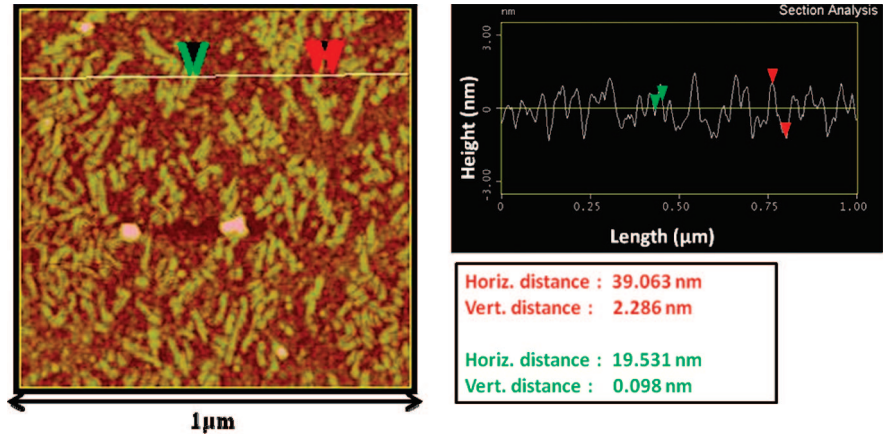

Figure 7. AFM topography image and section analysis of a hydrophobin LB film deposited on a silicon substrate. The rodlet height with respect to the LB monolayer is estimated as ~2.3 nm. The image size is $1 \times 1\ \mu m^2$, and height scale 7 nm.

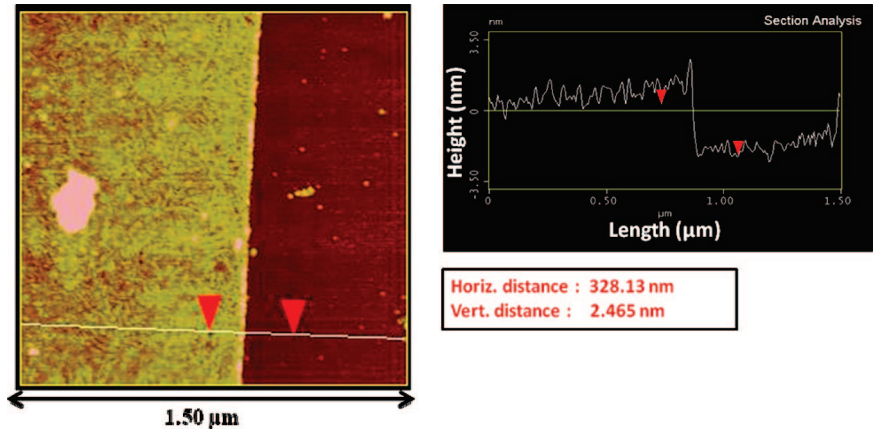

Figure 8. AFM topography image and section analysis of a hydrophobin LB film deposited on a silicon substrate. The thickness of the monolayer is estimated as ~2.5 nm. The image size is $1.5 \times 1.5\ \mu m^2$, and height scale 7 nm.

considering, for each fitting session, data collected in a fraction of the time needed for the whole isotherm acquisition. As result, we got a very good agreement between the experiment and the theoretical model. In doing this, we also noticed that the fit quality, expressed by the χ^2 value, although very good, reduces when the pressure increases. This could be due to the fact that the molecular depletion becomes more important at higher surface pressure values. The resulting curves are joined in the red one reported

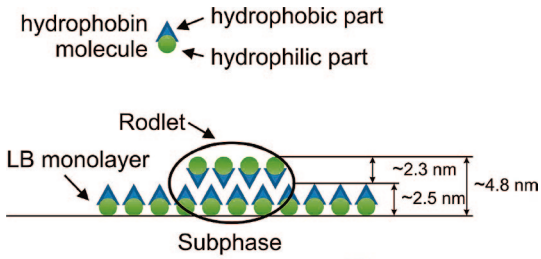

Figure 9. Oversimplified scheme of the molecular arrangement inside the LB monolayer and the observed rodlets.

in Figure 3. From both of the fitting methods, we obtained the same order of magnitude for the parameter n, in the order of 10^{14} molecules. From the same fit, we were also able to estimate the remaining parameter values in the model (eq 2), summarized in the Table 1.

We point out that the obtained value for the parameter m is consistent with those reported in ref 26. Also, the obtained values for the molecular area ω are in the correct order of magnitude for this kind of object.

By comparing this result to the number of molecules present in the hydrophobin solution introduced into the Langmuir trough, 2.5×10^{15} molecules, we deduce that only about $^1/_{10}$ of the total molecules contribute to the interfacial film formation. Using the obtained n values, we can now plot the experimental isotherm as a function of the area per molecule (Figure 4).

The effect of the surface molecule depletion is also evident in the compression−expansion cycle shown in Figure 5. In fact, the expansion curve is shifted toward lower areas with respect to the compression curve. For HFBI and HFBII hydrophobins, other authors attributed this shift to the formation of aggregates,[27] without highlighting molecule depletion. The formation of various aggregates by hydrophobins was noted very early. Takai described the formation of "rods" and "fibrils" by cerato-ulmin.[28]

The observed molecular depletion in our system is certainly at least partly associated with the formation of aggregates during the film compression that do not disassemble during the expansion. This hypothesis is supported by the AFM analysis.

Our AFM observations of LB hydrophobin films deposited onto hydrophilic silicon substrates revealed the coexistence of a hydrophobin monolayer and aggregates under the form of rodlets (Figure 6). In a very recent paper, Yu et al.[29] presented AFM images showing HGFI class I hydrophobin rodlets, but the coexistence with a LB monolayer was not evident.

The thickness of our hydrophobin monolayer, measured by AFM (Figure 8), is about 2.5 nm. From Figure 7, we have been able to estimate the rodlet size. The AFM image shows that the height of the rodlets, measured from the upper surface of the monolayer, is about 2.3 nm. Consequently, the rodlet height is ~4.8 nm, (2.3 + 2.5 nm). From these measurements, we can deduce that the rodlets are actually structured as bilayers. Their length ranges from 50 to 105 nm, and the width ranges from 19 to 24 nm. This last value has to be considered carefully because of the probe broadening effect.[30] Taking into account the broadening induced by a 10 nm end radius tip, an actual rodlet width ranging from 6 to 11 nm appears consistent with our data and in agreement with data reported by other authors[1] for different hydrophobins. On the contrary, measured heights are unaffected by this process and give a more reliable indication of particle size,[31] as well as the length if it is significantly larger than 10 nm. This latter value for the rodlet length appears smaller than those observed in ref 29.

As it can be clearly observed in the phase image reported in Figure 6, a phase contrast exists between the top of the rodlets and the underlying monolayer, indicating that the AFM tip does not interact in the same way with the monolayer and the rodlets. Because of the LB film transfer procedure, the upper surface of the hydrophobin monolayer must be hydrophobic. We conclude that the upper surface of the observed rodlets is hydrophilic and hence they are actually fragments of the bilayer, whose hydrophobic sides are in contact, sinking in the LB monolayer (Figure 9). The conclusion that the observed rodlets are hydrophilic suggests a possible molecular depletion mechanism: hydrophobins self-assemble into hydrophilic rodlets that can easily sink in the subphase. Other authors reported observations of the rodlets for other types of class I hydrophobins.[5,32,33] These rodlets are presumed to be insoluble in water and have not been shown to exist in solution.[34] It is noteworthy that in our samples the rodlet concentration is very high in the sample area close to the upper end of the film (Figure 8). This is likely due to the formation of aggregates close to the meniscus as a consequence of the Langmuir film perturbation at the very beginning of the substrate lifting. This strongly suggests that the rodlets are formed at the air−water interface, as also discussed in ref 29.

Conclusion

In this paper, we have investigated the formation and the features of LB films of a class I hydrophobin from *Pleurotus ostreatus*. Compression−expansion cycles and constant pressure measurements demonstrated that the film at the air−water interface exhibits a molecular depletion toward the subphase. As consequence, the number of molecules at the interface and hence the area per molecule are unknown. In order to estimate the surface molecular concentration, we analyzed the experimental pressure−area isotherms using a 2D equation of state (Volmer-like). Moreover, when the LB film is transferred onto the silicon substrate, AFM observations revealed the coexistence of a LB monolayer and rodlets. From these measurements, we were able to estimate the rodlet size and the monolayer thickness: we conclude that the observed rodlets are actually formed by hydrophobin bilayers embedded in the LB monolayer. The LB film transfer technique along with the AFM phase measurements demonstrate the hydrophilic character of the rodlets, supporting the hypothesis about a possible depletion mechanism occurring at least partly through the formation of hydrophilic rodlets.

Acknowledgment. This work has been performed in the frame of the Italian Consiglio Nazionale delle Ricerche (CNR) Project MD.P01.016.001. S.H. acknowledges the financial support from the Italian International Doctoral School of Hard Sciences "Bernardino Telesio". We thank Dr. M. Sposato and Mr. F. Capizzano from CaLCTec (Calabria Liquid Crystals Technology S.r.l) for the technical support.

LA802306R

(26) Wüstneck, R.; Fainerman, V. B.; Wüstneck, N.; Pison, U. *J. Phys. Chem. B* **2004**, *108*, 1766–1770.
(27) Paananen, A.; Vuorimaa, E.; Torkkeli, M.; Penttilä, M.; Kauranen, M.; Ikkala, O.; Lemmetyinen, H.; Serimaa, R.; Linder, M. B. *Biochemistry* **2003**, *42*, 5253–5258.
(28) Takai, S. *Nature* **1974**, *252*, 124–126.
(29) Yu, L.; Zhang, B.; Szilvay, G. R.; Sun, R.; Jänis, J.; Wang, Z.; Feng, S.; Xu, H.; Linder, M. B.; Qiao, M. *Microbiology* **2008**, *154*, 1677.
(30) Kirby, A. R.; Gunning, A. P.; Morris, V. J. *Biopolymers* **1996**, *38*, 355.
(31) Gunning, A. P.; de Groot, P. W. J.; Visser, J.; Morris, V. J. *J. Colloid Interface Sci.* **1998**, *201*, 118–126.
(32) Wösten, H. A.; Schuren, F. H.; Wessels, J. G. *EMBO J.* **1994**, *13*, 5848–5854.
(33) Mackay, J. P.; Matthews, J. M.; Winefield, R. D.; Mackay, L. G.; Haverkamp, R. G.; Templeton, M. D. *Structure* **2001**, *9*(2), 83–91.
(34) Stroud, P. A.; Goodwin, J. S.; Butko, P.; Cannon, G. C.; McCormick, C. L. *Biomacromolecules* **2003**, *4*, 956–967.

3.4.1 Protein immobilization

The hybrid interface of silicon and hydrophobin can act as an active substrate for non-covalently binding of different bioprobes, so that the quality and the characteristic of this proteins layer are key features for the entire device. Protein immobilization on the hydrophobin film has been verified and analyzed using labelled proteins, as fluorescent BSA, and enzymes, as laccase. These experiments are reported in:

<De Stefano L.; Rea I; De Tommasi E.; Rendina I.; Rotiroti L.; Giocondo M.; Longobardi, S.; ***Armenante A.****; Giardina P., "Bioactive Modification of Silicon Surface using Self-assembled Hydrophobins from Pleurotus ostreatus*". *Colloids and Surface B: Biointerfaces (submitted 24/09/2008)>*

Elsevier Editorial System(tm) for Colloids and Surfaces B: Biointerfaces
Manuscript Draft

Manuscript Number:

Title: Bioactive Modification of Silicon Surface using Self-assembled Hydrophobins from Pleurotus ostreatus.

Article Type: Full Length Article

Keywords: Hydrophobin, silicon surface, protein array

Corresponding Author: Dr Luca De Stefano,

Corresponding Author's Institution:

First Author: Luca De Stefano

Order of Authors: Luca De Stefano; Ilaria Rea; Edoardo De Tommasi; Ivo Rendina; Lucia Rotiroti; Michele Giocondo; Annunziata Armenante; Sara Longobardi; Paola Giardina

Abstract: A crystalline silicon surface can be made biocompatible and chemically stable by a self-assembled biofilm of proteins, the hydrophobins (HFBs) purified from the fungus Pleurotus ostreatus. The protein modified silicon surface shows an improvement in wettability and is suitable for immobilization of other proteins. Two different proteins were successfully immobilized on the HFBs coated chips: the bovine serum albumin and an enzyme, a laccase, which retains its catalytic activity even when bound on the chip. Variable angle spectroscopic ellipsometry (VASE), water contact angle (WCA), and fluorescence measurements demonstrated that the proposed approach in silicon surface bioactivation is a feasible strategy for the fabrication of a new class of hybrid biodevices.

Bioactive Modification of Silicon Surface using Self-assembled Hydrophobins from Pleurotus ostreatus.

L. De Stefano*[a], I. Rea [a,b], E. De Tommasi[a], I. Rendina[a], L. Rotiroti[a,c], M. Giocondo[d], S. Longobardi[e], A. Armenante[e], and P. Giardina [e].

[a] *Unit of Naples-Institute for Microelectronics and Microsystems, National Council of Research, Via P. Castellino 111, 80131, Naples, Italy Fax: +390816132598; Tel: +390816132375; E-mail: luca.destefano@na.imm.cnr.it*

[b] *Dept. of Physical Sciences, University of Naples "Federico II", Via Cintia 4, 80126, Naples, Italy.*

[c] *Dept. of Organic Chemistry and Biochemistry, University of Naples "Federico II", Via Cintia 4, 80126, Naples, Italy.*

[d] *LICRYL – INFM-CNR, Via P. Bucci, Cubo 33/B, 87036 Arcavacata di Rende, Cosenza, Italy.*

Abstract

A crystalline silicon surface can be made biocompatible and chemically stable by a self-assembled biofilm of proteins, the hydrophobins (HFBs) purified from the fungus *Pleurotus ostreatus*. The protein modified silicon surface shows an improvement in wettability and is suitable for immobilization of other proteins. Two different proteins were successfully immobilized on the HFBs coated chips: the bovine serum albumin and an enzyme, a laccase, which retains its catalytic activity even when bound on the chip. Variable angle spectroscopic ellipsometry (VASE), water contact angle (WCA), and fluorescence measurements demonstrated that the proposed approach in silicon surface bioactivation is a feasible strategy for the fabrication of a new class of hybrid biodevices.

Introduction

Biological molecules are more and more used in a large class of research and commercial applications such as biosensors, DNA and protein microarrays, cell culturing, immunological assays, and so on. The fabrication of a new generation of hybrid biodevices, where a biological counterpart is integrated in a micro or a nano-electronic platform, is strictly related to the bio-compatibilization treatments of the surfaces involved [1]. The design and the realization of bio/non-bio interfaces with specific properties of chemical stability, wettability, and biomolecules immobilization are key features in the miniaturization of devices needed in the development of genomic and proteomic research [2]. In particular, protein immobilization is a hot topic in biotechnology since commercial solutions such as the DNA array are not still available. Proteins

are, due to their composition, a class of very heterogeneous macromolecules with variable properties. For these reasons, it is extremely complex to find a common surface suitable for different proteins with a broad range in molecular weight and physical–chemical properties such as charge and hydrophobicity. A further aspect is the orientation of spotted compounds, that becomes of crucial relevance for some applications, like quantitative analysis, enzymatic reactions, interaction studies. Besides tethering the proteins to the surface by adhesion or non-oriented covalent attachment, recent developments for the directed immobilization of proteins are emerging. These efforts are addressing challenges such as loss of enzymatic activity due to unfavourable orientation of the immobilized enzyme [3]. Despite the development of many different surfaces in the last five years, notably only few systematic investigations have been conducted and yet, no universal surface ideal for all applications could be identified [4-8]. Among others, silicon is a very interesting platform due to its wide use in all the micro and nanotechnologies developed for the integrated circuits industry. Lot of studies about the chemical functionalization of silicon in order to make it compatible with the organic chemistry have been published in the last ten year [9]. A completely different approach is to use a biological substrate to passivate the silicon surface: recently, a nanostructured self-assembled biofilm of amphiphilic proteins, the hydrophobins, was deposited by solution deposition on crystalline silicon and proved to be efficient as masking material in the KOH wet etch of the crystalline silicon [10]. HFBs are a group of very surface active proteins [11]. They are small (about 10 kDa) proteins that originate from filamentous fungi, where they coat the spores and aerial structures, and they mediate the attachment of fungal structures to hydrophobic surfaces [12-13]. HFBs self-assemble at the air/water interface and lower the surface tension of water. Furthermore, they shown self-assembling properties also at interfaces between oil and water, and between water and a hydrophobic solid [14]. The primary structure of HFBs is characterized by a conserved pattern of eight cysteine residues, forming four intramolecular disulfide bridges [15]. HFBs are further divided into classes I and II based on their hydropathy patterns, although the amino acid sequence similarity both within and between the classes is small. Class I HFB assemblies are insoluble even in hot solutions of sodium dodecyl sulfate (SDS) and can only be dissolved in some strong acids, such as trifluoroacetic acid [11].

Some very recent applications of class II hydrophobins in protein immobilization have been reported, nevertheless only one example of enzyme immobilization on a Class I hydrophobin (SC3) layer formed on a glassy carbon electrode has been investigated [12]. Inspired by these very promising results, we have studied the immobilization of a fluorescent protein and an enzyme on a Class I hydrophobin layer when self-assembled on silicon surface.

Materials and methods

Protein purification. The HFB and the laccase POXC have been isolated from the culture broth of P. ostreatus (type: Florida ATCC no. MYA-2306). For HFBs production, mycelia have been grown at 28 °C in static cultures in 2 L flasks containing 500 mL of potato dextrose (24 g/l) broth with 0.5% yeast extract. After 10 days of fungal growth, the HFBs aggregates have been obtained by air bubbling of the culture broth by using a Waring blender. Foam has been then collected by centrifugation at 4000 g. The precipitate has been freeze dried, treated with 100% trifluoroacetic acid for 2h, and sonicated for 30 min. The sample has been dried again in a stream of air and then dissolved in 60% ethanol. The precipitate formed has been separated by centrifugation at 4000g. the homogeneity of the HFB sample has been ascertained by SDS-PAGE, by using a silver staining method. Mycelium growth and laccase purification have been carried out following the procedures described by Palmieri et al. [16].

Hydrophobin self-assembly on silicon chip. Silicon samples, single side polished, <100> oriented (chip size: 1cm×1cm), after standard cleaning procedure [17], have been washed in hydrofluoridic acid solution for three minutes to remove the native oxide thin layer (1-2 nm) due to silicon oxidation. Then samples have been incubated in HFBs solutions (0.1 mg/mL in 80% ethanol) for 1 h, dried for 10 min on the hot plate (80°C), and then washed by the solvent solution (80% ethanol in water).

Laccase immobilization method. A drop of the laccase solution has been deposited on HFB modified silicon surface, kept at 4 °C for 1 hour, and then rinsed over night in 50 mM phosphate buffer, pH 7. After 16 hours, the silicon biochip has been washed in the same buffer at 25°C till to complete loss of laccase activity in the washing buffer. Then each chip has been dust-protected and kept at constant humidity conditions when not in use.

BSA immobilization method. Bovine serum albumin (BSA) has been labelled by rhodamine, following the Molecular Probes© procedure MP06161, and solubilised in water at three different concentration (3, 6, 12 μM). To assess the protein binding on the chip surface, we have spotted on the chips covered by the HFBs biofilm 50 μl of water solution containing the labeled protein. The immobilization has been carried at 4°C over night. After incubation, the samples have been rinsed three times in deionized water at room temperature.

Enzyme assay Laccase activity has been assayed at 25°C using 2,6-dimethoxyphenol (DMP) 10mM in McIlvaine citrate–phosphate buffer, pH 5. Oxidation of DMP has been followed by the absorption increment at 477 nm (ε_{477}=14.8×10^3 M^{-1} cm^{-1}) using Beckman DU 7500 spectrophotometer (Beckman Instruments). Enzyme activity has been expressed in International Units (IU). Immobilized enzyme has been assayed by silicon dip in 10 ml of McIlvaine citrate–

phosphate buffer, pH 5. The absorption increment at 477 nm has been followed withdrawing 200 µl of reaction mixture each 30s for 10 min. The total immobilised activity per unit of silicon (chip) have been calculated as U/chip = $\Delta A_{min}^{-1}/\varepsilon\ 10^4$.

Optical Techniques. Ellipsometric characterization of the hydrophobin biofilm deposited on the silicon substrate has been performed by a variable-angle spectroscopic ellipsometry model (UVISEL, Horiba-Jobin-Yvon). Ellipsometric parameters Δ and Φ have been measured at an angle of incidence of 65° over the range of 360-1600 nm with a resolution of 5 nm. Fluorescence images were recorded by a Leica Z16 APO fluorescence macroscopy system. Contact angle measurements have been performed by using a KSV Instruments LTD CAM 200 Optical Contact Angle Meter: each contact angle has been calculated as the average between the values obtained from three drops having the same volume (about 3 µL), spotted on different points of the chip.

Results and Discussion

The main goal of this work is to demonstrate that the hybrid interface of silicon and HFB can act as an active substrate for non-covalent binding of different bioprobes. From this point of view the quality and the characteristic of the protein layer are key features for the entire device. The association of hydrophobins in solution and their self assembly have both been attributed to the amphiphilic structure of the HFB monomer [18-19]. The coating of a solid surface by solution deposition is not a finely controlled process, even if the covering substance has self-assembling properties, as it is the case of HFB. The result is that the HFB biofilms self-assembled on the silicon surface by deposition of equal concentration solutions could have variable thicknesses ranging between 10 and 30 nanometers. This behaviour could be ascribed to different local aggregation of HFB in the solution covering the silicon chip, due to the strong hydrophobic interactions among the protein molecules. In fact, during HFB deposition, solvent evaporation can determine local increases of protein concentration, thus favouring multimers and aggregate formation that can deposit on the layer. In this step there is no way to control the clustering and stacking of the proteins which are constituting the self-assembled biofilm.

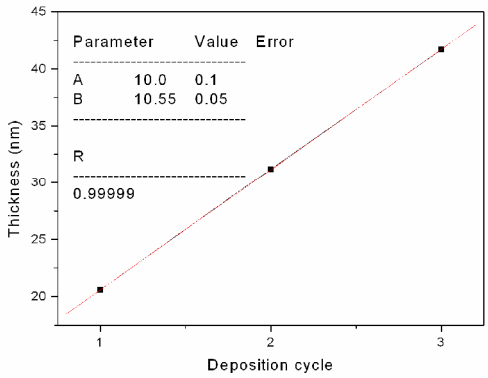

Figure 1. Growth of a thick HFB biofilm by repeated cycles of deposition on a hydrophobic silicon substrate.

However successive depositions of proteins form a biofilm having thickness proportional to the number of depositions, as it is shown in Figure 1: we have reported the thicknesses of the HFB films after each one of three consecutive depositions and plotted them as function of the deposition cycle. In a recent article, we have already demonstrated that the nanometric HFB biofilm uniformly covers the silicon surface [10]: on exposure to the potassium hydroxide (KOH), which anisotropically dissolves the silicon, a silicon wafer coated by HFB is completely shielded by the etching agent, at least for several minutes. The protection against KOH can be prolonged at any time by increasing the thickness of the HFB biofilm self-assembled on the silicon surface.

Before using the HFB biofilm as a nanostructured template for protein binding, we have tested its stability and some features by optical methods such as VASE, spectrophotometry, and WCA. The HFB biofilm self-assembled on the hydrophobic silicon shows a strong adhesion to the surface: the protein layers always exhibit great stability to alkaline solutions even at high temperature. After 10 minutes washing in sodium hydroxide and SDS at 100 °C, a residual biofilm is still present. It has a thickness of about 3.1±0.7 nm, independently from the starting value. The biofilm characterization has been performed by VASE on 12 samples realized in the same experimental conditions; the optical model for experimental data fitting has been developed in our previous work [10]. We believe that this is the thickness of a monolayer of HFBs when self-assembled on hydrophobic silicon: this value is also consistent with a typical molecular size and comparable to atomic force microscopy measurements [20]. According to the above described model, the washing step of the chip is strong enough to remove the aggregates deposited on the HFB monolayer that directly interacts with the hydrophobic silicon

surface.

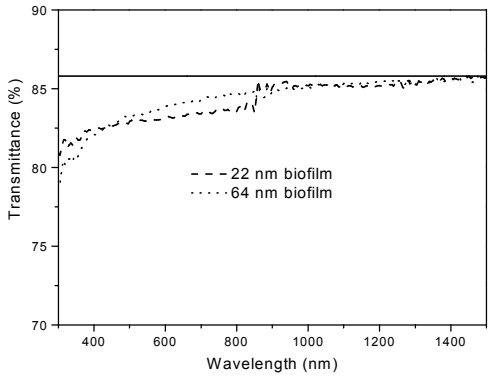

Figure 2. Transmission curves of two different samples of HFB self- assembled biofilm on silicon.

This behaviour points out the stronger interactions between the silicon surface and the HFB monolayer with respect to those between the HFB aggregates and the HFB monolayer.

The presence of the biofilms does not alter the optical behaviour of the silicon surface as it is shown in Figure 2, where the transmission curves of two different biofilms on silicon are reported. In both cases the self-assembled layer is transparent in a very large interval of wavelengths: the transmittance is still the 80 % at 290 nm.

The improvement in the silicon wettability is also a key features in biodevices realization: the silicon surface, after standard cleaning process and washing in HF, is hydrophobic, this occurrence can constitute a severe limit in the fabrication of microchannels for microfluidics applications. Since HFBs self-assemble in stable biofilm on a variety of different surfaces, such as mica, Teflon, and polydimethylsiloxane [6-7] due to the amphiphilic interaction with hydrophobic or hydrophilic surfaces, we can modify the silicon behaviour with respect to the water interaction by covering its surface by HFBs.

The changing in silicon wettability has been monitored by water contact angle measurements. In Figure 3 A and B are reported the WCA results in case of the bare silicon surface and after the deposition of the HFB biofilm. The dramatic increase in wettability of the silicon surface is well evident: in the first case, the WCA results in 90°±1°, so that the surface can be classified as hydrophobic, while after the HFB deposition the WCA falls down to 25°±2° so that the surface is clearly hydrophilic. The HFB modified silicon surface is highly stable and the WCA value does not change after months, even if stored at room temperature without particular saving condition.

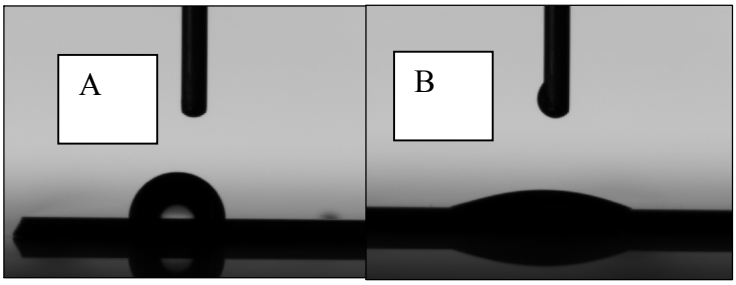

Figure 3. Changing the wettability of c-Si: the hydrophobin nanolayer turns the hydrophobic surface of c-Si into a hydrophilic one. A: a water drop on the c-Si after washing in hydrofluoridic acid forms a contact angle of 90°±1°. B: a water drop after the hydrophobin deposition forms a contact angle of 25°±2°.

The HFB modified silicon surface has been tested by BSA immobilization: solutions containing the rhodamine labelled protein, at different concentration, between 3 and 12 μM, have been spotted on the HFB film. The labelled bioprobes have been spotted also on other surfaces which have not been treated with the hydrophobins, as a negative control on the possible aspecific binding between the silicon and the probe. All the samples have been washed in deionized water to remove the excess of biological matter and observed by the fluorescence macroscopy system. By illuminating the fluorescent BSA samples, we found that the fluorescence is brighter than the negative control as it can be seen in Figure 4A and 4B. The fluorescence signal is also quite homogeneous on the whole surface, as confirmed by the intensity profile on a treated surface reported in Figure 4C. We have qualitatively tested the strength of the affinity bond between the HFB and the BSA, by washing the chip overnight in deionized water.

Since the fluorescent intensities before and after the washing step do not differ, we can conclude that the HFB-BSA system is very stable. We have also realized a dose-response curve of fluorescence intensity as function of BSA concentration, shown in Figure 4D, and we have estimated a saturation concentration equal to 6.05 μM corresponding to 300 fmol/cm^2.

Protein immobilization on the HFB film has been also verified and analyzed using an enzyme, POXC laccase. This enzyme is produced by the same fungus *P. ostreatus* [16], easily available in our laboratory and whose activity assay is simple and sensitive. The enzymatic assay on the immobilized enzyme has been performed dipping the chip into the buffer containing the substrate and following the absorbance change during several minutes. We chose to use a pH 5 buffer and DMP as a substrate, a good settlement between stability and activity of the enzyme. A volume of 30 μl of the enzyme solution (about 700 U/ml) have been deposited on the chips (10mm x 10mm) and, after several washing, an activity of 0.1÷0.2 U has been determined on

each chip (Figure 5), with an immobilization yield of 0.5÷1%.

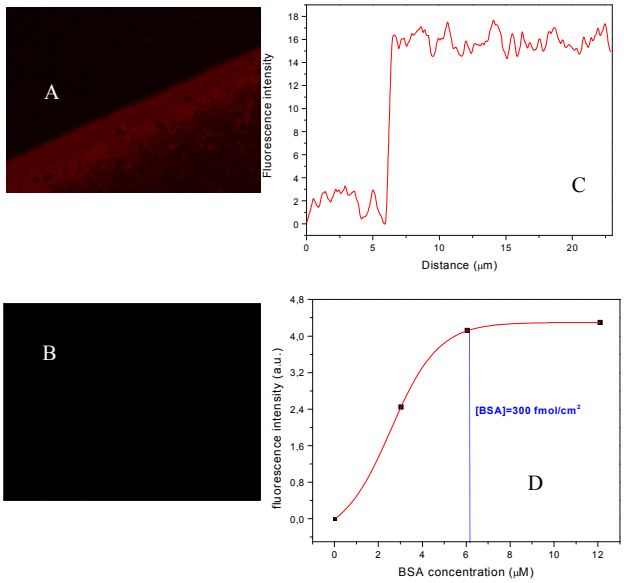

Figure 4. A: Fluorescence image of labelled BSA spotted on a silicon chip covered by HFBs. B: Negative control sample: BSA spotted directly on silicon. C: Intensity profile of fluorescencent BSA on HFB biofilm inside and outside the drop. D: The dose-response curve of fluorescence intensity as function of the BSA concentration.

This value is comparable to that one (7%) obtained in the optimized conditions for laccase immobilization on EUPERGIT C 250L©.[21] Taking into account the specific activity of the free enzyme (430 Umg^{-1}) and its molecular mass (59 kDa), 0.5µg of laccase corresponding to about 8 pmol (5 x 10^{12} molecules) have been immobilized on each chip. A reasonable evaluation of the surface occupied by a single protein molecule can be based on crystal structures of laccases [22-23] and homology among these proteins.

This surface should be 28 x 10^{-12} mm^2, considering the protein as a sphere with radius of 3 x 10^{-6} mm. On this basis the maximal number.of laccase molecule on each chip should be 3 x 10^{12}. These data can indicate that the number of active immobilized laccase molecules on each chip is of the same order of magnitude than the expected maximum. Laccase assays have been repeated on the same chip after 24 and 48 hours in the same conditions. Figure 6 shows that about one half of the activity was lost after one day, but no variation of the residual activity was observed after the second day.

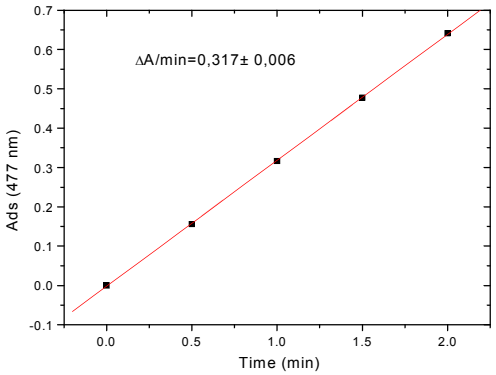

Figure 5. Enzymatic activity determination of POXC laccase immobilized on a chip

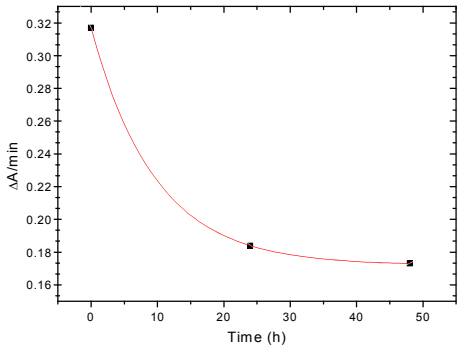

Figure 6. Time resolved profile of laccase activity of the immobilized enzyme.

Conclusions

We have demonstrated the bio-modification of the silicon surface by using the self-assembling features of the HFB, an amphiphilic protein purified by the fungus *P. ostreatus*. The nanometric monolayer of proteins, casted on the silicon surface by solution deposition, is very stable from the chemical point of view, since it is still present after strong washing in NaOH and SDS at 100 °C. The biofilm turns the hydrophobic silicon surface into a hydrophilic one, which can be very useful in microfluidic integrated application. Moreover, the biofilm can arrange both in a monolayer or in a multilayer stack of proteins depending on deposition conditions. The HFB monolayer acts as a bioactive substrate to bind other proteins, such as BSA and laccase. These results can be the starting point in the fabrication of a new generation of hybrid devices for proteomic applications.

ACKNOWLEDGMENT. The authors gratefully acknowledge dr. N. Malagnino of ST. Microelectronics in Portici (NA), Italy, for water contact angle measurements, Prof. P. Arcari (Dept. of Biochemistry and Medical Biotechnologies, University of Naples "Federico II") for fluorescent BSA, dr. F. Autore for the purification of POXC laccase and G. Armenante for technical support.

1. V.V. Tsukruk, *Adv Mat* **2001**, *13*, 95-108.
2. W. Xing and J. Cheng , Eds., *Frontiers in Biochip Technology*, **2006,** Springer.
3. Cha T, Guo A, Zhu XY. *Proteomics* **2005**, *5*, 416-419.
4. Angenendt P, Glokler J, Murphy D, Lehrach H, Cahill DJ. *Anal. Biochem.* **2002**, *309*, 253-260.
5. Angenendt P, Glokler J, Sobek J, Lehrach H, Cahill DJ. *J. Chromatogr.* A **2003**, *1009*, 97-104.
6. Qin, M.; Wang, L. K.; Feng, X. Z.; Yang, Y. L.; Wang, R.; Wang, C.; Yu, L.; Shao, B.; Qiao, M.Q. *Langmuir* **2007**, *23*, 4465-4471.
7. Wang, R.; Yang, Y. L.; Qin, M.; Wang, L. K.; .Yu, L; Shao, B.; Qiao, M. Q.; Wang, C.; Feng, X.Z. *Chem. Mater.* **2007**, *19*, 3227-3231.
8. Gutmann O, Kuehlewein R, Reinbold S, Niekrawietz R, Steinert CP, de Heij B, Zengerle R, Daub M. *Lab Chip* **2005**, *5*, 675-681.
9. Buriak, J. M. *Phil. Trans. Royal. Soc.* **2006***, 364,* 217-225.
10. De Stefano L., Rea I., Giardina P., Armenante A., Giocondo M., Rendina I.. *Langmuir* **2007**, 23, 7920,.
11. Hektor H.J., Scholtmeijer K. *Curr Op Biotechnol* **2005**, *16,* 434-439.
12. Sunde M., Kwan A.H.Y., Templeton M.D., Beever R.E., Mackay JP. *Micron* **2008,** *39*, 773-784
13. Linder MB, Szilvay GR, Nakari-Setälä T, Penttilä ME. *FEMS Microbiol Rev.* **2005**, *29*, 877-96.
14. Lumsdon SO, Green J, Stieglitz B. *Colloids Surf B Biointerfaces* **2005**, *44*, 172-8.
15. Kershaw M. J., Thornton C.R., Gavin E. Wakley and Talbot N. *Mol Microbiol* **2005**, *56(1)*, 117-125.
16. Palmieri G., Giardina P., Marzullo L., Desiderio B., Nitti G. Sannia G. *Appl. Microbiol. Biotechnol.*, **1993**, *39*, 632-636
17. Kern W **1993**, Ed., *Handbook of Semiconductor Cleaning Technology*, Noyes Publishing: Park Ridge, NJ, Ch 1.
18. Kisko K, Szilvay GR, Vainio U, Linder MB, Serimaa R. *Biophys J.* **2008**, *94*, 198-206.

19. Kwan AH, Winefield RD, Sunde M, Matthews JM, Haverkamp RG, Templeton MD, Mackay JP. *Proc Nat Acad Sci USA* **2006**, *103*, 3621-6.
20. Yu L, Zhang B, Szilvay GR, Sun R, Jänis J, Wang Z, Feng S, Xu H, Linder MB, Qiao M. *Microbiology,* **2008**, 154, 1677-85.
21. Russo M.E., Giardina P., Marzocchella A., Salatino P., Sannia G. *Enz. Microbiol. Biotechnol*., **2008**, *42*, 521–530
22. Piontek K, Antorini M, Choinowski T. *J Biol Chem.* **2002**; *77*, 37663-9.
23. Ferraroni M, Myasoedova NM, Schmatchenko V, Leontievsky AA, Golovleva LA, Scozzafava A, Briganti F. *BMC Struct Biol*. **2007**, *7*, 60.

3.4.2 Peptide immobilization

The hydrophobin biofilm was also used to immobilize peptides on an interesting surface, the MALDI sample plate used, for example, in the SELDI-TOF-MS. This technology is a variation of MALDI-MS that use a modified target to achieve biomedical affinity. The SELDI-TOF-MS represents the successful combination of retentate chromatography and mass spectrometry, and is an essential part of Protein Chip System. By performing protein analyses on a single experimental platform, it is possible to answer biomedical questions (127,128). This technology, utilizing Immobilized-Metal Affinity surfaces, can be used as a pseudo-specific chromatographic surface or as a biospecific interactive surface, for clinical applications and for research proteomic activity (129).

Preliminary results indicate that the steel surface of the MALDI sample plate can be modified by an hydrophobin biofilm, so changing the wettability of the sample plate and its affinity for biological molecules. Hydrophobin biofilm was deposited on the plate, washed as usual, than peptides were placed on it, and the plate washed several times under strong conditions. Peptide immobilization was analysed by MALDI-MS. MALDI spectra reported in figure 3.30 show several peaks corresponding to the expected peptides which were detected on the surface covered by the hydrophobin biofilm, whilst only few peptides could be detected in the absence of the biofilm. Taking into consideration the simplicity of obtaining the biofilm of these self-assembling proteins, we think that an improvement of the SELDI technique could be feasible due to use of hydrophobin biofilms.

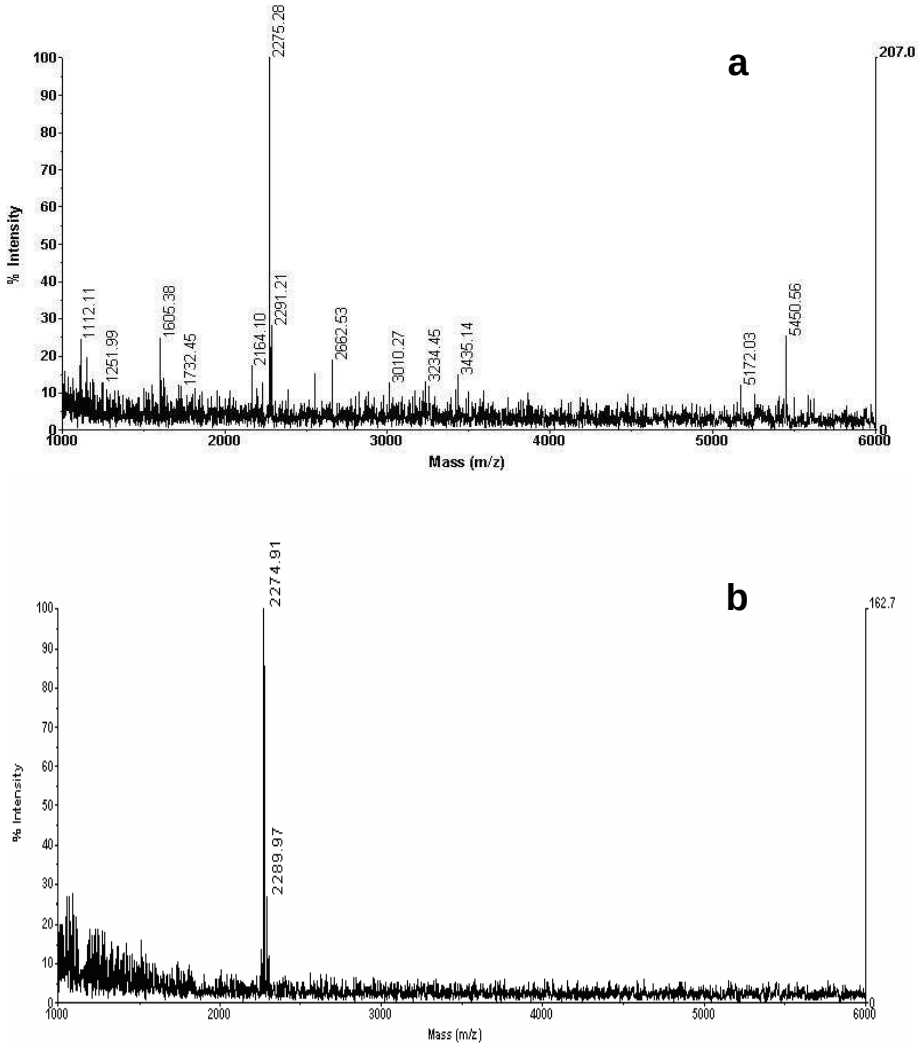

*Figure 3.30 Particular of MALDI-MS spectra of peptides immobilized on MALDI sample plates with (**a**) or without hydrophobin biofilms (**b**).*

3.4.3 Liquid crystals alignment

Liquid crystals (LCs) are very special kind of fluids showing long-range order of their molecules: this means that even if the mechanical properties, such as viscosity, of a LC is typical of that of a fluid, the diffraction pattern of a LC film shows characteristic diffraction peak as it happens in the case of crystalline solid. LCs are also non-Newtonian, optically anisotropic fluids, whose molecules can be re-oriented by external magnetic, electrical, thermal and optical fields so that they present a particularly interesting challenge in the context of material science. LCs are widely known for their applications in displays, telecommunications, and electro-optic devices. However, they are very important system model for a large class of biological organisms: membranes, cytoskeleton proteins, amino acids, viruses, and lipids can form LC phases not only *in vitro* but even *in vivo.* Anisotropic fluids can be found in medical applications in drug delivery, and also have relevance to diseases such as atherosclerosis and cystic fibrosis. Many everyday materials in household, such as soaps, detergents, dyes, food products, and colorants, exhibit LC polymorphism when dissolved in water (130,131).

The quality of LC based display strongly depends on the anchoring of LC molecules on the surface of the support material. Usually the LC molecules can be aligned parallel or perpendicular to the surface depending on the chemical substrate deposited on the surface. The common chemical agents for LC alignment are silanols or surfactant such as DMOAP. We have investigate the possibility to use the hydrophobin biofilm as aligning substrate on surfaces which could be of interest for opto-electronic industry, such as silicon or glass. The hydrophobin monolayer, self-assembled on these surfaces can induce a controlled alignment of liquid crystal molecules.

In particular, we found that the ordered hydrophobin monolayers can well align LC nematic phases (5CB), with oblique or homeotropic alignment (fig. 3.31). The alignment is influenced by the amphiphilic layer exposed by a hydrophobin biofilm, which can be different in case of LB or LS films. With this discovery it will be possible to substitute the aligned layer of organic synthesis with a biological one: the hydrophobin biofilm. In this way lower manufacture costs and lower environmental impact will be possible.

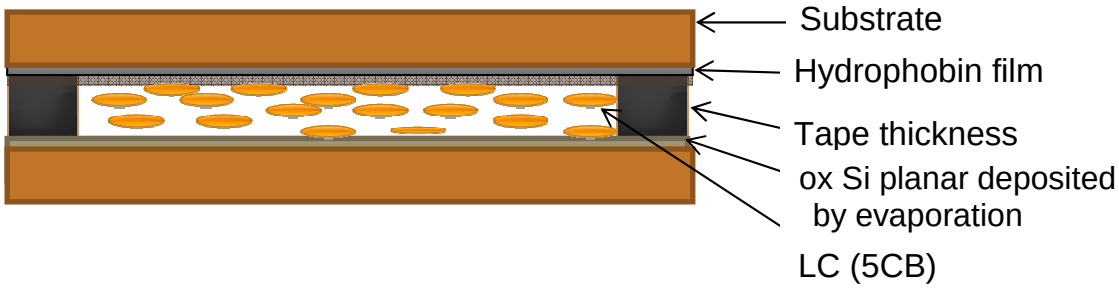

Figure 3.31 Schematic representation of hydrophobin biofilm planar cell.

The details of this inventions are reported in the italian patent:

<De Stefano L., Armenante A., Giardina P., Giocondo M., Rea I., Rendina I., "Un metodo per indurre l'allineamento dei cristalli liquidi nei dispositivi ottici a cristalli liquidi" n. NA2007A000077 del 21.06.2007>

Descrizione dell'Invenzione avente per Titolo:

Un metodo per indurre l'allineamento dei cristalli liquidi nei dispositivi ottici a cristalli liquidi.

a nome di: Luca De Stefano, residente in Via Jannelli 23, 80128, Napoli; Michele Giocondo, residente in via Paparelle 12/c 87100 Cosenza, tutti domiciliati elettivamente presso Luca De Stefano, Via Pietro Castellino, 111, 80131 (NA).

Autori: L. De Stefano, M. Giocondo, P. Giardina, A. Armenante, A. Mazzulla, F. Ciuchi, I. Rea, I. Rendina.

Riassunto

La presente invenzione riguarda l'utilizzo di materiale organico nella fabbricazione di dispositivi optoelettronici a cristalli liquidi in grado di indurre l'allineamento desiderato delle molecole del mezzo liquido cristallino. Il materiale organico biologico, in particolare proteine purificate da micro-organismi, è depositato, quale substrato allineante, con tecniche adeguate su materiali di supporto di comune utilizzo nei dispositivi basati sui cristalli liquidi, quali vetro e materiali semiconduttori. L'invenzione descrive inoltre la realizzazione di alcuni dispositivi ottici che utilizzano gli strati molecolari considerati.

Testo della descrizione

La presente invenzione riguarda l'allineamento dei cristalli liquidi in generale e la fabbricazione di dispositivi elettro-ottici basati sui cristalli liquidi. I cristalli liquidi sono ampiamente impiegati nella realizzazione di schermi di varia

dimensione utilizzati nelle televisioni a schermo piatto, nei telefoni cellulari, negli orologi digitali e in qualunque strumento per la visualizzazione di numeri o immagini. L'elemento base di questi prodotti è una cella, costituita da due vetri su ciascuno dei quali è stato depositato un elettrodo trasparente e uno strato sottile di materiale per l'allineamento, nella quale un cristallo liquido a seconda del tipo, nematico o ferroelettrico, assume una particolare distribuzione. Questa può od esempio essere "twisted", e cioè con una rotazione di 90° tra la direzione delle molecole in prossimità dell'elettrodo superiore rispetto a quello inferiore, oppure una configurazione "supertwisted", e cioè con una struttura in cui la direzione di allineamento delle molecole del cristallo liquido è ruotata di un angolo maggiore di 90°, ovvero altre distribuzioni, in modo da sfruttare la variazione di birifrangenza dovuta alla modulazione di un campo elettrico, applicato attraverso gli elettrodi trasparenti, che riorienta le molecole del cristallo liquido stesso. Il modo più comune di ottenere questi allineamenti è di depositare sui vetri della cella dei substrati polimerici (poliammide) o inorganici (SiOx). I primi necessitano di un ulteriore trattamento meccanico per definire la direzione di allineamento che altrimenti risulterebbe distribuita in modo casuale nel piano del substrato. Vi sono ulteriori tecniche di preparazione degli strati allineanti, riportate in letteratura scientifica o in brevetti, che permettono un orientamento perpendicolare alla superficie (omeotropico) oppure obliquo delle molecole di cristallo liquido nella cella. I requisiti degli strati allineanti sono: bassa oppure alta energia di ancoraggio secondo la particolare applicazione, trasparenza alla luce, buone proprietà dielettriche, stabilità ottica e termica a

lungo termine, ed in alcune applicazioni, l'esistenza di un angolo di pre-tilt uniforme su tutto lo strato.

Le idrofobine sono delle proteine di piccole dimensioni (100-130 aminoacidi) prodotte da diversi tipi di funghi e caratterizzate da una elevata attività superficiale. La loro più interessante proprietà consiste nella capacità di auto-assemblarsi in membrane anfifiliche quando vengono a contatto con superfici idrofobiche o idrofiliche sulle quali aderiscono stabilmente grazie ad interazioni non covalenti. Sia per le loro caratteristiche chimico-fisiche, sia per la possibilità di produrne quantitativi consistenti tramite opportune procedure di purificazione, le idrofobine sono state proposte o utilizzate per una serie di applicazioni tecnologiche che vanno dalla modifica della bagnabilità delle superfici, ai biosensori, o i a nuovi materiali biocompatibili. Le idrofobine si dividono in due classi in base alla stabilità del biofilm formato: le idrofobine di classe I formano uno strato molto stabile che si può sciogliere solo trattandolo con acidi forti (acido trifluoroacetico o acido formico). Le idrofobine di classe II formano invece delle strutture meno resistenti che possono essere sciolte anche in etanolo o in presenza di detergenti.

Attraverso studi sperimentali sulle tecniche di deposizione delle idrofobine, siamo riusciti a dimostrare che monostrati di idrofobine di classe I auto-assemblati sulla superficie del vetro, o di materiali di interesse per l'industria optoelettronica, sono in grado di indurre un allineamento controllato delle molecole di cristallo liquido, come mostrato nella Figura 1 dove lo strato A indica le molecole di cristallo liquido, lo strato B quello di idrofobine e lo strato C il supporto. Le idrofobine sostituiscono completamente gli strati allineanti di

origine organica sintetica con enormi possibilità di risparmio sui costi e di impatto ambientale sul ciclo di produzione dei dispositivi. La proprietà delle idrofobine di formare membrane auto-assemblate resistenti ai cambiamenti di temperatura, pressione e pH, dipendono esclusivamente dalla loro sequenza amminoacidica e di conseguenza dalla struttura tridimensionale, che è stata determinata solo per poche idrofobine (Kwan et al. PNAS, 2006, 103, 3621; Hakanpaa et al. Protein Sci. 2006, 15, 2129). In queste strutture sono evidenti due distinti domini, uno idrofobico e l'altro idrofilico. Queste proteine si ritrovano in forma solubile, fino a valori di concentrazione dell'ordine delle decine di microgrammi/millilitro, in dipendenza dalla natura del solvente. L'invenzione proposta consiste nella messa a punto di alcune tecniche di deposizione delle idrofobine su vetro, silicio, silicio poroso ed altre superfici di interesse tecnologico, inclusi i metalli ed i materiali plastici, con la finalità di modificarne la bagnabilità e di permettere opportuno allineamento delle molecole dei cristalli liquidi su di esse. L'invenzione ora verrà descritta in alcuni esempi non limitativi:

Esempio 1: Purificazione delle idrofobine.

Le idrofobine vengono purificate dal terreno di coltura (estratto di patata-destrosio 24 g/l, estratto di lievito 5 g/l) di un ceppo del fungo basidiomicete *Pleurotus ostreatus*. Sfruttando la peculiare tendenza di queste proteine a formare aggregati, si è messo a punto un protocollo di purificazione che prevede: **a)** l'aggregazione delle idrofobine per "bubbling" del brodo di coltura, **b)** il loro recupero per centrifugazione **c)** la risolubilizzazione con acido trifluoroacetico **d)** l'evaporazione dell'acido **e)** la dissoluzione del campione in etanolo al 60%, **f)** la

separazione per centrifugazione della componente polisaccaridica insolubile dalla proteina solubile. La proteina che viene così purificata è stata identificata come l'idrofobina Vmh2-1 da *Pleurotus ostreatus*.

Esempio 2: Deposizione delle idrofobine per adsorbimento.

Le idrofobine, in stato monomerico o polimerico, sono sciolte in soluzioni acquose o idro-alcoliche, in solventi polari o apolari, a carattere idrofobico o idrofilico e depositate sulla superficie di materiali, con superficie idrofobica o idrofillica, di interesse tecnologico quali semiconduttori, plastiche, polimeri e vetri in quantità sufficiente a ricoprire uniformemente tutta la zona interessata; una volta evaporato il solvente, i campioni sono posti su piastra riscaldante o in stufa alla temperatura di condizionamento (variabile da temperatura ambiente fino a 100 °C) per ottenere un biofilm auto-assemblato che risulti resistente ai solventi utilizzati per la deposizione ed in generale a tutte le sostanze che non siano acidi forti come l'acido trifluoroacetico o l'acido fluoridrico.

Esempio 3: Deposizione delle idrofobine con tecnica Languimir-Blodgett e Langmuir-Sheffer.

La tecnica di Langmuir consiste nel formare strati monomolecolari all'interfaccia aria acqua e di variarne la pressione superficiale comprimendo mediante barriere La deposizione su supporti solidi può avvenire tramite la tecnica di Langmuir-Blodgett (ovvero a pressione costante immergendo il substrato ripetutamente attraverso il film) o la tecnica Langmuir-Schaefer (sempre a pressione costante appoggiando il substrato orizzontalmente sulla superficie e ripetendo l'operazione più volte). Nel primo caso gli strati depositati

sono centrosimmetrici, nel secondo caso (a meno di riarrangiamenti posteriori) gli strati presentano una asimmetria. Una combinazione delle due tecniche permette di avere il numero di strati necessari (da uno a N) e le caratteristiche dell'ultimo strato idrofilico od idrofobico a seconda delle esigenze. Per ottenere una maggiore adesione del film al substrato sono auspicabili trattamenti specifici.

Esempio 4: Realizzazione di celle con allineamento dei cristalli liquidi.

Film mono-molecolari di Idrofobine ottenuti per mezzo della tecnica di LB descritta all'esempio 3, hanno la capacità di allineare gli usuali materiali liquido-cristallini in una maniera che dipende dai precedenti trattamenti subiti dal substrato su cui vengono depositate. Infatti il carattere anfifilico delle molecole di idrofobine è in grado di modificare le proprietà di bagnabilità dei substrati sui quali vengono depositati. Un film di idrofobine depositato su di un substrato idrofilico, quale è il vetro, si struttura in modo da esporre la parte idrofobica delle molecole e pertanto induce un allineamento perpendicolare sulle molecole di cristallo liquido. Viceversa, un film di idrofobine depositato su di un substrato reso idrofobico, ad esempio mediante silanizzazione, si struttura in modo da esporre le parti idrofiliche ed è quindi in grado di indurre un allineamento planare oppure obliquo sulle molecole dei cristalli liquidi. La tecnica di Langmuir adottata per depositare il film di idrofobine consente una strutturazione molecolare tale da definire la direzione di allineamento dei cristalli liquidi senza la necessità di ulteriori trattamenti. Tuttavia una maggiore uniformità dell'allineamento può essere ottenuta sottoponendo il film ad un usuale trattamento di rubbing.

Rivendicazioni

1- Si rivendica l'utilizzo delle proteine appartenenti alla famiglia delle idrofobine per il condizionamento di superfici di interesse tecnologico quali il silicio, il silicio poroso, il vetro, gli ossidi, i metalli, le plastiche, i materiali semiconduttori;

2- Come da rivendicazione n. 1, si rivendica l'utilizzo delle idrofobine per indurre un allineamento planare o omeotropico dei cristalli liquidi su di una superficie,

3- Come da rivendicazione n. 2, si rivendica l'utilizzo delle idrofobine per indurre l'allineamento desiderato dei cristalli liquidi in dispositivi optoelettronici o elettro-ottici comunemente utilizzati in ottica;

4- Come da rivendicazione n. 3, si rivendica l'utilizzo di proteine appartenenti alla famiglia delle idrofobine come tali o prodotti e/o modificati mediante la tecnologia del DNA ricombinante, derivatizzati con fluorofori, sequenze tag o cromogeni;

5- Come da rivendicazione n. 4, si rivendica l'utilizzo delle idrofobine quale substrato attivo per l'interazione proteina-proteina per la realizzazione di biochip ottici o elettrici utilizzabili in studi di proteomica;

6- Come da rivendicazione n. 5, si rivendica l'utilizzo delle idrofobine quali elementi chelanti in grado di trattenere i metalli pesanti presenti in soluzione e quindi utilizzabili nella realizzazione di biosensori.

7- Come da rivendicazione n. 6, si rivendica l'utilizzo delle idrofobine quale materiale di protezione per le superfici di interesse biotecnologico, quali metalli, vetri, polimeri e semiconduttori, durante i trattamenti di fabbricazione chimico-fisici.

Figura 1

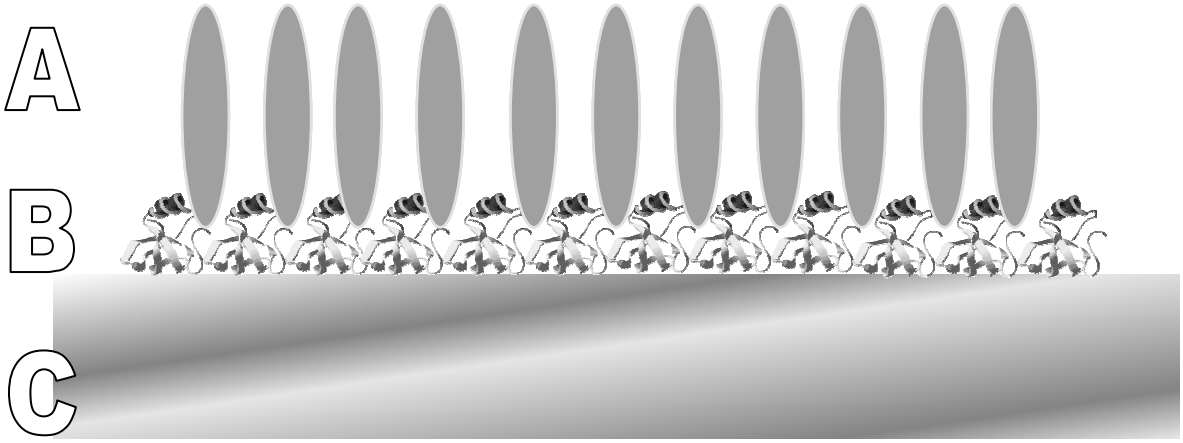

4 Discussion

A hydrophobin from the basidiomycete fungus *Pleurotus ostreatus* was purified, and identified as vmh2-1, whose encoding gene, specifically expressed in the vegetative mycelium, had been previously isolated by Penas et al. (100). The protein undergoes a proteolytic processing, since the N terminus is either T25 or D26, whereas the expected signal peptide is M1-A21, according to the SignalP prediction program (http://www.cbs.dtu.dk/services/SignalP/). Sequence analysis (hydropathy pattern and spacing between the cysteine residues) and robustness of the aggregates (dissolved only in 100% TFA) demonstrate that it belongs to Class I hydrophobins.

Although hydrophobins are generally reported to share low sequence identity percentage (24), comparison of the sequence of the often-used example of class I hydrophobin, SC3, with that of vmh2 reveals a 46% identity of the whole sequence, raising to 62% if the fragment starting from the first Cysteine of the disulfide pattern is considered. The main difference between the two sequences lies in the T stretch upstream of the first C of SC3, that is absent in vmh2. This T stretch in SC3 is reported to be O-linked to mannose residues, thus further increasing the hydrophilicity of that region and consequently, of the whole protein (25). The absence of this region in vmh2 could suggest a higher hydrophobicity of the *P. ostreatus* protein with respect to SC3.

Our results conclusively demonstrate that pure vmh2 is not soluble in water. The other two Class I hydrophobin, SC3 and EAS of *N. crassa*, which were also studied, can be dissolved in water up to 1 mg ml^{-1}(132), furthermore, class II hydrophobins are reported to be much more soluble (up to 10 mg ml^{-1}) (133). Therefore to the best of our knowledge, vmh2 is the most hydrophobic hydrophobin characterized so far.

Analysed protein samples purified from culture medium containing amylose (PDY) have shown the presence of glycans in the hydrophobin aggregates. The protein-glycans complex is soluble in water, whereas the free protein is not. If the complex is dissolved in 60% ethanol, the glycan fraction precipitates, leaving the protein free in this solution. However, the protein purified from ME broth or from a minimum medium (in the absence of amylose) is not water soluble whilst it is soluble in 60% ethanol. Therefore, we can conclude that the interaction with glycans enables the protein to be water soluble.

The structure of the glycans matched to α 1-4 linked glucose. Moreover the data indicated the absence of reducing ends, pointing towards a cyclic structure containing from six to sixteen monomers, namely α, β, γ cyclodextrins and higher homologues. It is well known that cyclodextrins can accommodate hydrophobic guest molecules, thus changing their solubility (134). In particular, the more studied α, β, and γ cyclodextrins exhibit a truncated cone-shaped structure. The cavity of the torus is hydrophobic, while the rest of it is hydrophilic, making the cavities favourable places for hydrophobic interactions to occur thus enabling the formation of inclusion complexes.

Enzymatic activities like 4-α-glucanotransferase can be responsible for the synthesis of cyclodextrins (135). These enzymes are widely distributed in bacteria, yeasts, plants, and mammals and an increasing number of 4-α-glucanotransferases from different sources are known to be able to catalyze cyclization reactions to produce cycloamylose (136).

It has been demonstrated and hence worth noting the Alzheimer's amyloid β-peptide interacts with β-cyclodextrin and this interaction reduces fibril formation and

neurotoxicity (137,138). This interaction is considered to be hydrophobic in nature which suggests that it involves aromatic side chains of the peptide and the hydrophobic cavity of the cyclodextrin. Therefore this interaction might interfere with the oligomerization process of amyloid β-peptide.

Our results on the vmh2-cyclodextrins interactions strengthen the similarity of the behaviors of Class I hydrophobins and amyloid peptides. In the case of the highly hydrophobic protein vmh2, cyclodextrins could play a similar role increasing vmh2 hydrophilicity thus permitting its solubility in water, but not preventing vmh2 self aggregation.

The behaviour of vmh2-cyclodextrins complex is similar to that described for the multiple assembled states of SC3 (139). Three different states depending upon experimental conditions had been pointed out by these authors: soluble SC3, consisting of unimers or multimers in micelle-like association (U-SC3), solution-assembled SC3 (S-SC3), resulting from time dependent ordering in aqueous media without external perturbation (obtained when U-SC3 was allowed to stand undisturbed over a considerable period of time) forming SDS-insoluble structures, and I-SC3 inter-facially assembled structures obtained immediately by vortexing of U-SC3 solution.

As a matter of fact the vmh2-cyclodextrins complex dissolved in water is prone to self assemble when was allowed to stand undisturbed over a period of time as S-SC3, (as demonstrated by the decrease of the protein concentration and of the SDS PAGE band intensity during time). An even higher propensity to form aggregates is shown in buffered solutions, (where SDS insoluble multimers are detectable by SDS-PAGE, the concentration of the protein in solution decreases very rapidly, and an intense band corresponding to a multimer is present in FFF fractogram). Therefore comparison of the buffered or water solution indicated a quicker shift in equilibrium towards the solution-assembled protein in the buffered solution.

Moreover, the vmh2-cyclodextrins complex, dissolved in water or buffered solutions, forms inter-facially assembled structures, as I-SC3, obtained immediately by vortexing of monomeric hydrophobin.

On the other hand, when pure protein is dissolved in a less polar solvent (60% ethanol) no propensity to self assemble is observed (no decrease in the protein concentration and of the SDS PAGE band intensity during time) and no conformational change has been observed upon vortexing the solution (by CD analyses). In these conditions vmh2 differs from SC3 because of the absence of detectable inter-facially or solution assembled structures (I-SC3 or S-SC3). Even when the pure hydrophobin is dissolved in a more polar solvent (20% ethanol), no change of the CD spectrum is observed after agitation of the protein solution. On the other hand a different behaviour is observed in this condition as far as the protein concentration is concerned. The amount of soluble protein is much lower than that achieved in 60% ethanol and protein concentration decreases during time. Further investigations are needed to explore the occurrence of the different aggregation states of the vmh2 hydrophobin in different solvents.

The behaviour of the aggregates was investigated by analysing the biofilms, obtained by depositing either on hydrophobic or hydrophilic surfaces, the pure protein in ethanol or the cycloamylose-protein complex in water. The biofilms were always washed out with hot SDS, and thereafter the thicknesses of the biofilm was determined using spectroscopic ellipsometry.

Pure hydrophobin vmh2, dissolved in the apolar solvent (60% ethanol), forms a very stable biofilm on a hydrophobic surface when conditions favouring self assembling are used, such as incubation at 80℃. Ethanol evaporation quickly occurs at high temperature, thus leading to a reduction of monomeric hydrophobin solubility. Moreover, changes of the secondary structure (shown by CD analysis) takes place between 70 and 80 ℃, similar to that observed when the aggregation process was induced by agitation of a hydrophobin water solution.

When the pure protein was deposited on a hydrophilic surface, oxidized silicon, the biofilm could not be detected. It is worth noting that pure vmh2 can form a biofilm on oxidized porous silicon, a hydrophilic surface. This result can be explained considering that the protein was not only deposited on the surface of the porous silicon but adsorbed by infiltration. Therefore other interactions can contribute to stabilize the biofilm in this case. The vmh2 hydrophobin forms also Languimir Film (LB) deposited on hydrophilic surfaces (es. ITO), but in this case the hydrophobin self-assembling occurs at the water-air interface and then the biofilm is deposited on a hydrophilic surface. Moreover in this case the stability of the monolayer biofilm on hydrophilic surfaces is lower than the stability of a biofilm on hydrophobic surfaces as demonstrated by the different resistances to rubbing (in the patent ref).

Using the cyclodextrin-vmh2 complex dissolved in water, biofilms have been obtained on both surfaces, hydrophilic or hydrophobic. Therefore we can conclude that cyclodextrins are necessary for vmh2 assembly into films on hydrophilic surfaces, whereas the pure vmh2 can assembly only on hydrophobic surface.

Martin et al (77) demonstrated that *Schizophyllum commune* produces and excretes a high molecular weight polysaccharide, schizophyllan that stabilizes small hydrophobin multimers in solution, and proposed a model in which the polysaccharide acts as a hydrophilic stabilizer. Moreover schizophyllan is necessary for SC3 assembly into films on hydrophilic surfaces, whereas SC3 alone can assemble only on hydrophobic surfaces. From these points of view the function of cyclodextrins towards vmh2 is similar to that of schizophyllan towards SC3.

Biofilms obtained on hydrophylic or hydrophobic surfaces using the cyclodextrin-vmh2 complex dissolved in water have thicknesses always higher but much more variable then that obtained from pure protein on crystalline silicon. According to the model proposed by *Martin et al*. (77), the presence of schizophyllan enhances adhesion to hydrophilic surfaces thereby exposing the hydrophobic portion of the protein molecules. However this model could be too simple to explain the behaviour of the vmh2-cyclodextrin system. The variability and the high thicknesses of the biofilms obtained in our experiments on hydrophilic or hydrophobic surfaces, is not easily described by a simple double layer of polysaccharides and proteins. In our case more complex interactions have to occur, probably the complexity and variety of the polysaccharide molecules has to be taken into account to explain the observed behaviour.

The vmh2 biofilm on Si is very stable from a chemical point of view, since it is still present after strong denaturing washing in SDS at 100℃ as other class I biofilm (46). The resistant modification of the silicon surface can be used to protect the nanocrystalline material from basic dissolution in NaOH and for the fabrication process, such as the KOH wet etch, which is the basis of silicon micromachining techniques. Under these conditions we have also demonstrated that the amphiphilic properties of these proteins led to changing of the wettability of silicon surfaces (from ~90° for the

silicon surface to ~ 60° for the silicon coated by biofilm). The change in the nature of surfaces is a well known phenomenon, and it is a fact that other hydrophobins such as SC3 when dried on hydrophobic surfaces, such as Teflon, change the water contact angle (from ~100° to about 60° for surface coated b y biofilm) (46). The nanometric biofilm can turn the hydrophobic silicon surface into a hydrophilic one, but it also leaves unaltered the sensing ability of such an optical transducer, adding chemical stability, which can be a key factor in biomolecular experiments. The wettability changes were also demonstrated with porous silicon both from a hydrophobic surface into a hydrophilic and viceversa. The ability to switch between two different wettability regimes could be a key feature in designing bioactive interfaces for miniaturization not only for biosensors but also for medical devices.

AFM observations of LB films revealed the coexistence of monolayer and rodlets. From these measurements we were able to estimate the size of the rodlets and the monolayer thickness: we conclude that the observed rodlets are actually formed by hydrophobin bilayers embedded in the LB monolayer. The rodlets of vmh2 were of a lower thickness than other class I Hydrophobin (5 nm for vmh2 and 10 nm for SC3) but at the same time they are not easily dissociated (140).

Moreover the monolayer can act as substrate to bind peptides or proteins, such as BSA and enzymes such as laccase.

These results can be the starting point in the fabrication of a new generation of hybrid devices for biosensing research, encompassing such micro technology of micro-electrodes, microfluidic devices, lab-on-a-chip, which all call for restricted equipment sizes, limited quantity of bioactive molecules and therefore high efficiency of biomaterial utilization.

5 References

1. Wessels J.G.H., de Vries O.M.H., Ásgeirsdóttir S.A., Springer J., The *thn* mutation of *Schizophyllum commune,* which suppresses formation of aerial hyphae, affects expression hydrophobin gene. *J. Gen. Microbiol*., 1991b, 137: 2439-2445.
2. Stringer M.A., Dean R.A., Sewall T.C. and Timberlake W.E., Rodletness, a new *Aspergillus* developmental mutant induced by directed gene inactivation. *Genes Dev*., 1991, 5: 1161-1171.
3. Bell-Pedersen D., Dunlap J.C., Loros, J.J., The *Neurospora* circadian clock-controlled gene, *ccg-2*, is allelic to *eas* and encodes a fungal hydrophobin required for formation of the conidial rodlet layer. *Genes Dev.*,1992, 6: 2382-2394.
4. Wösten, H.A.B., de Vries, O.M.H. and Wessels, J.G.H. (1993). Interfacial self-assembly of a fungal hydrophobin into a hydrophobic rodlet layer*. Plant Cell,* 1993, 5: 1567-1574.
5. Wösten H.A.B., van Wetter M.-A., Lugones L.G., van der Mei H.C., Busscher, H.J. and Wessels J.G.H., How a fungus escapes the water to grow into the air. *Curr. Biol*., 1999, l9: 85-88.
6. Wösten H.A.B., Schuren F.H.J. and Wessels J.G.H., Interfacial self-assembly of a hydrophobin into an amphipathic membrane mediates fungal attachment to hydrophobic surfaces. *EMBO J*.,1994, 13: 5848-5854.
7. Lugones, L.G., Wösten, H.A.B., Birkenkamp, K.U., Sjollema, K.A., Zagers, J.,and Wessels, J.G.H., Hydrophobins line air channels in fruiting bodies of *Schizophyllum commune* and *Agaricus bisporus*. *Mycol. Res.,* 1999, 103: 635-640.
8. van Wetter M.-A., Wösten H.A.B. and Wessels J.G.H., SC3 and SC4 hydrophobins have distinct roles in formation of aerial structures in dikaryons of *Schizophyllum commune*. *Mol. Microbiol*., 2000, 36: 201-210
9. Wessels, J.G.H., Hydrophobins: proteins that change the nature of a fungal surface. *Adv. Microb. Phys., 1997,* 38: 1-45.
10. Wösten H.A., Hydrophobins: multipurpose proteins. *Annu Rev Microbiol*., 2001, 55: 625-46.
11. Linder M.B., Szilvay G.R., Nakari-Setälä T., Penttilä, M.E., Hydrophobins: the protein amphiphiles of fungi. *FEMS Microbiol. Rev., 2005,* 29 : 877-896.
12. Claessen, D., Stokroos, I., Deelstra, H.J., Penninga, N.A., Bormann, C., Salas, J.A.,Dijkhuizen, L., and Wösten, H.A., The formation of the rodlet layer of *Streptomycetes* is the result of the interplay between rodlins and chaplins. *Mol. Microbiol*., 2004*,* 53: 433-443.
13. Linder MB, Szilvay GR, Nakari-Setälä T, Penttilä ME. Hydrophobins: the protein-amphiphiles of filamentous fungi. FEMS Microbiol Rev. 2005, 29(5): 877-896.
14. Kazmierczak P, Kim DH, Turina M, Van Alfen NK.A Hydrophobin of the chestnut blight fungus, Cryphonectria parasitica, is required for stromal pustule eruption. *Eukaryot Cell.* 2005, 4(5): 931-936.
15. St. Leger, R.J., Staples, R.C., and Roberts, D.W., Cloning and regulatory analysis of starvation-stress gene, *ssgA*, encoding a hydrophobin-like protein from the entomopathogenic fungus, *Metarhizium anisopliae*. *Gene,* 1992*,* 120(1): 119-124.
16. Talbot N.J., Ebbole D.J., Hamer J.E., Identification and characterization of MPG1, a gene involved in pathogenicity from the rice blast fungus Magnaporthe grisea. *Plant Cell*., 1993; 5(11): 1575-1590.

17. Talbot N.J., Kershaw M., Wakley G.E., de Vries O.M.H., Wessels J.G.H. and Hamer J.E., *MPG1* encodes a fungal hydrophobin involved in surface interactions during infection related development of the rice blast fungus *Magnaporthe grisea*. *Plant Cell,* 1996*,* 8: 985-999.
18. Viterbo A., and Chet I., *TasHyd1*, a new hydrophobin gene from the biocontrol agent *Trichoderma asperellum*, is involved in plant root colonization. *Molecular Plant Pathology,* 2006, 7: 249-258.
19. Tagu D. and Martin F., Molecular analysis of cell wall proteins expressed during the early steps of ectomycorrhiza development. *New Phytol*., 1996, 133: 73-85.
20. Tagu D., De Bellis R., Balestrini R., De Vries O.M.H., Piccoli G., Stocchi V., Bonfante P., Martin F., Immunolocalization of hydrophobin HYDPt-1 from the ectomycorrhizal basidiomycete Pisolithus tinctorius during colonization of *Eucalyptus globulus* roots. *New Phytol*., 2001, 149: 127-135.
21. Mankel A., Krause K., Kothe E., Identification of a hydrophobin gene that is developmentally regulated in the ectomycorrhizal fungus *Tricholoma terreum*. *Appl. Environ. Microbiol.,* 2002, 68: 1408-1413.
22. Honegger R., Developmental biology of lichens. *New Phytol.,* 1993, 125: 659-677.
23. Ikeno S., Szilvay G.R., Linder M., Aritomi H., Ajimi M., Haruyama T.,. Protein dot stamp using hydrophobin as immobilization carrier. *Sensorsand Materials,* 2004, 16: 413-420.
24. Sunde M., Kwan A.H., Templeton M.D., Beever R.E., Mackay J.P., Structural analysis of hydrophobins. *Micron,* 2008, 39(7): 773-784.
25. de Vocht M.L., Scholtmeijer K., van der Vegte E.W., de Vries O.M.H., Sonveaux N., Wösten H.A.B., Ruysschaert J.-M., Hadziioannou G., Wessels J.G.H., Robillard G.T., Structural characterization of the hydrophobin SC3, as a monomer and after self-assembly at hydrophobic/hydrophilic interfaces. *Biophys. J.,* 1998, 74: 1-10.
26. Fan H., Wang X., Zhu J., Robillard G.T., Mark A.E., Molecular dynamics simulations of the hydrophobin SC3 at a hydrophobic/hydrophilic interface. *Proteins,* 2006, 64: 863-873.
27. Kwan A.H.Y., Winefield R.D., Sunde M.,. Matthews J.M,. Haverkamp R.G, Templeton M.D.,. Mackay J.P., Structural basis for rodlet assembly in fungal hydrophobins. *PNAS*., 2006, 103: 3621-3626.
28. Kwan A.H.Y, Macindoe I., Vukasin P.V., Morris V.K., Kass I., Gupte R., Mark A.E., Templeton M.D., Mackay J.P., Sunde M., The Cys3-Cys4 loop of the hydrophobin EAS is not required for rodlet formation and surface activity. *J Mol Biol*., 2008, 10, 382(3): 708-720.
29. Hakanpaa J., Paananen A., Askolin S., Nakari-Setälä T., Parkkinen T., Penttila M., Linder M.B., Rouvinen J., Atomic resolution structure of the HFBII: a self-assembling amphiphile. *J. Biol. Chem.,* 2004, 279: 534-539.
30. Hakanpää J., Linder M., Popov A., Schmidt A., Rouvinen J. Hydrophobin HFBII in detail: ultrahigh-resolution structure at 0.75Å. *Biological Crystallography, 2006a,* 62: 356–367.
31. Hakanpää J., Szilvay G.R., Kaljunen H., Maksimainen M., Linder M., Rouvinen J., Two crystal structures of *Trichoderma reesei* hydrophobin HFBI. The structure of a protein amphiphile with and without detergent interaction. *Protein Sci., 2006b,* 15: 2129-2140.

32. Wessels J.G.H., Hydrophobins: Proteins that change the nature of the fungal surface. *Adv. Microb. Physiol*.,1997, 38: 1-45.
33. Wösten H.A.B. and de Vocht M.L., Hydrophobins, the fungal coat unravelled. *Biochim. Biophys. Acta*, 2000, 1469, 79-86.
34. Wösten H.A.B. and Wessels J.G.H., Hydrophobins, from molecular structure to multiple functions in fungal development. *Mycoscience*, 1997, 38: 363-374.
35. Wessels J.G.H., Developmental regulation of fungal cell wall formation. Ann. *Rev. Phytopathol*., 1994, 32: 413-437
36. Wang X., Shi, Wösten F., Hektor H.A.B, Poolman H.B., Robillard, G.T., The SC3 Hydrophobin Self-Assembles into a Membrane with Distinct Mass Transfer Properties. *Biophys. J.,* 2005, 88(3): 434-443.
37. Lumsdon S.O., Green J. and Stieglitz B., Adsorption of hydrophobin proteins at hydrophobic and hydrophilic interfaces. Colloids Surf., 2005, 44: 172-178.
38. Linder M.B., Szilvay G.R., Nakari-Setälä T., and Penttilä M.E., Hydrophobins: the protein amphiphiles of fungi. *FEMS Microbiol. Rev,* 2005, 29, 877-896.
39. Lugones L.G., Bosscher J.S., Scholtmeyer K., de Vries O.M., Wessels J.G., An abundant hydrophobin (ABH1) forms hydrophobic rodlet layers in Agaricus bisporus fruiting bodies. *Microbiology*., 1996, 142(5): 1321-1329.
40. Lugones L.G., Wösten H.A.B. and Wessels J.G.H., A hydrophobin (ABH3) specifically secreted by vegetatively growing hyphae of *Agaricus bisporus* (common white button mushroom). *Microbiology*, 1998, 144: 2345-2353
41. Mackay J.P., Matthews J.M., Winefield R.D., Mackay L.G., Haverkamp, R.G., Templeton M.D., The hydrophobin EAS is largely unstructured in solution and functions by forming amyloid-like structures. *Structure*, 2001, 9: 83-91.
42. Scherrer,S., de Vries O.M.H., Dudler R., Wessels J.G.H. and Honegger R., Interfacial self-assembly of fungal hydrophobins of the lichen-forming ascomycetes *Xanthoria parietina* and *X*. *ectaneoides*. *Fungal Genet. Biol*, 2000, 30: 81-93.
43. de Vocht M.L., Structural changes that accompany the self-assembly of hydrophobins. *Ph.D. Thesis. Groningen: University of Groningen*. 2001, 1-97.
44. Dempsey G.P., Beever R.E., Electron microscopy of the rodlet layer of Neurospora crassa conidia. *J Bacteriol*., 1979, 140(3): 1050-1062.
45. Girardin H., Paris S., Rault J., Bellon-Fontaine M.N. Latgé J.P., The role of the rodlet structure on the physicochemical properties of Aspergillus conidia. *Lett Appl Microbiol*. 1999, 29(6): 364-369.
46. Wosten H.A.B., de Vocht M.L., Hydrophobins, the fungal coat unravelled. *Biochim. Biophis Acta,* 2000, 1469 (2): 79-86.
47. Butko P., Buford J.P., Goodwin J.S., Stroud P.A., McCormick C.L., Cannon G.C., Spectroscopic evidence for amyloid-like interfacial selfassembly of hydrophobin Sc3. *Biochem. Biophys. Res. Commun.,* 2001, 280: 212-215.
48. Wang X., Shi F., Wösten H.A., Hektor H., Poolman B., Robillard G.T., The SC3 hydrophobin self-assembles into a membrane with distinct mass transfer properties. *Biophys J.,* 2005, 88(5): 3434-3443.
49. van der Vegt W, van der Mei HC, Wösten HA, Wessels JG, Busscher HJ. A comparison of the surface activity of the fungal hydrophobin SC3p with those of other proteins. *Biophys Chem*., 1996, 57(2-3): 253-60.

50. Mackay J.P., Matthews J.M., Winefield R.D., Mackay L.G., Haverkamp R.G., Templeton M.D., The hydrophobin EAS is largely unstructuredin solution and functions by forming amyloid-like structures. *Structure,* 2001, 9: 83-91.
51. Russo P.S., Blum F.D., Ipsen J.D., Miller W.G., Abul-Hajj Y.J., The surface activity of the phytotoxin cerato-ulmin. *Can. J. Bot,* 1982, 60: 1414-1422.
52. De Vries O.M., Moore S., Arntz C., Wessels J.G., Tudzynski P., Identification and characterization of a tri-partite hydrophobin from Claviceps fusiformis. A novel type of class II hydrophobin. *Eur J Biochem.*, 1999, 262(2): 377-385.
53. Paananen A., Vuorimaa E., Torkkeli M., Penttilä M., Kauranen M., Ikkala O., Lemmetyinen H., Serimaa R., Linder M.B,. Structural hierarchy in molecular films of two class II hydrophobins. *Biochemistry*., 2003, 42(18): 5253-5258.
54. Torkkeli M., Serimaa R., Ikkala O., Linder M., Aggregation and self-assembly of hydrophobins from Trichoderma reesei: low-resolution structural models. *Biophys J.,* 2002, 83(4): 2240-2247.
55. de Vocht M.L., Reviakine I., Ulrich W.P., Bergsma-Schutter W., Wösten H.A.B., Vogel H., Brisson A., Wessels J.G.H., Robillard G.T., Self-assemblyof the hydrophobin SC3 proceeds via two structural intermediates. *Protein Sci.,* 2002, 11, 1199-1205.
56. de Vocht M.L., Reviakine I., Wösten H.A., Brisson A., Wessels J.G., Robillard GT., Structural and functional role of the disulfide bridges in the hydrophobin SC3. *J Biol Chem.,* 2000, 275(37): 28428-28432.
57. Askolin S., Penttilä M., Wösten H.A., Nakari-Setälä T., The *Trichoderma reesei* hydrophobin genes *hfb1* and *hfb2* have diverse functions in fungal development. *FEMS Microbiol. Lett.,* 2005, 253: 281-288
58. Askolin S., Linder M., Scholtmeijer K., Tenkanen M., Penttilla M., de Vocht M.L., Wosten H.A.B., Interaction and Comparison of a Class I Hydrophobin from Schizophyllum commune and Class II Hydrophobins from Trichoderma reesei. *Biomacromolecules*, 2006, 7: 1295-1301.
59. Szilvay G.R., Kisko K., Serimaa R., Linder M.B., The relation between solution association and surface activity of the hydrophobin HFBI from Trichoderma reesei. *FEBS Lett.* 2007, 581(14): 2721-2726.
60. Scholtmeijer K., Wessels J.G., Wösten H.A., Fungal hydrophobins in medical and technical applications. *Appl. Microbiol. Biotechnol.,* 2001, 56: 1-8.
61. Takai S., Pathogenicity and cerato-ulmin production in Ceratocystis ulmi. *Nature*, 1974, 252(5479): 124-126.
62. Takai, S.,Richards W.C., Cerato-ulmin, a wilting toxin of *Ceratocystis ulmi*: Isolation and some properties of cerato-ulmin from the culture of *C. ulmi*. *Phytopath. Z*., 1978, 91: 129-146.
63. Schuurs T.A., Schaeffer E.A.M., Wessels J.G.H., Homology-dependent silencing of the SC3 gene in Schizophyllum commune. *Genetics*, 1997, 147: 589-596.
64. Scholtmeijer K., Janssen M.I., Gerssen B., de Vocht M.L., van Leeuwen B.M., van Kooten T.G., Wösten H.A., Wessels J.G., Surface modifications created by using engineered hydrophobins. *Appl. Environ Microbiol*., 2002, 68(3): 1367-1373.
65. Peñas M.M., Asgeirsdottir S.A., Lasa I., Culianez-Macia F.A., Pisabarro A.G., Wessels J.G., Ramirez L. Identification, characterization, and In situ detection of a fruit-body-specific of *Pleurotus ostreatus. Appl. Environ. Microbiol*., 1998, 64(10): 4028-4034.

66. de Vries O.M.H., Fekkes M.P., Wösten H.A.B., Wessels J.G.H., Insoluble hydrophobin complexes in the walls of *Schizophyllum commune* and other filamentous fungi. *Arch. Microbiol.,*1993, 159: 330-335.
67. Wessels J.G.H., de Vries O.M.H., Ásgeirsdóttir S.A., Schuren F.H.J., Hydrophobin genes involved in formation of aerial hyphae and fruit bodies in *Schizophyllum commune*. *Plant Cell,* 1991a, 3: 793-799.
68. de Groot P.W.J., Schaap P.J., Sonnenberg A.S.M., Visser J., van Griensven L.J.L.D., The *Agaricus biosporus hypA* gene encodes a hydrophobin and specifically accumulates in peel tissue of mushroom caps during fruit body development. *J. Mol. Biol.,* 1996, 257: 1008-1018.
69. Asgeirsdóttir S.A., Halsall J.R., Casselton L.A., Expression of two closely linked hydrophobin genes of Coprinus cinereus is monokaryon-specific and down-regulated by the oid-1 mutation. *Fungal Genet Biol*., 1997, 22(1): 54-63.
70. Spanu P., HCF-1, a hydrophobin from the tomato pathogen *Cladosporium fulvum*. *Gene*, 1997, 193: 89-96.
71. van Wetter M.A., Wösten H.A.B., Wessels J.G.H., SC3 and SC4 hydrophobins have distinct roles in formation of aerial structures in dikaryons of *Schizophyllum commune*. *Mol. Microbiol*., 2000, 36: 201-210.
72. Trembley M.L., Ringli C., Honegger R., Hydrophobins DGH1, DGH2, and DGH3 in the Lichen-Forming Basidiomycete *Dictyonema glabratum*. *Fungal Genet. Biol*., 2002, 35: 247-259.
73. Paris S., Debeaupuis J.-P., Crameri R., Carey M., Charlès F., Prévost M. C., Schmitt C., Philippe B. and Latgé J.P., Conidial hydrophobins of *Aspergillus fumigatus*. *Appl. Environ. Microbiol*., 2003, 69: 1581-1588.
74. Templeton M.D., Greenwood D.R. and Beever R.E., Solubilization of *Neurospora crassa* rodlet proteins and dentification of the predominant protein as the proteolytically processed eas (ccg-2) gene product. *Exp. Mycol.,* 1995, 19: 166-169.
75. Mackay J.P., Matthews J.M., Winefield R.D., Mackay L.G., Haverkamp R.G., Templeton M.D., The Hydrophobin EAS Is Largely Unstructured in Solution and Functions by Forming Amyloid-Like Structures of polypeptide chains, has actually been applied in nature to form these remarkable structures. *Structure*. 2001, 9, 83–91.
76. Takahashi T., Maeda H., Yoneda S., Ohtaki S., Yamagata Y., Hasegawa F., Gomi K., Nakajima T., Abe K., The fungal hydrophobin RolA recruits polyesterase and laterally moves on hydrophobic surfaces. *Mol. Microbiol*., 2005, 57: 1780-1796.
77. Martin G.G., Cannon G.C. and McCormick C.L., Sc3p hydrophobin organization in aqueous media and assembly onto surfaces as mediated by the associated polysaccharide Schizophyllan. Biomacromolecules, 2000, 1: 49-60.
78. Wang X., de Vocht M.L., Jonge J.D., Poolman B. and Robillard G.T., Structural changes and molecular interactions of hydrophobin SC3 in solution and on a hydrophobic surface. *Protein Sci.,* 2002, 11: 1172-1181.
79. Carpenter C.E., Mueller R.J., Kazmierczak P., Zhang L., Villalon D.K. and van Alfen N.K., Effect of virus on accumulation of a tissue-specific cellsurface protein of the fungus *Cryphonectria* (*Endothia*) *parasitica*. *Mol. Plant Microbe Interact*, 1992, 4: 55-61.

80. Nakari-Setäl T., Aro N., Ilmen M., Kalkkinen N. and Penttilä M., Differential expression of the vegetative and spore-bound hydrophobins of *Tricoderma reesei*, Cloning and characterization of the *hfb2* gene. *Eur. J. Biochem*., 1997, 248: 415-423.
81. Nakari-Setälä T., Aro N., Kalkkinen N., Alatalo E. and Penttilä M., Genetic and biochemical characterization of the *Tricoderma reesei* hydrophobin HFBI. *Eur. J. Biochem*., 1996, 235: 248-255.
82. Janssen M.I., van Leeuwen M.B., Scholtmeijer K., van Kooten, T.G., Dijkhuizen L., Wösten, H.A., Coating with genetic engineered hydrophobin promotes growth of fibroblasts on a hydrophobic solid. *Biomaterials,* 2002, 23: 4847-4854.
83. Kleemola, T., Nakari-Setälä, T., Linder, M., Penttilä, M., Kotaviita, E., Olkku, J.and Haikara, A.. Characterisation and detection of the gushing factors produced by fungi. In: *Proc. E.B.C. 28th Congr., Budapest*. ,2001, 1-10.
84. Scholtmeijer K., Wessels J.G., Wösten H.A., Fungal hydrophobins in medical and technical applications. *Appl. Microbiol. Biotechnol.,* 2001, 56*,* 1-8.
85. Nakari-Setälä T., Azeredo J., Henriques M., Oliveira R., Teixeira J., Linder M., Penttilä M., Expression of a fungal hydrophobin in the *Saccharomyces cerevisiae* cell wall: effect on cell surface properties and immobilization. *Appl. Environ. Microbiol*., 2002, 68: 3385-3391.
86. Linder M., Szilvay G.R., Nakari-Setälä T., Söderlund H. and Penttilä M., Surface adhesion of fusion proteins containing the hydrophobins HFBIand HFBII from *Trichoderma reesei*. *Protein Sci*. 2002, 11: 2257-2266
87. Palomo J.M., Peñas M.M., Fernández-Lorente G., Mateo C., Pisabarro A.G., Fernández-Lafuente R., Ramirez L., Guisán J.M., Solid-phase handling of hydrophobins: immobilized hydrophobins as a new tool to study lipases. *Biomacromolecules,* 2003, 4: 204-210.
88. Linder M., Szilvay G.R., Nakari-Setälä T., Söderlund H., Penttilä M., Surface adhesion of fusion proteins containing the hydrophobins HFBI and HFBII from *Trichoderma reesei*. *Protein Sci*., 2002, 11, 2257-2266.
89. Collen A., Persson J., Linder M., Nakari-Setälä T., Penttilä M., Tjerneld F., Sivars U., A novel two-step extraction method with detergent/polymer systems for primary recovery of the fusion protein endoglucanase I -hydrophobin I. *Biochim. Biophys. Acta*., 2002, 1569: 139-150.
90. Chang R., Functional properties of edible mushrooms. *Nutr. Rev*., 1996, 54: 91–93.
91. Ballero M., E. Mascia A. Rescigno and E. S. Use of *Pleurotus* for transformation of polyphenols in waste waters from olive presses into proteins. *Micol. Italiana*, 1990, 19: 39–41.
92. Puniya A., Shah K.G., Hire S.A., Ahire R.N., Rathod M.P., Mali R.S., Bioreactor for solid-state fermentation of agro-industrial wastes. *Indian J. Microbiol*.,1996, 36: 177–178.
93. Giardina P., Aurilia V., Cannio R., Marzullo L., Amoresano A., Siciliano R., Pucci P., Sannia G., The gene, protein and glycan structures of laccase from *Pleurotus ostreatus*. Eur*. J. Biochem.,* 1996, 235: 508–515.
94. Gunde-Cimerman N., Medicinal value of the genus *Pleurotus* (Fr.) P. Karst. (*Agaricales* s.l., *Basidiomycetes*). *Intl. J. Med. Mushrooms*, 1999,1: 69–80.
95. Marzullo L., Cannio R., Giardina P., Santini M., Sannia G., Veratryl alcohol oxidase from *Pleurotus ostreatus* participates in lignin biodegradation and prevents

polymerization of laccase-oxidized substrates. *J. Biol. Chem.,* 1995, 270: 3823–3827.
96. Axtell C., Johnston C.G., Bumpus J.A., Bioremediation of soil contaminated with explosives at the Naval Weapons Station Yorktown. *Soil Sediment Contam*., 2000, 9: 537–548.
97. Abdellah M.M.F., Emara M.F.Z., Mohammady T.F., Open field interplanting of oyster mushroom with cabbage and its effect on the subsequent eggplant crop. *Ann. Hortic. Sci. Cairo,* 2000, 45: 281–293.
98. Asgeirsdottir S.A., de Vries O.M., Wessels J.G., Identification of three differentially expressed hydrophobins in *Pleurotus ostreatus* (oyster mushroom). *Microbiology*, 1998144: 2961–2969.
99. Peñas M.M., Hidrofobinas asociadas a diferentes fases del desarrollo del hongo *Pleurotus ostreatus*. *Ph.D thesis, Universidad Pu´blica de Navarra, Pamplona, Spain*. 1999, 1-185.
100. Peñas M.M., Rust B., Larraya L.M., Ramírez L., Pisabarro A.G., Differentially regulated, vegetative-mycelium-specific hydrophobins of the edible basidiomycete Pleurotus ostreatus. *Appl Environ Microbiol.,* 2002, 68(8): 3891-3898.
101. Ásgeirsdóttir S.A., de Vries O.M.H., Wessels J.G.H., Identification of three differentially expressed hydrophobins in *Pleurotus ostreatus* (oyster mushroom), *Microbiology,* 1998, 144: 2961-2969.
102. Ma A, Shan L, Wang N, Zheng L, Chen L, Xie B., Characterization of a Pleurotus ostreatus fruiting body-specific hydrophobin gene, Po.hyd. *J Basic Microbiol*., 2007, 47(4): 317-324.
103. Chaplin M. F.; Kennedy J. F., In *Carbohydrate Analysis: A Practical approach*; 2nd ed.; D. Rickwood and D. Hames, Eds.; IRL press: London, UK, 1994
104. Cleveland D. W., Fischer S.G., Kirschner M. W., Laemmli U.K., Peptide mapping by limited proteolysis in sodium dodecyl sulfate and analysis by gel electrophoresis *J Biol Chem.*, 1977, 252,:1102-1106.
105. Leontein K., Lönngren J., Assignment of absolute configuration of sugars by g.l.c. of their acetylated glycosides formed from chiral alcohols, *Methods Carbohydr. Chem.,* 1978, 62: 359-362.
106. Molinaro A., De Castro C., Lanzetta R., Parrilli M., Petersen B.O., Broberg A., Duus J., NMR and MS evidences for a random assembled O-specific chain structure in the LPS of the bacterium Xanthomonas campestris pv. Vitians. A case of unsystematic biosynthetic polymerization. *Eur J Biochem*., 2002, 269(17): 4185-4193.
107. Hakomori S., A rapid permethylation of glycolipid and polysaccharide catalyzed by methylsulfinyl carbanion in dimethyl sulfoxide. J. Biochem. *J. Biochem*., 1964, 55: 205-208.
108. States D.J., Haberkorn R.A., Ruben D.J., A Two-Dimensional Nuclear Overhauser Experiment with Pure Absorption Phase in Four Quadrants *J. Magn. Reson*., 1982, 48: 286-292.
109. Wang X., Permentier H.P., Rink R., Kruijtzer J.A., Liskamp R.M., Wösten H.A., Poolman B., Robillard G.T., Probing the self-assembly and the accompanying structural changes of hydrophobin SC3 on a hydrophobic surface by mass spectrometry. *Biophys. J.,* 2004b, 87: 1919-1928.

110. Swatkoski S., Russel S. C., Edwards N.,, Fenselau C., Rapid chemical digestion of small acid –soluble spore proteins for analysis of bacillus spores. *Analytical Chemistry*, 2006, 78: 181-188.
111. Lin S.S., Wu C. H., Sun M.C., Sun C.M., Ho Y.P., Microwave –assisted enzyme-catalyzed reactions in various solvent systems. J*. Am. Soc. Mass Spectrom.* 2005, 16: 581-588.
112. Hua L., Low T.Y., Sze K.S., Micowave –assisted specifiv chemical digestion for rapid protein identification. *Proteomics*, 2006, 6: 586-591.
113. Inglis A.S., Cleavage at aspartic acid Methods Enzymol., 1983; 91: 324-332**.**
114. Kyte J., Doolittle R.F., A simple method for displaying the hydropathic character of a protein. *J Mol Biol,* 1982, 157: 105–132.
115. Reschiglian P., Zattoni A., Cinque L., Roda B., Dal Piaz F., Roda A., Moon M.H., Min B.R., Hollow-Fiber Flow Field-Flow Fractionation for Whole Bacteria Analysis by Matrix-Assisted Laser Desorption/Ionization Time-of-Flight Mass Spectrometry. *Anal. Chem.,* 2004, 76: 2103-2111.
116. Reschiglian P., Moonb M.H., Flow field-flow fractionation: A pre-analytical methodfor proteomics. *J. of Proteomics*, 2008, 71: 265-276.
117. Reschiglian P., Zattoni A., Roda B., Nichelini E., Roda A., Field-flow fractionation and biotechnology, *TRENDS in Biotecnology*, 2005, 23: 475-483.
118. Roda B., Reschiglian P., Zattoni A., Tazzari P., Buzzi M., Ricci F., Contadini A., Human lymphocyte sorting by gravitational field-flow fractionation. *Anal Bioanal Chem*, 2008, 392: 137–145.
119. Chaniotakis N, Sofikiti N., Novel semiconductor materials for the development of chemical sensors and biosensors: a review. *Anal Chim Acta*., 2008, 615(1): 1-9.
120. De Stefano L., Rossi M., Staiano M., Mamone G., Parracino A., Rotiroti L., Rendina I., Rossi M., D'Auria S., Glutamine-Binding Protein from Escherichia coli Specifically Binds a Wheat Gliadin Peptide Allowing the Design of a New Porous Silicon-Based Optical Biosensor. *Journal of Proteome Research,* 2006, 5: 1241-1245.
121. Kane R.S., Stroock A.D., Nanobiotechnology: Protein-Nanomaterial Interactions. *Biotechnol. Prog*., 2007, 23: 316-319.
122. J. Buriak, High surface area silicon materials: fundamentals and new Phil. Trans*. R. Soc. A* , 2006, 364: 217–225.
123. L. De Stefano, L. Rotiroti, I. Rendina, L. Moretti, V. Scognamiglio, M. Rossi, S. D'Auria, Porous silicon-based optical microsensor for the detection of l-glutamine, Biosensors and Bioelectronics, 2006, 21, 1664–1667.
124. Zasadzinski J.A., Viswanathan R., Madsen L., Garnaes J., Schwartz D.K., Langmuir-Blodgett films. *Science*, 1994, 263(5154): 1726-1733.
125. Girard-Egrot A.P., Godoy S., Blum L.J., Enzyme association with lipidic Langmuir-Blodgett films: interests and applications in nanobioscience., *Adv Colloid Interface Sci.,* 2005, 116(1-3): 205-225.
126. Szilvay G.R., Self-assembly of hydrophobin proteins from the fungus Trichoderma reesei P*h.D. Thesis, VTT Technical Research Centre of Finland University of Helsinki,* 2007, 1-64.
127. White C.N., Zhang Z., Chan D.W, Quality control for SELDI analisys, *Clin Chem. Lab. Med.,* 2005, 43(2): 125-126.

128. Poon TC., Opportunities and limitations of SELDI-TOF-MS in biomedical research: practical advices. *Expert Rev Proteomics,* 2007; 4(1): 51-65.
129. Tang N., Tornatore P., Weinberger S.R., Current developments in SELDI technology. *Mass spectrometry reviews*, 2003, 23(1): 34-44.
130. Gleeson F.H., Wood T.A., Dickinson M., Laser manipulation in liquid crystals: an approach to microfluidics and micromachines. *Phil. Trans. R. Soc. A*, 2006, 364, 2789–2805.
131. Höger S., Weber J., Lepper A., Enkelmann V., Shape-persistent macrocycles with intraannular alkyl groups: some structural limits of discotic liquid crystals with an inverted structure. *Beilstein Journal of Organic Chemistry,* 2008, 4(1): 1-6.
132. Wang X., Graveland-Bikker J.F., de Kruif C.G., Robillard, G.T., Oligomerization of hydrophobin SC3 in solution: from soluble state to selfassembly. *Prot. Sci.,* 2004a, 13: 810-821.
133. Kisko K., Szilvay G.R., Vainio U., Linder M.B., Serimaa R., Interactions of hydrophobin proteins in solution studied by small-angle X-ray scattering. *Biophys J.,* 2008, 94(1): 198-206.
134. Lindner K., Saenger W., Crystal structure of the gamma-cyclodextrin n-propanol inclusion complex; correlation of alpha-, beta-, gamma- cyclodextrin geometries. *Biochem Biophys Res Commun.,* 1980. 92(3): 933-938.
135. Takaha T., Smith S.M., The functions of 4-alpha-glucanotransferases and their use for the production of cyclic glucans. B*iotechnol Genet Eng Rev.,* 1999, 16: 257-280.
136. Yanase M., Takata H., Takaha T., Kuriki T., Smith S.M., Okada S., Cyclization reaction catalyzed by glycogen debranching enzyme (EC 2.4.1.25/EC 3.2.1.33) and its potential for cycloamylose production. *Appl Environ Microbiol*., 2002, 68(9): 4233-4239.
137. Camilleri P., Haskins N.J., Howlett D.R., Beta-Cyclodextrin interacts with the Alzheimer amyloid beta-A4 peptide. *FEBS Lett.,* 1994, 21, 341(2-3): 256-258.
138. Danielsson J., Jarvet J., Damberg, P., Gräslund A., Two-Site Binding of b-Cyclodextrin to the Alzheimer Ab(1-40) Peptide Measured with Combined PFG-NMR Diffusion and Induced Chemical Shifts. *Biochemistry*, 2004, 43: 6261-6269.
139. Stroud P.A., Goodwin J.S., Butko P., Cannon G.C., McCormick C.L., Experimental evidence for multiple assembled states of Sc3 from Schizophyllum commune. *Biomacromolecules.*, 2003, 4(4): 956-967.
140. Yu L,, Zhang B., Szilvay G.R., Sun R., Jänis J., Wang Z., Feng S., Xu H., Linder M.B., Qiao M., Protein HGFI from the edible mushroom Grifola frondosa is a novel 8 kDa class I hydrophobin that forms rodlets in compressed monolayers. *Microbiology*, 2008; 154: 1677-1685.

Publications

- L. De Stefano, I. Rea, **A. Armenante**, P. Giardina, M. Giocondo, I. Rendina “Self-Assembled Biofilm of Hydrophobins Protects the Silicon Surface in the KOH Wet Etch Process” *Langmuir* 2007; 23(15): 7920-7922

- L. De Stefano, **A. Armenante**, P. Giardina, M. Giocondo, I. Rea, I. Rendina “Un metodo per indurre l'allineamento dei cristalli liquidi nei dispositivi ottici a cristalli liquidi" n. NA2007A000077 del 21.06.2007 *(national patent)*

- L. De Stefano, I. Rea, P. Giardina, **A. Armenante**, I. Rendina “Protein-Modified Porous Silicon Nanostructures” *Advanced Materials* 2008, 20(8): 1529-1533

- S. Houmadi, F. Ciuchi, M. De Santo., L. De Stefano, I. Rea., P. Giardina., **A. Armenante,** E. Lacaze., M. Giocondo "Langmuir Blodgett film of hydrophobin protein from *Pleurotus ostreatus* at the air-water interface" *Langmuir* 2008, DOI:10.1021/la802306r

- L. De Stefano, I. Rea, E. De Tommasi, I. Rendina, L. Rotiroti, M. Giocondo, S. Longobardi, **A. Armenante**, and P. Giardina “Bioactive Modification of Silicon Surface using Self-assembled Hydrophobins from *Pleurotus ostreatus*” *Colloids and Surface B: Biointerfaces* (submitted 24/09/2008)

- **A. Armenante**, S. Longobardi, I. Rea, L. De Stefano, M. Giocondo, A. Silipo, A. Molinaro, P. Giardina. “The *Pleurotus ostreatus* hydrophobin vmh2 and its association with glucans” *Biomacromolecules* (submitted 16/10/2008)

Communications

- L. De Stefano, **A. Armenante,** I. Rea, I. Rendina, P. Giardina "Protein modified porous silicon structures” NanoSmat 2007 (Nano porous semiconductors), Algarve, Portugal, 9-11July 2007.

- L. De Stefano, I. Rea, **A. Armenante**, M. Giocondo, I. Rendina, P. Giardina Merging bio/non-bio interfaces for advanced hybrid optical icrosystems", Oral, Optical Microsystems 2007, Capri (Napoli), Italia, 30 September-3 October, 2007.

- **A. Armenante**, P. Giardina, L. De Stefano, I. Rea, I. Rendina, M. Giocondo “Hydrophobins from *Pleurotus ostreatus*: characterization and applications” Annual workshop of the COST 868 action on *Biotechnical functionalisation of renewable polymeric materials* Graz, Austria 12-14 September, 2007.

- L. De Stefano, I. Rea, L. Rotiroti, I. Rendina, P. Giardina, **A. Armenante**, S. Longobardi, “Bio/non-bio interfaces for a new class of proteins microarrays” XIII Conferenza Nazionale *AISEM*, Roma, Italia, 19-21 February, 2008.

- L. De Stefano, I. Rea, P. Giardina, **A. Armenante**, I. Rendina, "Porous silicon devices modified by self-assembled molecular biofilm" 6th International Conference on *Porous Semiconductuctors-Science and Technology*, Mallorca, Spagna, 10-14 March, 2008.

- I. Rea, E. De Tommasi, I. Rendin, P. Giardina, **A. Armenante**, S. Longobardi, and L. De Stefano, “Ellipsometric Characterization of Self-assembled Biological Films on Silicon based Substrate” *European optical society Annual Meeting* EOS, Parigi, Francia, 29 october-2 November, 2008

Acknowledgments

I wish to thank the Coordinator of the Doctorate, Prof. G. Sannia who gave me the possibility to work on a very interesting project and all Professors that worked to make unforgettable these years of the Doctorate.
I am grateful to the Dean of the Faculty of “Scienze Biotecnologiche” Prof. Gennaro Marino for the helpful discussions and for his critical reading of the manuscript.

I owe my deepest gratitude to my tutor, Prof. Paola Giardina, for all her advice, her support, and care-taking, her broad-minded way of thinking. She was precious in every moment. I wish to thank all the members of the BMA group (especially Prof. P. Pucci and L. Birolo), and other the members of the Department (especially Prof. A. Molinaro, D. Picone, C. Ercole and A. Silipo) for their skilled technical support and for the helpful advice. I thank all the past and present members of the “Fungi” group (Annalisa, Alessandra, Claudia, Donata, Flavia, Rosario, Maria, Maidia, Cinzia, Jianbin, Giovanna) for their kindness, their support during these years and for enjoyable atmosphere they helped to create. I thank Dr. Cinzia Pezzella e Giovanni Chiappetta, who were not only good colleagues but also precious friends of this adventure.

Special thanks go to the little group of “hydrophobins”, Enzo, Nunzio and Sara, for their help. It has been great to work with them! I thank them because my work is also their work!

This work was carried out in collaboration with the group of Luca De Stefano at CNR of Naples. I warmly thank Luca and his group (especially Lucia and Ilaria) for providing us with the silicon and other materials to study the self-assembled hydrophobins, letting us exploit their vast knowledge about surfaces and for inspiring meetings and conversations. I’m especially grateful to Luca who has believed in me and was supporter of my thesis.

I am really grateful to Michele Giocondo and the CNR-INFM LICRYL group because they have believed in the hydrophobins and their potential.

I wish to thank Prof. Pierluigi Reschiglian and Barbara Roda for analyzing hydrophobins with the new generation instrument, GrFFF.

I thank my parents who believe in me and are the most important things in my life. I also thank my sister Valentina, she is very important for me and I think she is special. I am very grateful for the love and support that I received from my whole family.

Finally, I find myself out words when trying to express my gratitude to and love for my husband Vittorio. I cherish the life that we share and I warmly thank you for understanding and encouragement.

Appendix I

The Pleurotus ostreatus hydrophobin vmh2 and its association with glucans

Journal:	*Biomacromolecules*
Manuscript ID:	bm-2008-01182t
Manuscript Type:	Article
Date Submitted by the Author:	17-Oct-2008
Complete List of Authors:	Armenante, Annunziata; University "Federico II", Organic Chemistry and Biochemistry Longobardi, Sara; University "Federico II", Organic Chemistry and Biochemistry Rea, Ilaria; National Council of Research, Institute for Microelectronics and Microsystems De Stefano, Luca; National Council of Research, Institute for Microelectronics and Microsystems Giocondo, Michele; National Council of Research-INFM LICRYL, Liquid crystal Laboratory Silipo, Alba; University "Federico II", Organic Chemistry and Biochemistry Molinaro, Antonio; University "Federico II", Organic Chemistry and Biochemistry Giardina, Paola; University "Federico II", Organic Chemistry and Biochemistry

The *Pleurotus ostreatus* hydrophobin vmh2 and its association with glucans

Annunziata Armenante[1], *Sara Longobardi*[1], *Ilaria Rea*[2], *Luca De Stefano*[2], *Michele Giocondo*[3], *Alba Silipo*[1], *Antonio Molinaro*[1], *Paola Giardina*[1*]

[1]Dept. of Organic Chemistry and Biochemistry, University of Naples "Federico II", Via Cintia 4, 80126, Naples, Italy.

[2]Unit of Naples-Institute for Microelectronics and Microsystems, National Council of Research, Via P. Castellino 111, 80131, Naples, Italy.

[3]CNR-INFM LICRYL – Liquid Crystals Laboratory, c/o Dipartimento di Fisica Università della Calabria, 87036 Rende – Italy

[*]corresponding author, E-mail: giardina@unina.it

ABSTRACT

Hydrophobins are small self-assembling proteins, produced by fungi. A Class I hydrophobin secreted by the basidiomycete fungus *Pleurotus ostreatus* has been purified and identified. The pure protein is not water soluble, whereas complexes formed between the protein and glycans, present in culture broth containing amylose, are soluble in water. Glycan structure matched to cyclic structures of α 1-4 linked glucose containing from six to sixteen monomers (cyclodextrins). They increase hydrophilicity of the hydrophobin but do not prevent its self aggregation. Conformational changes of the protein in the aqueous solution after vortexing have been observed. The pure protein dissolved in less polar solvent is not prone to self assembly and no conformational change is observed upon vortexing the solution. When the pure protein was deposited on a hydrophobic surface, crystalline silicon, it forms a very stable biofilm, whereas the biofilm has not been detected on a hydrophilic surface, oxidised silicon. When the water-soluble cyclodextrin-hydrophobin complex was used, thick biofilms were obtained on both surfaces.

INTRODUCTION

Hydrophobins are small proteins (about 100 amino-acid residues) produced by fungi as soluble forms, self-assembling into an amphipatic membrane when they reach an interface (e.g. medium-air or cell wall-air). Because of their properties, these proteins play a role in the formation of aerial hyphae, spores, in fruiting body and in the attachment of hyphae to hydrophobic surfaces during symbiotic or pathogenic interactions[1]. The intriguing properties of these proteins make them of great interest to biotechnologists, as they have potentialities for numerous applications[2]. They could be used as coatings to increase biocompatibility of medical implants, to immobilize enzymes on surfaces, in cosmetic industry for hair-care products, in drug delivery, etc.

At the molecular level, hydrophobins have low sequence identity, but for the presence of eight cysteine residues, forming a conserved four disulfide bonding pattern[3]. Analysis of fungal genomes indicates that hydrophobins are encoded as gene families ranging from two to seven members, but for *Coprinus cinereus* genome which has 23 genes. The proteins have been distinguished in two types, class I and class II hydrophobins, based on the differences in their hydropathy patterns, spacing of aminoacids between the cysteine residues and properties of the aggregates they form[4]. Class I hydrophobins generate very insoluble assemblies, which can only be dissolved in strong acids (i.e. 100% TFA). Assemblies of Class II can be more easily dissolved in ethanol or sodium dodecyl sulphate. Class II hydrophobins have been only detected in Ascomycetes, while class I have been identified in Ascomycetes and Basidiomycetes. One distinguishing feature of class I hydrophobins is the characteristic rodlet structure observed on the hydrophobic side of an amphipathic protein film. The morphology of isolated rodlets is reminiscent of amyloid fibrils whereas the aggregates of Class II hydrophobins lack the rodlet morphology, are non-amyloid, and needle like.

SC3 from *Schyzophyllum commune* is one of the most characterized member of the Class I hydrophobin family. SC3 contains approximately 20 mannose residues, possibly O-linked through threonine residues in the N-terminal region of the protein, modification that increases the

hydrophilicity of that region of the polypeptide chain[5]. When SC3 is induced to self-organize at the air/water or Teflon/water interface, a small, transient increase in α-helical secondary structure is observed, followed by an increase in *β*-sheet structure[6-7]. More recently the structure in solution of another Class I hydrophobin, EAS from *Neurospora crassa*, has been resolved[8]. EAS forms a β-barrel structure interrupted by some disordered regions and displays a complete segregation of charged and hydrophobic residues on its surface. This structure has been used to propose models for the polymeric rodlet structure formation.

Class II hydrophobins are more easily handled, because of their less tendency to aggregate. The crystal structures of two class II hydrophobins, HFBI and HFBII of *Thrichoderma reesei* have been determined, and several other studies on these two proteins have been performed[9-10]. The amino acid sequence of HFBII is 70% similar to HFBI, their 3D structures are similar and they form similar, hexagonally ordered films[11]. The assemblies of HFBI have been recently shown to be more stable than those of HFBII, as the former could tolerate changes in temperature and pH and addition of ethanol better than the latter[12]. The differences in their behaviour could reflect different roles in fungal life.

Aside from these studies, very little is known about other hydrophobins, their characteristics and the films they can form. This could be mainly due to the difficulties in extracting and handling these self-assembling proteins. A deeper knowledge of the properties and behaviours of other fungal hydrophobins, both in solution or assembled, is needed to generalize results obtained so far. We are contributing to this goal by studying hydrophobins secreted by the basidiomycete fungus *Pleurotus ostreatus*. It is a well known edible mushroom and its ligninolytic and biodegradative abilities have been widely reported[13]. Several hydrophobin encoding genes have been identified in *P. ostreatus* and their expression in different growth stages or culture times have been studied[14-15], whereas very little is known on the encoded proteins, their structures and their potential applications.

We have purified the hydrophobin secreted by *P. ostreatus* mycelia. The solubility characteristics of the aggregates formed by this protein clearly indicate that it is a member of Class I

hydrophobin[16]. Actually chemically and mechanically stable mono- and multilayers of self-assembled proteins have been obtained by deposition of the protein on crystalline silicon[17]. The biomolecular membrane changes the wettability of the silicon surface. It has been characterized by variable-angle spectroscopic ellipsometry (VASE) and used as masking material in the KOH wet etch of the crystalline silicon[16]. Because of the high persistence of the protein biofilm, the hydrophobin-coated silicon surface has been perfectly protected during the standard KOH micromachining process. Furthermore we have demonstrated the passivation of some optical devices based on Porous Silicon (PSi) technology when infiltrated by this hydrophobin[18]. The self-assembled protein biofilm changes the wettability of the PSi structures. Moreover this membrane not only protects the nanocrystalline material from basic dissolution in NaOH, but also leaves unaltered the sensing ability of such an optical transducer, adding chemical stability.

In this paper we analyse at molecular level this *P. ostreatus* hydrophobin, its behaviour in solution and that of complexes formed between the protein and cyclodextrins, present in fungal culture broth containing amylose.

EXPERIMENTAL SECTION

Fungal growth and protein purification

White-rot fungus, *P. ostreatus* (Jacq.:Fr.) Kummer (type: Florida) (ATCC no. MYA-2306) was maintained through periodic transfer at 4 °C on potato dextrose agar (Difco) plates in the presence of 0.5 % yeast extract (Difco). Mycelia were inoculated (by adding six agar circles of 1 cm diameter) in 2 l flasks containing 500 ml potato dextrose (24 g/l) broth supplemented with 0.5% yeast extract (PDY) or 2% malt extract (ME) and grown at 28 °C in static cultures.

After 10 days of fungal growth, hydrophobins released into the medium were aggregated by air bubbling using a Waring blender. Foam was then collected by centrifugation at 4,000 x *g*. The precipitate was freeze-dried, treated with TFA for 2hr and sonicated for 30 min. After centrifugation at 3200 x *g* for 20 min, the supernatant was dried again in a stream of air, and then dissolved in water (Hyd-w) or 60% ethanol (Hyd-et). In the latter case, the solution was kept at 4 °C overnight and then centrifuged at 3200 x *g* for 10 min.

Before use the protein was always disassembled with pure TFA, dried, and then the monomeric protein dissolved.

Protein concentration was evaluated by bicinchoninic acid (BCA) assay (Pierce, Rockford, IL) using bovine serum albumin as standard or evaluated by measuring the absorbance band at 280 nm, using a value of ε=1.44 ml mg^{-1} cm^{-1}, when the hydrophobin was dissolved in EtOH solution. This extinction coefficient has been estimated on the basis of the concentration determined using the protein dissolved in water and tested by BCA assay.

Phenol-sulphuric acid test[19]

The glycan solution (200µl) was mixed to 5% phenol (200ml) and sulphuric acid (1ml). This mixture was incubated for 10 min at room temperature and 20 min at 37 °C and then absorbance at 485 nm was determined. Standard curve was performed using from 2 to 200 µg of glucose.

HPLC

A HPLC system (HP 1100 series Agilent Technologies) equipped with a analytical reverse phase Vydac C4 column (25×0.21 cm, 5 µm) (The Separation Group, Hesperia, CA, USA) was used for chromatographic separation. 0.1% trifluoroacetic acid and 10% isopropanol was used as solvent A; 0.1% trifluoroacetic acid in 90% acetonitrile and 10% isopropanol was used as solvent B. A linear gradient of solvent B from 10 to 95% in 65 min at flow rate of 1 ml/min was employed. UV absorbance of the eluent was monitored at 220 nm.

SDS-PAGE

SDS-polyacrylamide gel electrophoresis (SDS-PAGE) was performed at 15% polyacrilamide concentration using the Bio-Rad Mini Protean III apparatus. ß-galactosidase (117 kDa), bovine serum albumine (85.0 kDa), ovalbumin (49 kDa), carbonic anidrase (34.0 kDa), β̃-lactoglobulin (25.0 kDa), lisozyme (19 kDa) were used as standards (Fermentas Inc., Glen Burnie, MD, USA).

The gels were stained by silver staining or by periodic acid staining (GelCode Glycoprotein Staning Kit 24562, Pierce).

Complex reconstitution

PDY broth or an aqueous solution of the previously separated glycans, were added to the dried, TFA treated Hyd-et, and the procedure used for hydrophobin purification (air bubbling, centrifugation, lyophilisation and TFA treatment) was performed. Alternatively Hyd-et (dissolved in 60% ethanol) was diluted up to 4% ethanol and then the aqueous solution of the glycans was added. The sample was then vortexed for 10 min, the aggregates centrifuged, lyophilised, TFA treated and solubilised in water.

Mass spectrometry

MALDI mass spectra were recorded on a Voyager DE Pro MALDI-TOF mass spectrometer (Applied Biosystems, Foster City, CA). The analyte solutions were mixed with sinapinic acid (20 mg/ml in 70% acetonitrile, TFA 0.1% v/v), or 2,5-Dihydroxybenzoic acid (DHB) (25 mg/ml in 70% acetonitrile) or α-cyano-4-hydroxycinnamic acid (10mg/ml in 70% acetronitrile, TFA 0.1%

(v/v) as matrixes, applied to the sample plate and air-dried. The spectrometer was used in the linear or reflectron mode. Spectra were calibrated externally.

In situ hydrolysis was carried out on the silver-stained protein bands excised from a 15% polyacrylamide gel run under denaturing conditions[20]. Excised bands were extensively washed with acetonitrile and then with 0.1 M of ammonium bicarbonate. Protein samples were reduced by incubation in 10 mM dithiothreitol for 45 min at 56°C and carboxamidomethylated by using 55 mM iodoacetamide for 30 min, in the dark, at room temperature. The gel particles were then washed with ammonium bicarbonate and acetonitrile. Enzymatic digestion was carried out with 15 mg/ml trypsin (Sigma-Aldrich, St.Louis, MO, USA) in 10 mM of ammonium bicarbonate, at 4°C for 2 h. The buffer solution was then removed and a new aliquot of buffer solution was added for 18 h at 37°C. A minimum reaction volume, sufficient for complete rehydration of the gel was used. Peptides were then extracted washing the gel particles with 20 mM of ammonium bicarbonate and 0.1% trifluoroacetic acid in 50% acetonitrile at room temperature and then lyophilized. Aliquots of the digests were concentrated and directly analyzed by MALDI-MS.

Peptides from *in situ* hydrolysis were analyzed by LCQ ion trap (Finnigan Corp.) coupled to a 250×2.1 nm, 300 Å Phenomenex Jupiter C18 column on an HP 1100 HPLC (Agilent Technologies). Peptides were eluted at a flow rate of 0.5 ml/min with a 5%–65% gradient of 95% acetonitrile, 5% formic acid and 0.05% TFA in 60 min.

Carbohydrate analysis

GLC and GLC-MS were all carried out as described[21,22]. Monosaccharides were identified as acetylated O-methyl glycosides derivatives. After methanolysis (2M HCl/MeOH, 85°, 24 h) and acetylation with acetic anhydride in pyridine (85°, 30 min) the sample was analyzed by GLC-MS. Linkage analysis was carried out by methylation of the complete core region as described[23]. The sample was hydrolyzed with 2 M trifluoroacetic acid (100°C, 2 h), carbonyl-reduced with $NaBD_4$, , acetylated and analyzed by GLC-MS.

NMR spectroscopy

All spectra were recorded on a solution of 1 mg in 0.5 mL of D_2O, at 300 K, at pD 7. NMR experiments were carried out using a Bruker DRX-600 spectrometer. Chemical shift are in ppm with respect to the 0 ppm point of the manufacturer indirect referencing method. Nuclear Overhauser enhancement spectroscopy (NOESY) was measured using data sets (t1 × t2) of 2048 × 256 points, and 16 scans were acquired. A mixing time of 100 ms was used. Double quantum-filtered phase-sensitive correlation spectroscopy (DQF-COSY) experiment was performed with 0.258 s acquisition time, using data sets of 2048 x 1024 points, and 64 scans were acquired. Total correlation spectroscopy experiments (TOCSY) were performed with a spinlock time of 120 ms, using data sets (t1 × t2) of 2048 × 256 points, and 16 scans were acquired. In all homonuclear experiments the data matrix was zero-filled in the F1 dimension to give a matrix of 4096 x 2048 points and was resolution enhanced in both dimensions by a shifted sine-bell function before Fourier transformation. Heteronuclear single quantum coherence (HSQC) was measured in the 1H-detected mode via single quantum coherence with proton decoupling in the ^{13}C domain, using data sets of 2048 × 256 points, and 64 scans were acquired for each t1 value. Experiments were carried out in the phase-sensitive mode according to the method of States et al[24].

Circular dichroism spectroscopy

Far-UV CD spectra were recorded on a Jasco J715 spectropolarimeter equipped with a Peltier thermostatic cell holder (Jasco model PTC-348), in a quartz cell (0.1-cm light path) from 190 to 250 nm. The temperature was kept at 20° C and the sample compartment was continuously flushed with nitrogen gas. The final spectra were obtained by averaging three scans, using a bandwidth of 1 nm, a step width of 0.5 nm, and a 4 sec averaging per point. The spectra were then corrected for the background signal using a reference solution without the protein.

CD spectra of the protein were also recorded by varying the temperatures from 30 a 90°C at a rate of 1 °C /min with 10°C step.

Biofilm on silicon chip.

Silicon samples, single side polished, <100> oriented (chip size: 1cmx1cm), after standard cleaning procedure have been washed in hydrofluoridic acid solution for three minutes to remove the native oxide thin layer (1-2 nm) due to silicon oxidation. To obtain oxidized silicon, samples have been thermally oxidized in O_2 atmosphere, at 1100 °C for 1 hr, resulting in a oxide thickness of about 80 nm. Samples have been incubated in hydrophobin solutions (0.1 mg/ml in 80% ethanol or water) for 1 h, dried for 10 min on the hot plate (80°C), washed by the solvent solution, and then by 2% SDS at 100 °C for 10 min. At least six different experiments have been performed in each condition.

RESULTS

Purification of the protein

P. ostreatus was grown in static cultures using potato dextrose broth containing yeast extract (PDY) till to the complete coverage of the liquid surfaces by mycelia. The amount of the lyophilised material, obtained after air bubbling into the liquid broths and centrifugation, ranged from 5 to 10 mg/L. After the TFA treatment, the dried material was dissolved in water (Hyd-w) and analysed by SDS-PAGE, showing an unique protein band at about 10 kDa (Fig. 1a). Since about 0.5-1 mg of proteins per litre of culture broth were determined by BCA protein assay, non proteic components have to be present in the dried material obtained after bubbling. Further treatment of this material with 60% ethanol, extracted the hydrophobin in the ethanol solution (Hyd-et), as verified by SDS-PAGE (Fig.1A), leaving the non-proteic component as insoluble precipitate. The presence of glycans in Hyd-w and in the ethanol precipitate was demonstrated by the phenol-sulphuric acid test and by periodic acid staining of the SDS-PAGE (Fig. 1B).

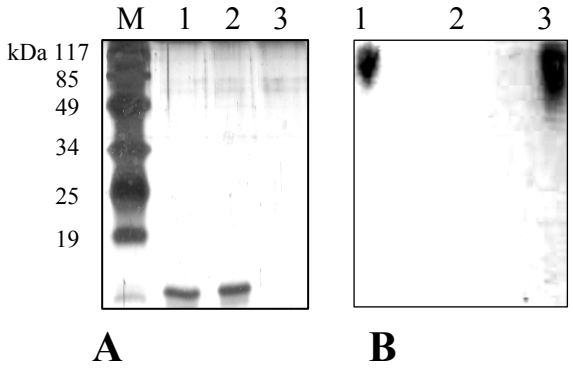

Figure 1 SDS-PAGE of Hyd-w (lane 1); Hyd-et (lane 2); and the precipitate obtained from Hyd-et (lane 3). M: M_w markers. Panel A: Silver stained gel; Panel B: periodic acid stained gel

After glycan separation by precipitation in 60% ethanol, the protein is only soluble in the presence of ethanol, not in pure water. Therefore these glycans, when present, co-aggregate during air-bubbling with hydrophobins, making the protein soluble in water.

However if the hydrophobin was purified from *P. ostreatus* grown in malt extract (ME) cultural broth, the protein was not soluble in water, but in 60% ethanol. In this condition no precipitate was

formed, indicating the absence of the glycan component in this sample. This evidence has been confirmed by the lack of any detectable band when the sample was loaded on periodic acid stained SDS-PAGE .

The maximal concentration of hydrophobin achievable in water is about 0.3 mg ml^{-1}, whereas a concentration of 2 mg ml^{-1} was obtained in 60% ethanol.

To investigate the interactions between the hydrophobin and glycans, an analytical reverse phase chromatography procedure has been set up. Elution of the proteins from the C4 column was only obtained in conditions less polar than the standard (in the presence of 10% isopropanol). Very different elution volumes of Hyd-w and Hyd-et (before and after glycans removal) were observed. As shown in Fig. 2, a single peak eluting at about 10 min was detected, when Hyd-w was loaded on the column, whereas a heterogeneous peak centred at 57 min was eluted when Hyd-et was loaded. The presence of the hydrophobin in these peaks has been confirmed by SDS-PAGE, whereas the simultaneous presence of glycans in the peak eluting at 10 min was confirmed by the phenol-sulfuric acid test. These results indicate that a complex, stable in the conditions used for the chromatography, is formed between the hydrophobin and glycans.

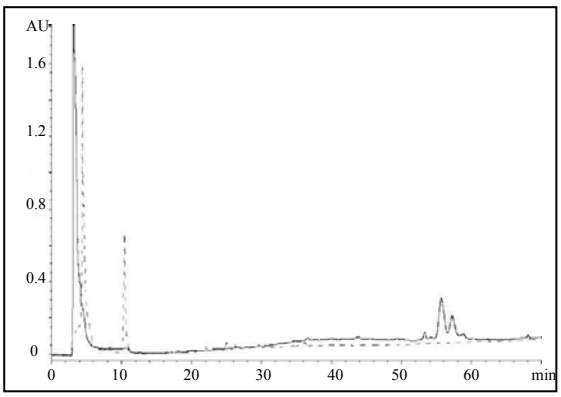

Figure 2 Reverse phase chromatography of Hyd-w (dotted line) and Hyd-et (solid line).

Several conditions have been explored to reconstitute the hydrophobin-glycan complex starting from the dried pure hydrophobin, in order to re-obtain a water soluble protein, but all of them were unsuccessful. The protein was insoluble either in aqueous solution of the glycans or in the PDY broth. The water soluble protein-glycan complex could be re-obtained only when the aqueous

solution of the glycans is added to the Hyd-et solution and the usual aggregation procedure was performed. As a result, co-aggregation of the two components allows the formation of the protein-glycan complex, obtaining the hydrophobin in aqueous solution.

Structural analysis

MALDI MS spectra of the samples (Hyd-w and Hyd-et) show two peaks at 8463 and 8564 m/z (Fig. 3), with the relative intensity of the latter always higher than the former.

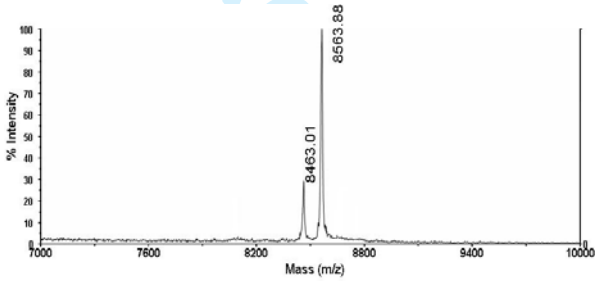

Figure 3 MALDI-MS spectrum of Hyd-w performed in linear mode using sinapinic acid as matrix..

According to Penãs *et al.*[14], *P. ostreatus* hydrophobins undergo a proteolytic processing after signal peptide removal. The peak at 8564 m/z can be attributed to vmh2-1 (TrEMBL accession number Q8WZI2) starting from T25 and with the eight cysteines linked by four disulphide bridges, and the peak at 8463 m/z to the same protein after further removal of the N terminal threonin residue. Analysis of the MALDI-MS spectrum of the tryptic peptides, obtained by *in situ* hydrolysis, showed the presence of the expected peaks at 2001.9 m/z (D26-K44) and 2102.9 m/z (T25-K44), whereas the other expected peak at 6938.6 m/z (corresponding to the peptide A45-L113) was not detected. The absence of this peak could be due to the difficult extraction of such a large peptide by the polyacrylamide gel.

The identity of the protein and its N-terminal processing was confirmed by LC-MS-MS analysis. Fragmentation of the 2102.9 and 2001.9 m/z peak led to the sequences SCSTGSLQC (S29-C37) and CSTGSLQCCSSV (C30-V41) (Supporting information Fig. 1) respectively.

The protein was purified from fungal cultures grown at different times (5, 10, 15 or 20 days), and a relative increase of the intensity of the peak corresponding to the form D26-L113, in respect to

that corresponding to T25-L113, was observed in older cultures. Furthermore a peak at 8349.5 m/z probably corresponding to the form lacking also D26, was detected in the preparation from 15 and 20 days old cultures.

The glycan component of Hyd-w was also subjected to chemical and spectroscopic analyses after purification by ethanol precipitation. Carbohydrate analysis by GLC-MS revealed exclusively the presence of 4-linked D-Glucose in pyranose form (4-D-Glc*p*), no terminal residues were detected, neither reducing nor non-reducing. The ^{1}H NMR spectum of this glucan showed proton signals in the anomeric and ring sugar regions. The water dissolved precipitate was fully assigned by 2D NMR spectroscopy that confirmed the presence of a single component, the α-(1→4) glucan. It is worth to note that reducing ends were undetectable in NMR spectra.

Analysis of MALDI MS spectra of such glucan showed the presence of several peaks whose molecular masses agreed with the theoretical values for cyclic glucans with degree of polymerization from 6 to 16. As a matter of fact, a cyclodextrin blend should have a mass of 162*n*, whereas glucans in any non-cyclic structure should have a molecular mass of 162*n* + 18.

Incubation of the cyclic glucan at 110 °C for two hours at pH 3 led to partial hydrolysis of the cyclic glucans (peaks corresponding to molecular masses of 162*n* + 18), as shown in the MS spectrum reported in Fig. 4A. In agreement, in the ^{1}H NMR spectrum of this sample (Fig. 4B) the presence of anomeric reducing signals was detectable.

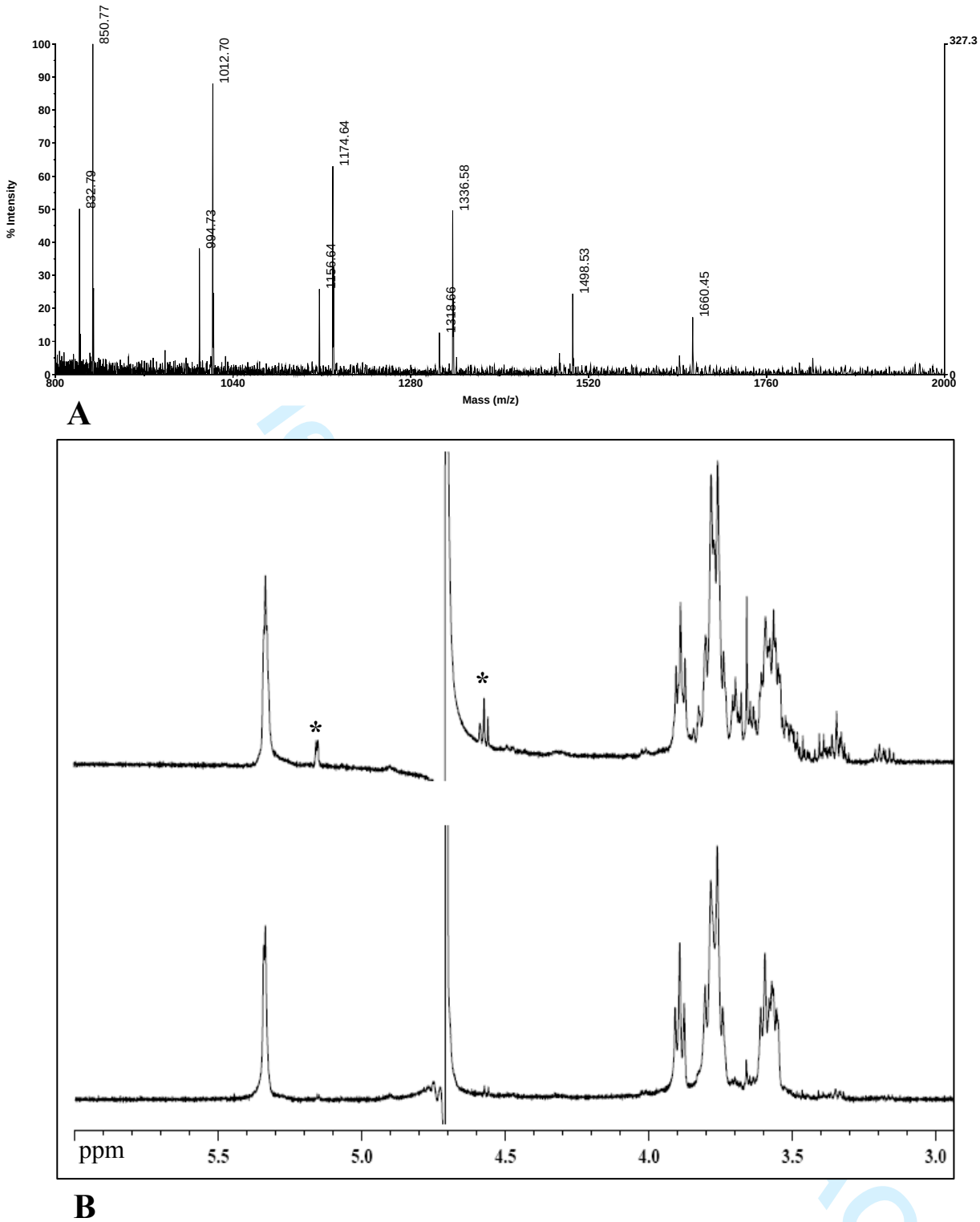

Figure 4 Panel A: MALDI MS analysis (performed in reflectron mode using DHB as matrix) of glycans after incubation at 110 °C for two hours at pH 3. Peaks corresponding to cyclic structures (162*n*), and peaks corresponding to linear structures (162*n* + 18) are shown. Panel B: Comparison

of the ^{1}H NMR spectrum of the α-(1→4) glucan before (bottom) and after (up) the acid hydrolysis. The anomeric signals of the reducing units are labelled.

It is worth noting that amylose ((α-(1→4)-Glc)$_n$glucan), a component of the PDY cultural broth coming from potato infusion, is absent in the ME culture broth. The lack of glycans in the hydrophobin preparation from the latter cultural broth indicated that the cyclodextrins are produced by the fungus when grown in the presence of amylose.

Analysis of hydrophobin aggregation

Since hydrophobins are prone to interfacial self assembly in response to external stimuli like agitation of the solution, we have investigated the hydrophobin behaviour in water (in the presence of glucans) or ethanol solution by analyses of SDS-PAGE, protein concentration and CD spectra, before and after vortexing.

A remarkable decrease of Hyd-w concentration was observed after vortexing. It dropped down (i.e. from 0.7 to 0.2 mg/ml), as well as the intensity of the relative SDS PAGE band (Fig. 5A).

CD spectra of Hyd-w slightly varied from sample to sample (Fig. 5B) even when the same dried sample was apparently suspended in the same conditions. These differences could be due to the diverse protein/glucans ratio of each single sample preparation. In all the samples, however, a significant contribution of random structure was noticed. Conformational changes with large shift towards β structure were observed after vortexing (Fig. 5B).

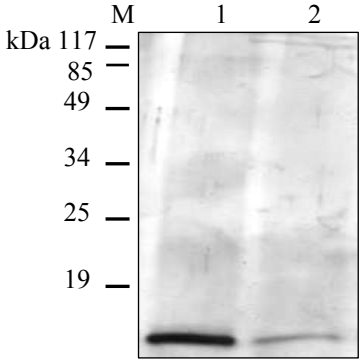

A

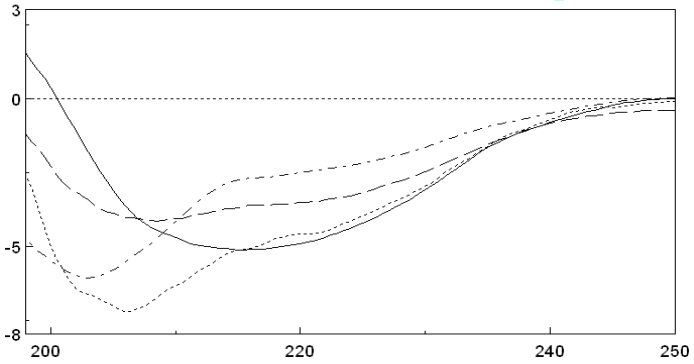

B

Figure 5 Panel A: SDS-PAGE of Hyd-w (lane 1); Hyd-w after vortexing (lane 2). Panel B**:** CD spectra of Hyd-w (sample 1 – · – · – ; sample 2 ····· and sample 3 — —), and sample 1 after vortexing (———).

Significant changes of the secondary structure were also observed between 70 and 80 °C, registering CD spectra of Hyd-w at different temperatures in the range from 30 to 90 °C.

When the pure protein was dissolved in 60% ethanol (Hyd-et) protein concentration was estimated by absorbance at 280nm, because of the interference of ethanol in the BCA assay. No variation of this values as well as band intensities on SDS-PAGE was observed after vortexing (Fig. 6A). CD spectra of Hyd-et were recorded showing a significant contribution of α helix to the secondary structure of the protein (Fig. 6B). It is worth noting that no change of the spectrum was detectable after vortexing of these samples.

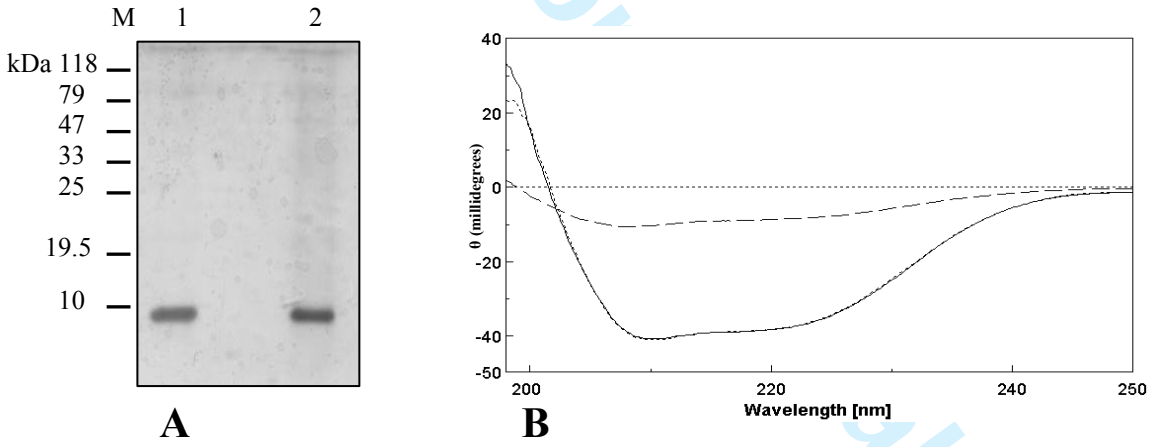

Figure 6 Panel A: SDS-PAGE of Hyd-et (lane 1); Hyd-et after vortexing (lane 2). Panel B**:** CD spectra of Hyd-et in 60% ethanol (solid lane), Hyd-et after vortexing (dotted lane); and Hyd-et in 20% ethanol (dashed line).

We also tried to suspend dried Hyd-et in 20% ethanol. Protein concentration was lower (about 30%) then that one obtained in 60% ethanol, and CD spectrum showed similar profile but at lower intensity (Fig. 6B). No variation of these parameters was observed after vortexing, as for Hyd-et in 60% ethanol.

Biofilm analyses

In order to analyse the vmh2 aggregates, biofilms have been formed on hydrophobic (silicon) or hydrophilic (oxidized silicon) surfaces using both Hyd-w or Hyd-et. The biofilm characterization has been performed by VASE on at least 6 samples prepared in the same experimental conditions; the optical model for experimental data fitting has been developed in a previous work[16]. Hyd-et forms a very stable biofilm on silicon whose thickness is 3.1±0.7 nm, whereas Hyd-et did not stably interact with oxidized silicon, thus the biofilm was not detectable. On the other hand, Hyd-w (in the presence of glucans) forms biofilms whose thickness was highly variable, sometimes significantly thicker than when Hyd-et was used on crystalline silicon. The Hyd-w biofilms thickness ranged from 3.5 to 30 nm on the silicon surface and from 6 to 38 nm on the oxidized silicon surface.

DISCUSSION

A hydrophobin secreted by the basidiomycete fungus *Pleurotus ostreatus* was purified, and identified as vmh2-1. Its encoding gene and cDNA had been previously isolated and sequenced by Penãs *et al.*[14]. The secreted protein undergoes a proteolytic processing, since the N terminus is either T25 or D26, whereas the expected signal peptide is M1-A21 according to the SignalP prediction program (http://www.cbs.dtu.dk/services/SignalP). Sequence analysis (hydropathy pattern and spacing between the cysteine residues) and robustness of the aggregates (dissolvable in 100% TFA) demonstrate that it belongs to Class I hydrophobins. As previously reported, the vmh2 biofilm is stable in 2% sodium dodecyl sulphate (SDS) at 100 °C for 10 minutes[16].

Although hydrophobins are generally reported to share low sequence identity percentage[3], comparison of the sequence of the often-used example of class I hydrophobin, SC3, with that of vmh2 reveals 46% of identity on the whole sequence, raising to 62% if the fragment starting from the first C of the disulfide pattern is considered. The main difference between the two sequences lies in the T stretch upstream the first C of SC3, that is absent in vmh2. This T stretch in SC3 is reported to be O-linked to mannose residues, thus further increasing the hydrophilicity of that region and consequently, of the whole protein[5]. The absence of this region in vmh2 could suggest a higher hydrophobicity of the *P. ostreatus* protein with respect to SC3. As a matter of fact our results show that pure vmh2 is not soluble in water. The two more studied Class I hydrophobin, SC3 and EAS of *N. crassa*, can be dissolved in water up to 1 mg/ml[25], and class II hydrophobins are reported to be even much more soluble (up to 10 mg/ml[26]). Therefore to the best of our knowledge, vmh2 is the most hydrophobic hydrophobin characterized so far.

Analyses of protein samples purified from culture medium containing amylose have shown the presence of glycans in the hydrophobin aggregates. If the complex is dissolved in 60% ethanol, the glycan fraction precipitates, leaving the protein free in this solution. The protein-glycans complex is soluble in water, but not the free protein. Therefore only the interaction with glycans enables the protein to be water soluble.

The structure of the water-soluble glycans matched to α 1-4 linked glucose. Moreover the data indicated the absence of reducing ends, pointing towards cyclic structure containing from six to sixteen monomers, namely α, β, γ cyclodextrins and higher homologues. It is well known that cyclodextrins can accommodate hydrophobic guest molecules, thus changing their solubility[27]. The most studied α, β, and γ cyclodextrins exhibit a truncated cone-shaped structure. The cavity of the torus is hydrophobic, while the rest is hydrophilic, making the cavities favourable places for hydrophobic interactions thus enabling the formation of inclusion complexes.

Enzymatic activities like 4-α-glucanotransferase can be responsible for the synthesis of cyclodextrins[28]. These enzymes are widely distributed in bacteria, yeasts, plants, and mammals and an increasing number of 4-α-glucanotransferases from different sources are known to be able to catalyze cyclization reactions to produce cycloamylose[29].

Aggregates can be obtained by vortexing the aqueous solution of the hydrophobin-glycans complex. The conformational changes observed for Class I hydrophobins after self-assembling, i.e. increase in β sheet structure, have been demonstrated for vmh2 upon vortexing. On the other hand when the pure protein is dissolved in a less polar solvent (60% ethanol) the propensity to self assemble is greatly reduced and no conformational change has been observed upon vortexing the solution.

It is worth to note that interactions of fibrillary prone peptides, such as the Alzheimer's amyloid β-peptide, with β-cyclodextrin have been demonstrated and these interactions reduce fibril formation[30,31]. They are considered to be hydrophobic in nature and involve aromatic side chains of the peptide and the hydrophobic cavity of the cyclodextrin, thus interfering with the oligomerization process of amyloid β-peptide. Our results on the vmh2-cyclodextrins interactions strengthen the similarity of the behaviors of Class I hydrophobins and the amyloid β-peptide.

Interaction between the most studied Class I hydrophobin, SC3 from *Schizophyllum commune* and polysaccharides has been reported[32]. *S. commune* produces and excretes a high molecular weight polysaccharide, schizophyllan[33]. Martin et al.[32] demonstrated that this polysaccharide

stabilizes small hydrophobin multimers in solution, and proposed a model in which the polysaccharide acts as hydrophilic stabilizer, and prevents hydrophobin self-aggregation. In the case of the high hydrophobic protein vmh2, cyclodextrins play a role in increasing its hydrophilicity thus allowing its solubility in water, but are not able to prevent vmh2 self aggregation.

The behaviour of the vmh2 aggregates have been investigated analysing the biofilms, obtained by depositing the pure protein in ethanol or the cycloamylose-protein complex in water, either on hydrophobic or on hydrophilic surfaces. When pure protein was deposited on the hydrophobic surface, crystalline silicon, a very stable biofilm was formed, whereas biofilm could not be detected on a hydrophilic surface, the oxidised silicon. On the other hand biofilms have been obtained on both surfaces using the cyclodextrin-hydrophobin complex dissolved in water and their thicknesses were always higher but much more variable then that obtained from the pure protein on crystalline silicon. Studies performed on the interaction between SC3 and schizophyllan, using other analytical methods, led the authors to the conclusion that schizophyllan is necessary for SC3 assembly into films on hydrophilic surfaces, whereas the hydrophobin alone can assembly only on hydrophobic surface[32]. Our studies led to similar conclusion as far as vmh2 and cyclodextrins are concerned. On the other hand the model proposed by Martin et al.[32] in which the presence of schizophyllan enhances adhesion to a hydrophilic surfaces thereby exposing the hydrophobic portion of the protein molecules, could be too simple to explain the behaviour of the vmh2-cyclodextrins system. The variability and the high thicknesses of the biofilms obtained in our experiments on hydrophilic or hydrophobic surfaces, can not be easily described by a simple double layer of polysaccharides and proteins. In our case more complex interactions have to occur, probably even because of the complexity and variety of the polysaccharide molecules involved. Further investigation are needed to analyse at molecular level the hydrophobin-cyclodextrins interactions and the specificity of this interaction, i.e. by using distinct cyclodextrin molecules.

ACKNOWLEDGMENT. This work was supported by the European Commission, Sixth Framework Program (QUORUM contract NMP-2004-032811).

The authors gratefully acknowledge proff. Gennaro Marino, Delia Picone and Leila Birolo for the helpful discussion.

REFERENCES

(1) Wösten, H. A. *Ann. Rev. Microbiol.*, **2001**, *55*, 625-646.

(2) Hektor, H. J.; Scholtmeijer, K. *Curr. Opin. Biotechnol*., **2005**, *16*, 434-9.

(3) Sunde, M.; Kwan, A. H.; Templeton, M. D.; Beever, R. E.; Mackay, J. P. *Micron*; **2008**, *39*, 773-784.

(4) Linder, M. B.; Szilvay, G. R.; Nakari-Setälä, T.; Penttilä; M. E. *FEMS Microbiol. Rev*., **2005**, *29*, 877-896.

(5) de Vocht, M. L.; Scholtmeijer, K.; van der Vegte, E. W.; de Vries, O. M.; Sonveaux, N.; Wösten, H. A.; Ruysschaert, J. M.; Hadziloannou, G.; Wessels, J. G.; Robillard, G. T. *Biophys. J*., **1998**, *74*, 2059-2068.

(6) Wang, X.; de Vocht; M. L.; de Jonge, J.; Poolman, B; Robillard, G. T. *Protein Sci,*. **2002**, *11*, 1172-81.

(7) Wang, X.; Permentier, H. P.; Rink, R.; Kruijtzer, J. A.; Liskamp, R. M.; Wösten, H. A.; Poolman, B.; Robillard, G. T. *Biophys. J.,* **2004**, *87*, 1919-1928.

(8) Kwan, A. H.; Winefield, R. D.; Sunde, M.; Matthews, J. M.; Haverkamp, R. G.; Templeton, M. D.; Mackay, J. P. *Proc. Natl. Acad. Sci. U S A.,* **2006**, *103,* 3621-6.

(9) Hakanpää, J.; Szilvay, G. R.; Kaljunen, H.; Maksimainen, M.; Linder, M.; Rouvinen, J. *Protein Sci.,* **2006**, *15*, 2129-2140.

(10) Hakanpää, J.; Linder, M.; Popov, A.;, Schmidt, A.;, Rouvinen, J. *Acta Crystallogr. D Biol. Crystallogr*., **2006**, *62*, 356-367.

(11) Szilvay, G. R.; Paananen, A.;, Laurikainen, K.; Vuorimaa, E.; Lemmetyinen, H.; Peltonen, J.; Linder, M. B. *Biochemistry*, **2007**, *46*, 2345-2354.

(12) Kisko, K.; Szilvay, G. R.; Vainio, U.; Linder, M. B.; Serimaa, R. *Biophys. J.*, **2008**, *94*, 198-206.

(13) Cohen, R.; Persky, L.; Hadar, Y. *Appl. Microbiol. Biotechnol.*, **2002**, *58*, 582-594.

(14) Peñas, M. M.; Rust, B.; Larraya, L. M.; Ramírez, L.; Pisabarro, A.G. *Appl. Environ. Microbiol.,* **2002**, *68*, 3891-3898.

(15) Peñas, M. M.; Asgeirsdóttir, S. A.; Lasa, I.; Culiañez-Macià, F. A.; Pisabarro, A.G.; Wessels, J. G.; Ramírez, L.; *Appl. Environ. Microbiol.*, **1998**, *64*, 4028-4034.

(16) De Stefano, L.; Rea, I.; Armenante, A.; Giardina, P.; Giocondo, M.; Rendina, I.; *Langmuir*, **2007**, *23*, 7920-7922.

(17) Houmadi, S.; Ciuchi, F.; De Santo, M. P.; De Stefano, L.; Rea, I.; Giardina, P.; Armenante, A.; Lacaze, E.; Giocondo M. *Langmuir,* **2008,** DOI: 10.1021/la802306r

(18) De Stefano, L.; Rea, I.; Giardina, P.; Armenante, A.; Rendina, I. *Adv. Mater.* **2008**, *20*, 1529–1533

(19) Chaplin, M. F.; Kennedy, J. F. In *Carbohydrate Analysis: A Practical approach*; 2nd ed.; D. Rickwood and D. Hames, Eds.; IRL press: London, UK, 1994.

(20) Cleveland, D. W.; Fischer, S.G.; Kirschner, M. W.; Laemmli, U. K. *J. Biol. Chem.*, **1977**, *252*, 1102-6.

(21) Leontein, K.; Lönngren, J. *Methods Carbohydr. Chem.,* **1978**, *62*, 359-362.

(22) Molinaro, A.; De Castro, C.; Lanzetta, R.; Evidente, A.; Parrilli, M.; Holst, O. *J. Biol. Chem*., **2002**, *277*, 10058-10063.

(23) Hakomori, S. *J. Biochem*., **1964,** *55*, 205-208.

(24) States, D. J., Haberkorn, R. A., Ruben, D. J. *J. Magn. Reson*., **1982**, *48*, 286-292.

(25) Wang, X.; Graveland-Bikker, J. F.; de Kruif, C. G.; Robillard, G. T. *Protein Sci.*, **2004**, *13*, 810-821.

(26) Kisko, K.; Szilvay, G. R.; Vainio, U.; Linder, M. B.; Serimaa, R. *Biophys. J.*, **2008,** *94*, 198-206.

(27) Lindner, K.; Saenger, W. *Biochem. Biophys. Res. Commun*., **1980**, *92*, 933-938

(28) Takaha, T.; Smith, S. M.. *Biotechnol. Genet. Eng. Rev.*, **1999**, *16*, 257–280.

(29) Yanase, M.; Takata, H.; Takaha, T.; Kuriki, T.; Smith, S. M.; Okada, S. *Appl. Environ. Microbiol.,* **2002**, *68*, 4233-4239

(30) Camilleri, P., Haskins N. J., Howlett D. R., *FEBS Lett*. **1994**; *341*, 256-258.

(31) Danielsson, J., Jarvet J., Damberg, P., Gräslund, A., *Biochemistry*, **2004,** *43*, 6261-6269.

(32) Martin, G. G.; Cannon, G. C.; McCormick, C. L. *Biomacromolecules*, **2000**, *1*, 49-60.

(33) Steiner, W.; Lafferty, R. M.; Gomes, I.; Esterbauer, H. *Biotechnol. Bioeng.,* **1987**, *30*, 169-178.